Technical Report Documentation Page

1. Report No.	2. Government Accession No.	3. Recipient's Catalog No.
FHWA/TX-88/01		

4. Title and Subtitle	5. Report Date
PREVENTION OF LONGITUDINAL CRACKING IN SURFACES AND FILLS	January, 1991
	6. Performing Organization Code
	8. Performing Organization Report No.

7. Author(s)	
Warren K. Wray and C. B. Ellepola	

9. Performing Organization Name and Address	10. Work Unit No. (TRAIS)
Dept. of Civil Engineering Texas Tech University Lubbock, TX 79409-1023	11. Contract or Grant No. 11-8-89-1214
	13. Type of Report and Period Covered Final September, 1988 - August, 1990
12. Sponsoring Agency Name and Adress Texas State Dept of Highways & Public Transportation P. O. Box 5051 Austin, TX 78763	14. Sponsoring Agency Code

15. Supplementary Notes

This study was conducted in cooperation with the U.S. Dept. of Transportation, Federal Highway Administration.

16. Abstract

Cracking parallel to the highway alignment (longitudinal cracking) was discovered in flexible pavement constructed over high-PI clay embankments retained by reinforced soil retaining walls (RSRWs). The cracks were noted to occur at approximately the location of the interface between the clay embankment and the cohesionless backfill of the RSRW. Coring of the crack revealed the crack to be wider at the bottom than at the top suggesting that the tensile force causing the cracking was being applied at the bottom of the pavement structure. All Texas State Dept. of Highways and Public Transportation (SDHPT) Districts were queried to learn the extent of the longitudinal cracking problem. Only District 16, headquartered at Corpus Christi, was found to be experiencing the problem.

Using soil from the same source as was used to construct embankments and RSRW backfill, four large laboratory models were constructed of the field situation. Each of the tests demonstrated that a vertical separation would occur between the clay embankment and sand backfill as a result of lateral shrinking of the high-PI clay over time due to climate. The third test showed that the vertical crack would propagate upwards through the flexible base material. The fourth test produced a crack through the flexible base but failed to produce a crack through the overlying HMAC because the HMAC adhered to the walls of the test box and separated from the caliche base.

Lateral stresses imposed on the flexible base by the laterally shrinking clay embankment were found to be approximately 366 psi in the laboratory tests, well exceeding the tensile strength of normal HMAC.

continued on back of page

17. Key words	18. Distribution Statement
clay embankments, expansive soil, field instrumentation, lateral stresses, longitudinal cracking, pavement cracks, reinforced soil retaining walls, soil suction, shrinking stresses	No restrictions. This document is available to the public through National Technical Information Service, Springfield, VA 22161.

19. Security Classif. (of this report)	20. Security Classif. (of this page)	21. No. of Pages	22. Price
UNCLASSIFIED	UNCLASSIFIED	143	

continued from other side

Thus, it was concluded that the longitudinal cracks observed in the District 16 pavements constructed over high-PI clay embankments retained by reinforced earth retaining walls were the result of the clay embankments laterally drying beneath the installed pavement.

Field instrumentation installed during the study was inconclusive with respect to measuring soil moisture condition changes occurring beneath the pavement because the monitoring sites were not paved until nearly the end of the study. However, the instruments showed that a change in soil suction pressures of up to 25 atmospheres of pressure had occurred during the 1-year monitoring period as a result of changes in climate only.

Four recommendations for dealing with the problem were made for those instances when high-PI clay material cannot be avoided in constructing reinforced earth retained embankments: (1) construct a zone of mixed soil with a lower PI across the clay-sand interface; (2) construct a sand subbase between the clay subgrade and the flexible pavement base; (3) permit the crack to occur, repair the crack, and apply a final lift of HMAC; and (4) spray cut-back asphalt to encapsulate the clay embankment and prevent any change in soil moisture conditions.

PREVENTION OF LONGITUDINAL CRACKING IN SURFACES AND FILLS

by

Warren K. Wray
C. B. Ellepola

Research Report Number 11-8-89-1214

conducted for

Texas State Department of Highways
and Public Transportation

In cooperation with the U.S. Department of Transportation
Federal Highway Administration

by the

DEPARTMENT OF CIVIL ENGINEERING
TEXAS TECH UNIVERSITY

JANUARY 1991

Any opinions, findings, and conclusions or recommendations expressed in this material are those of the authors and do not necessarily reflect the views or policies of the Federal Highway Administration or the Texas State Department of Highways and Public Transportation. This report does not constitute a standard, a specification, or regulation.

There was no invention or discovery conceived or first actually reduced to practice in the course of or under this contract, including any art, method, process, machine, manufacture, design or composition of matter, or any new and useful improvement thereof, or any variety of plant which is or may be patentable under the patent laws of the United States of America or any foreign country.

ACKNOWLEDGEMENTS

This study was accomplished under Study No. 11-8-89-1214 from the Texas State Department of Highways and Public Transportation (SDHPT). The Technical Coordinators for the study were William M. Isenhower, Ph.D., P.E. of SDHPT Division 8 and Mark McClelland of SDHPT Division 5.

Special thanks is given to many members of the SDHPT District 16 who provided valuable assistance in many ways during the period of the study. Included in this group of District 16 engineers were Mr. Nino Gutierrez, P.E., District Engineer; Mr. James B. Opiela, P.E., Assistant District Engineer and District Construction Engineer; Mr. Dallas Comuzzie, P.E., Supervising Resident Engineer, Corpus Christi residency; and Mr. Richard A. Terry, P.E., Senior Resident Engineer, Corpus Christi residency. The District 15 soil drilling rig crew were a pleasure to work with; their professional approach to carefully securing valuable soil samples was very much appreciated.

The considerable assistance and advice provided to the research team by SDHPT Division 10-Research personnel was also invaluable to the success of this study. Mr. Jon Underwood, P.E., Research and Development Engineer, provided invaluable guidance on SDHPT procedures and methods, and Lana Ashley and Sheila Stiffelmeir always seemed to know the right answer to many research team questions.

The authors want to particularly express our appreciation to Mrs. Judy Hardin for her day-to-day work on the project; Mr. Richard Dillingham for his editorial expertise in preparing the final report; Mrs. Rebecca Foster for her excellent preparation of the draft and final versions of the study report; Mr. Brian Riha for tirelessly producing the figures presenting the results of the study tests and field monitoring; and Graduate Research Assistant Patty Pomper and Technician I Arnold Fernandez for their uncomplaining and tireless toiling in installing the field instrumentation and making numerous subsequent round trips between

Corpus Christi and Lubbock to read the instruments. Thanks is also expressed to Graduate Research Assistants Edward Lee and Wes Bratton for their timely and valuable assistance--deadlines came and were met in a timely manner.

ABSTRACT

Cracking parallel to the highway alignment (longitudinal cracking) was discovered in flexible pavements constructed over high-PI clay embankments retained by reinforced soil retaining walls (RSRWs). The cracks were noted to occur at approximately the location of the interface between the clay embankment and the cohesionless backfill of the RSRW. Coring of the crack revealed the crack to be wider at the bottom than at the top suggesting that the tensile force causing the cracking was being applied at the bottom of the pavement structure. All Texas State Dept. of Highways and Public Transportation (SDHPT) Districts were queried to learn the extent of the longitudinal cracking problem. Only District 16, headquartered at Corpus Christi, was found to be experiencing the problem.

Using soil from the same source as was used to construct embankments and RSRW backfill, four large laboratory models of the field situation were constructed. Each of the tests demonstrated that a vertical separation would occur between the clay embankment and sand backfill as a result of lateral shrinking of the high-PI clay over time due to climate. The third test showed that the vertical crack would propagate upwards through the flexible base material. The fourth test produced a crack through the flexible base but failed to produce a crack through the overlying HMAC because the HMAC adhered to the walls of the test box and separated from the caliche base.

Lateral stresses imposed on the flexible base by the laterally shrinking clay embankment were found to be approximately 366 psi in the laboratory tests, well exceeding the tensile strength of normal HMAC. Thus, it was concluded that the longitudinal cracks observed in the District 16 pavements constructed over high-PI clay embankments retained by reinforced soil retaining walls were the result of the clay embankments laterally drying beneath the installed pavement.

Field instrumentation installed during the study was inconclusive with respect to measuring soil moisture condition changes occurring beneath the pavement because the monitoring sites were not paved until nearly the end of the study. However, the instruments showed that a change in soil suction pressures of up to 25 atmospheres of pressure had occurred during the 1-year monitoring period as a result of changes in climate only.

Four recommendations for dealing with the problem were made for those instances when high-PI clay material cannot be avoided in constructing reinforced soil retained embankments: (1) construct a zone of mixed soil with a lower PI across the clay-sand interface; (2) construct a sand subbase between the clay subgrade and the flexible pavement base; (3) permit the crack to occur, repair the crack, and apply a final lift of HMAC; and (4) spray cut-back asphalt to encapsulate the clay embankment and prevent any change in soil moisture conditions.

METRIC CONVERSION FACTORS

Approximate Conversions to Metric Measures

Symbol	When You Know	Multiply by	To Find	Symbol
		LENGTH		
in	inches	*2.5	centimeters	cm
ft	feet	30	centimeters	cm
yd	yards	0.9	meters	m
mi	miles	1.6	kilometers	km
		AREA		
in^2	square inches	6.5	square centimeters	cm^2
ft^2	square feet	0.09	square meters	m^2
yd^2	square yards	0.8	square meters	m^2
mi^2	square miles	2.6	square kilometers	km^2
	acres	0.4	hectares	ha
		MASS (weight)		
oz	ounces	28	grams	g
lb	pounds	0.45	kilograms	kg
	short tons (2000 lb)	0.9	tonnes	t
		VOLUME		
tsp	teaspoons	5	milliliters	ml
Tbsp	tablespoons	15	milliliters	ml
fl oz	fluid ounces	30	milliliters	ml
c	cups	0.24	liters	l
pt	pints	0.47	liters	l
qt	quarts	0.95	liters	l
gal	gallons	3.8	liters	l
ft^3	cubic feet	0.03	cubic meters	m^3
yd^3	cubic yards	0.76	cubic meters	m^3
		TEMPERATURE (exact)		
°F	Fahrenheit temperature	5/9 (after subtracting 32)	Celsius temperature	°C

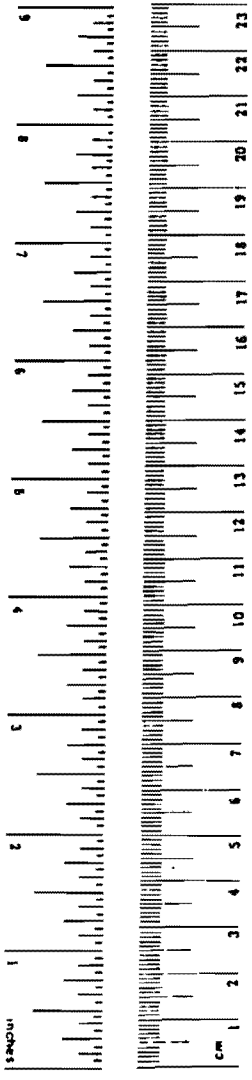

Approximate Conversions from Metric Measures

Symbol	When You Know	Multiply by	To Find	Symbol
		LENGTH		
mm	millimeters	0.04	inches	in
cm	centimeters	0.4	inches	in
m	meters	3.3	feet	ft
m	meters	1.1	yards	yd
km	kilometers	0.6	miles	mi
		AREA		
cm^2	square centimeters	0.16	square inches	in^2
m^2	square meters	1.2	square yards	yd^2
km^2	square kilometers	0.4	square miles	mi^2
ha	hectares (10,000 m^2)	2.5	acres	
		MASS (weight)		
g	grams	0.035	ounces	oz
kg	kilograms	2.2	pounds	lb
t	tonnes (1000 kg)	1.1	short tons	
		VOLUME		
ml	milliliters	0.03	fluid ounces	fl oz
l	liters	2.1	pints	pt
l	liters	1.06	quarts	qt
l	liters	0.26	gallons	gal
m^3	cubic meters	35	cubic feet	ft^3
m^3	cubic meters	1.3	cubic yards	yd^3
		TEMPERATURE (exact)		
°C	Celsius temperature	9/5 (then add 32)	Fahrenheit temperature	°F

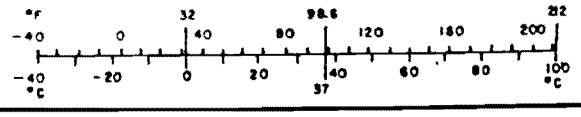

TABLE OF CONTENTS

LIST OF FIGURES

LIST OF TABLES

1. INTRODUCTION

Retaining walls are often employed on highway embankments when there is a limitation on the land area available for highway right-of-way. Reinforced soil retaining walls (RSRWs) have often been found to provide an economical substitute for conventional reinforced concrete retaining walls in these instances. RSRWs limit the land required for the embankment by maintaining a vertical profile, thus reducing the land required for the construction of highway overpass embankments.

Two advantages of using RSRW systems are that they are considerably less expensive to build than the more conventional gravity retaining wall or cantilever retaining wall systems and they are faster to construct. Using an RSRW system, the entire retaining structure may increase by two or three panel heights in a single day. This is an important factor in dealing with public funded engineered structures, since it permits public work departments to show the public that they are working quickly and efficiently to bring the project to a successful completion (Comuzzie, 1989). Walkinshaw (1975) reports that RSRW structures have been proved to be economical and have saved hundreds of thousands of dollars in construction costs on projects where they have been used. RSRW structures are highly recommended for use when the foundation soils are poor and settlements are anticipated which could be detrimental to conventional retaining structures.

Reinforced soil retaining walls derive their stability from the interaction of select granular backfill and steel reinforcement straps or grids attached to the back of the wall panels and embedded horizontally in compacted granular backfill. The weight of the backfill acts normally on the steel straps or grids and the frictional force occurring between the backfill and the steel strips or straps resists any attempt by the RSRW structure to move away from the backfill. This frictional force inhibits further movement of the RSRW wall.

The Texas State Department of Highways and Public Transportation (SDHPT) employed RSRWs in its embankment construction--particularly in association with overpass bridge construction--through most of the 1980s. Most of RSRW applications have been in urban environments and have proved to perform successfully subsequent to being placed in the inventory and opened to public use. However, SDHPT District 16, headquartered in Corpus

Christi, began encountering development of longitudinal cracking occurring in the flexible pavement structures placed over embankments constructed with RSRWs.

It was observed by District 16 personnel that the cracking usually occurred in the shoulders of the paved section but the cracking sometimes occurred in the right wheel path as the embankment height increased. Subsequent measurements showed that the location of the cracks roughly approximated the location of the interface between the compacted earth embankment and the compacted select granular RSRW backfill. Shortly after the initiation of the study, District 16 personnel cored one of the longitudinal cracks on SH 358 and reported that the crack was discovered to be wider at the bottom than at the surface of the pavement.

Concern over this possible deficiency in using RSRW structures generated the study being reported. The cause of the longitudinal cracking and recommendations for solving or avoiding this problem were the principal objectives of the study.

2. REVIEW OF THE TECHNICAL LITERATURE

A. GENERAL

There are at least three possible causes of the longitudinal cracking that has been observed in flexible pavements constructed over RSRW-retained embankments. These three possibilities include:

1. Subsidence of the cohesionless select granular backfill material's horizontal surface due to a rotational movement of the vertical face of the RSRW about its base.

2. Differential settlement of the embankment and the adjacent select granular backfill.

3. Lateral shrinkage of the high-PI cohesive soil away from the interface with the cohesionless select granular backfill due to change in soil moisture content in the clay embankment.

Each possibility will be considered in detail. In this chapter each possibility is closely examined, including concept, theory, documented cases of failure, and conclusions about each possibility. This chapter will be solely devoted to developing an understanding of the three possible causes of longitudinal cracking.

B. BACKFILL SUBSIDENCE DUE TO ROTATION OF RSRW FACE ABOUT ITS BASE

1. General Principles of Reinforced Soil. Reinforced soil is a composite material which consists of two materials (Vidal, 1969): soil grains and reinforcement. An analogy of reinforced soil is reinforced concrete. Reinforced concrete, too, is a composite material, consisting of concrete and steel reinforcement. In both cases, the reinforcement is used in the direction of the greatest stress, and, in particular, to resist those stresses inducing tension in the matrix material (Walkinshaw, 1975). The reinforcement in the reinforced soil, however, does not include any glue-type bonding material like cement in reinforced concrete or the clay of adobe walls (Vidal, 1978). The reinforced soil concept is not an anchorage technique. The RSRW reinforcement is flexible and can follow the movement of the soil.

The most common configuration of reinforced soil retaining walls is depicted in Fig. 2.1. In the structures in Fig. 2.1, the reinforcement consists of horizontal layers of metal strips

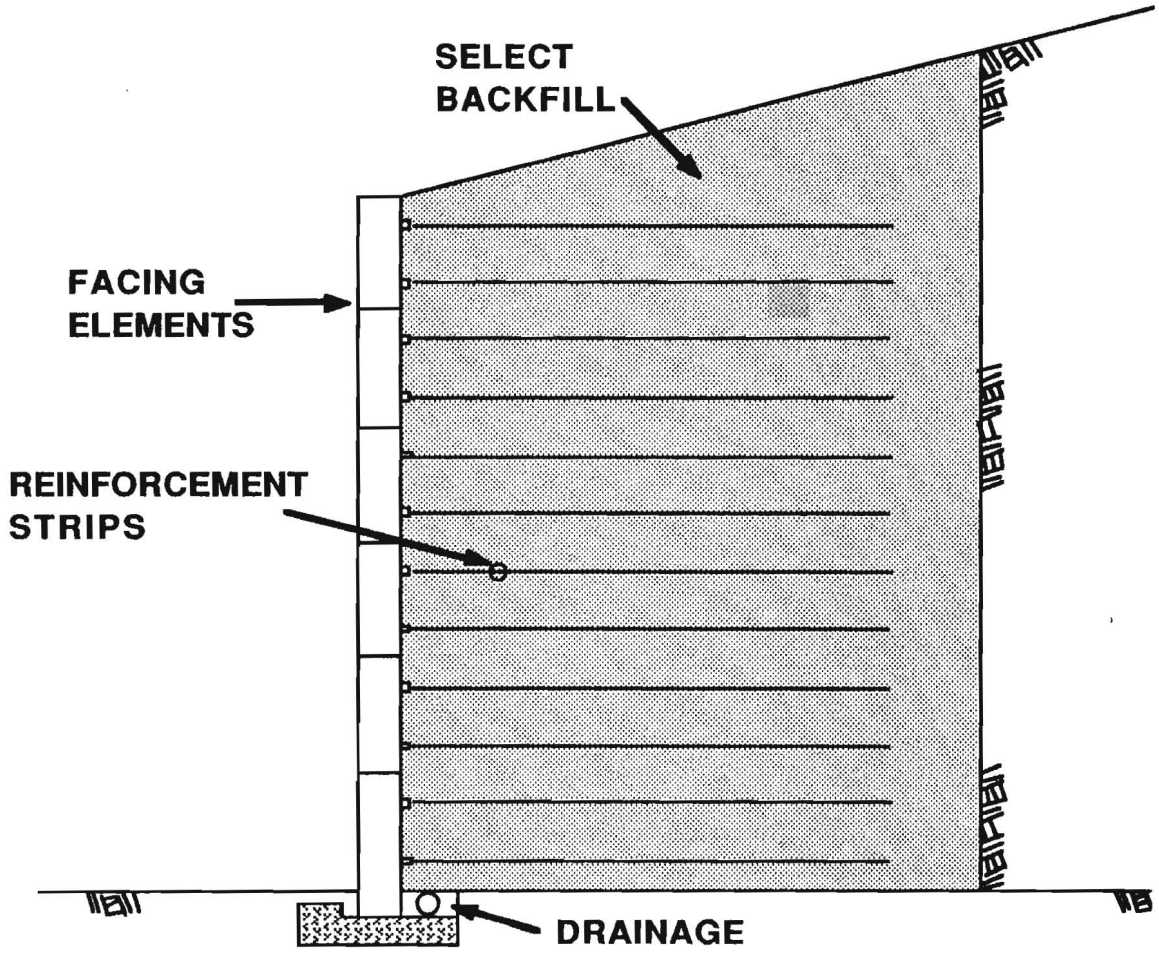

Fig. 2.1. The typical reinforced soil retaining wall configuration.

within the soil mass. The four principal elements of the reinforced soil retaining walls as shown in Fig. 2.1 are (Walkinshaw, 1975; Lee, 1978):

1. *Backfill.* This cohesionless material extends from the back of the facing wall panel to a short distance beyond the ends of the reinforcing strips, and is commonly called the "reinforced volume." This provides bulk, weight, compression resistance, and shearing strength. This material must meet certain size and gradation specifications. These specifications may change from project to project, but are typically stated in the project engineering construction specifications.

2. *Reinforcing Strips.* Manufactured from either metal or geogrid material, the strips are fastened only to the back face of the facing elements. The dimensions of these strips (length, width, and thickness) will depend on the external loading and the height of the structure. The metal strips are usually galvanized steel, but in some cases aluminum magnesium alloy (for bulkhead walls in sea water), stainless steel, or polypropylene geogrids have been used. These strips help bend the soil into a pseudo coherent material and resist tensile stresses (Lee, 1978).

3. *Facing Elements.* These units may be constructed of either galvanized steel or precast concrete panels. These panels do not carry any structural load. The main function of the facing elements is to prevent backfill ravelling or sand grains from slipping away at the open end. They also fulfill an aesthetic effect. Thus, the panel could be manufactured out of virtually any material since it does not have to meet strict structural requirements. Recent trends indicate that precast concrete panels predominate, especially in the state of Texas.

4. *Mechanical Connections.* This is the method of connecting the reinforcements to the facing elements.

According to Vidal (1969), Walkinshaw (1975), and Lee (1978), the basic mechanism of the reinforced earth structure is the friction between the strips and the earth. The friction is generated by an infinitesimal movement of the facing panel. Walkinshaw (1975) states that friction without slippage between the backfill and the strips is possible if the backfill soil has minimal frictional characteristics. Consequently, the backfill material used in the reinforced volume of a reinforced soil structure is commonly required to have a minimum angle of internal friction of approximately 25 degrees with no more than approximately 15 percent of the backfill passing the No. 200 sieve (75 μm).

Since no slippage occurs between the strips and the backfill soil, tensile forces are resisted by the reinforcing strips, and the associated strains are, therefore, controlled by this stiffer material. With proper spacing (both vertically and horizontally) and length of the reinforcing strips, the reinforced earth volume is internally stable between each layer of strips, and the facing element is required only to prevent the outward flow of the soil at the boundary (Lee et al., 1972; Walkinshaw, 1975).

The length of the reinforcing strips is dependent upon the height of the wall, external loadings, and site conditions. The internal design of a reinforced earth structure includes the determination of strip spacing, width, length, and thickness. While every reinforced earth structure is a unique structure, where the local site and atmospheric conditions must be considered, experience has shown that the length of the strips should be approximately 80 percent of the wall height for routine retaining applications. Walkinshaw (1975) claims that this length of strip embedment gives excellent wall stability.

According to McKittrick (1978), the topics that pertain to reinforced earth structures can be arranged in the following manner:

1. Basic mechanics of reinforced earth
    a. State of stress in a reinforced earth structure
    b. Frictional relationship between soil and reinforcement
2. Selection of soil for use in reinforced earth structures
3. Durability of buried metal reinforcements

2. Basic Mechanics of Reinforced Earth. A series of triaxial tests done on sand reinforced with aluminum disks by Long et al. (1983), at the Laboratoire Central des Ponts at Chaussee (LCPC), Paris, under the supervision of Professor F. Schlosser, was one of the very first scientific tests done on reinforced earth to investigate its behavioral mechanism. What is evident from this test is that the reinforcing strips give the reinforced earth an "apparent" or "pseudo" cohesion. The points found were on a line, which is parallel to the line of the same sand without the reinforcements, and the "cohesion" was found to be proportional to the resistance of the reinforcement.

It has been shown in laboratory experiments that an axial load on a sample of granular material will result in lateral expansion in dense materials. Because of dilation, the lateral strain is more than one half of the axial strain. However when reinforcing elements are placed within the soil mass, no lateral deformation takes place. The lateral extension of each layer of sand located between two adjacent reinforcement plates is being restrained by means of friction mobilized at the interfaces between the soil and the reinforcing element. The generated shear stresses result in the development of the tensile forces in the reinforcements and in the increase of the average confining pressure within the soil giving an anisotropic "cohesion" to the sample (Juran et al., 1978). This lateral restraining load is equal to the lateral earth pressure at rest ($K_o\sigma_v$) (McKittrick, 1978). Each element of the soil mass is acted upon by a lateral stress equal to $K_o\sigma_v$. Therefore, as the vertical pressure increases, the horizontal restraining force due to the reinforcement also increases in direct proportion. Consequently,

for any value of internal friction, ϕ, typically associated with granular soils, the stress circle lies well below the rupture curve at all points. Therefore, failure can only occur by the loss of friction between the soil and the reinforcements or by tensile failure of the reinforcements. This was examined and confirmed by Schlosser and Long (1969) and Hausmann and Lee (1976).

The theoretical relationships between the spacing and tensile resistance of the reinforcements and the increase in "anisotropic pseudocohesion" of the reinforced materials were presented above. Since these conclusions were restrictive of the wider application of soil reinforcing, Bassett and Last (1978) further investigated this concept with analyses of a non-cohesive soil reinforced with a uni-directional reinforcement system subjected to plane strain. Using a Mohr's circle of strain, the investigators determined the directions of the major and minor principal strains, ε_1 and ε_3, and the direction of the zero strain planes, α and β, which define an arc segment containing the minor principal strain direction, ε_3, within which all normal strains would be tensile and reinforcement horizontally in line with the maximum principal tensile strain. This direction is used in actual reinforced soil retaining walls. Since the modulus of elasticity of the reinforcing material is generally very much greater than that of the soil, and as efficient frictional force transfer occurs between the soil matrix and the reinforcements, the direction of the reinforcements must be aligned with one of the zero extension characteristics; i.e., the β characteristics of a composite material would be rotated to become very nearly horizontal and the α characteristics would be forced to follow. The potential rupture or failure mechanism would also attempt to realign with these new characteristics. Such realignment is in substantial conformity to the locus of maximum tensile strains measured in several full-scale structures (Schlosser, 1978).

Vidal (1966) intuitively assumed that reinforced soil acts like a coherent gravity structure. However, many researchers have done extensive studies and have tried to analyze the reinforced earth structure as a tieback structure. It, therefore, becomes imperative to consider the body of research done world wide in order to validate one of the two differing hypotheses.

The major assumption made, which is accepted by both hypotheses, is that the reinforced soil wall will move by an infinitesimal amount sufficient to cause active earth pressure failure of the soil mass behind the wall (Vidal, 1969). Now the question which arises is "Where is the failure plane located?" The **tieback structure analysis hypothesis** assumes that the active pressure plane begins at the bottom of the wall and, according to Rankine theory, rises through the reinforced soil backfill mass, intersecting the horizontal surface behind the top of the wall at an angle of $45° + \phi/2$, thus intersecting the horizontal surface behind the top of the

wall at a distance of H·Tan (45° - ϕ/2). Here H is the height of the wall and ϕ is the angle of internal friction of the reinforced volume.

A very simple and rudimentary explanation of the **coherent gravity hypothesis** is that the reinforced soil structure acts as and like a single, united, integrated and fused structure, akin to a monolithic massive. In this hypothesis, the assumption is that the failure plane initiates at the base of the wall but rises very rapidly in a curvilinear fashion, quickly turning almost vertical until it intersects the horizontal surface behind the wall at a distance equal to approximately 0.3H. This distance is significantly less than H·Tan (45° - ϕ/2). Fig. 2.2 compares the two methods of analysis.

Two foundation failures at Aguadilla, Puerto Rico and Roseburg, Oregon (McKittrick, 1978) strongly support the coherent gravity structure theory.

(a) State of Stress in a Reinforced Soil Structure. The determination of the lateral stresses which must be resisted by the reinforcement is the most important aspect in reinforced soil design. An overstress could cause tensile failure of the reinforcement, resulting in structural collapse. Determination of the sliding resistance between the soil and reinforcement is not critical since slippage will cause a redistribution of the stress and a slow deformation of the soil mass (McKittrick, 1978).

The state of stress in reinforced soil structures has been shown to vary and, thus, cannot always be predicted (Schlosser and Elias, 1978). This variance can be explained by the relationship between critical void ratio and applied stress. The results of the test performed by Schlosser and Elias (1978) indicate that the most important parameter is the ratio of the relative volume of the fine grained portion to the granular portion. The internal friction angle decreases when the fine grained portion increases and can be explained as follows:

1. As long as the fine grain portion is small, the number of contacts between the grains of the granular soil "skeleton" do not vary. Therefore, the value of the internal friction angle remains constant.

2. When a critical value of the relative volume of fines is exceeded, the number of contacts between the grains of the soil "skeleton" decreases causing the internal friction angle to decrease.

3. When there is no more contact between grains of the granular soil "skeleton," the value of the internal friction angle becomes zero and the soil is then purely cohesive.

Studies by Castro (1969) have shown that the critical void ratio decreases with increasing stress. Thus, the relative extension of the soil compared with the reinforcing strips

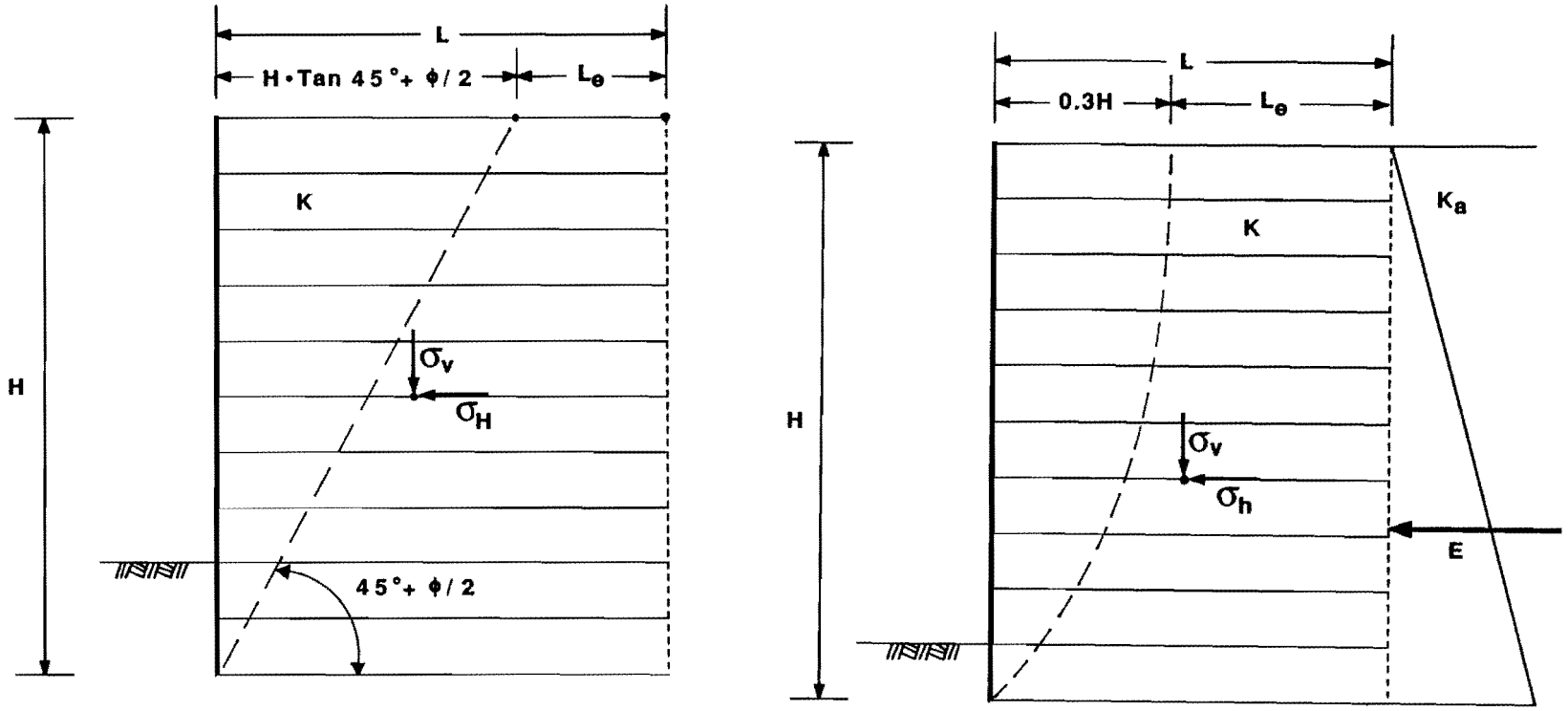

Fig. 2.2. A representation of the two types of reinforced soil performance or analysis hypotheses: (a) tieback structure analysis hypothesis, and (b) coherent gravity analysis hypothesis.

becomes less for higher walls with their correspondingly higher stresses. Therefore, for higher structures the effective lateral stress is reduced and approaches an active state.

The effect of the factor of safety in design is to move the Mohr's circle away from the failure envelope resulting in designing for a K_o (coefficient of lateral earth pressure at rest) greater than K_a (coefficient of active earth pressure). Thus, K_o must be determined with sufficient accuracy and precision.

The coefficient of earth pressure at rest is defined as the ratio of the horizontal to the vertical stress, $\frac{\sigma_h}{\sigma_v}$, under zero lateral strain conditions (Tavenas et al., 1975). However, using the condition of effective stress:

$$K_o = \frac{\sigma_h - u}{\sigma_v - u} \qquad (2.1)$$

where σ_h = stress acting in the horizontal direction

σ_v = stress acting in the vertical direction

u = pore water pressure

Jacký (1944) suggested a semi-empirical relationship for normally consolidated soils (clays):

$$K_o = \left(1 + \frac{2}{3}\,\mathrm{Sin}\,\phi\right)\frac{1-\sin\phi}{1+\sin\phi} \qquad (2.2)$$

where ϕ = effective angle of friction.

However, an approximation for this relationship often sufficiently accurate for engineering purpose is usually used:

$$K_o = 1 - \sin\phi \qquad (2.3)$$

Janbu (1972) suggested an analytical approach for the determination of K_o for $c - \phi$ (soils having both cohesion and a high angle of internal friction):

$$\phi_o = \frac{2}{3}\phi \ (\phi \text{ as determined by direct shear test}) \qquad (2.4)$$

where ϕ_o = angle of internal friction at rest.

$$\text{Therefore, } K_o = \frac{1 - \sin\phi_o}{1 + \sin\phi_o} \qquad (2.5)$$

The cohesion at rest, c_o, may be determined as:

$$c_o = \frac{c\,\mathrm{Cot}\,\phi}{\mathrm{Cot}\,\phi o} \qquad (2.6)$$

where c, ϕ are parameters determined by the direct shear test and K_o is determined from the relation as:

$$\sigma_{o3} = \sigma_1 K_o + 2C_o K_o \tag{2.7}$$

where σ_{o3} = pressure of soil at rest

σ_1 = overburden of soil

c_o = cohesion at rest

(b) Frictional Relationship Between Soil and Reinforcement. Once the horizontal stress has been determined, the cross sectional area of the reinforcement strips and their horizontal and vertical spacing can be calculated. Now all that remains is to determine whether that horizontal stress can be effectively and efficiently transferred to the soil mass. The factor of safety should be calculated also. The equations that govern these relationships are (e.g., Vidal, 1969):

$$FS_{bond} = \frac{2bf^{*}L_e\sigma_v}{(K\sigma_v)\,S_xS_y} \tag{2.8}$$

or

$$FS_{bond} = \frac{2bf^{*}L_e}{(K)A} \tag{2.9}$$

where FS_{bond} = factor of safety

b = width of reinforcement

f^{*} = apparent coefficient of friction

L_e = length of reinforcement effective in stress transfer

K = earth pressure coefficient

S_xS_y = influence area of reinforcement

The apparent coefficient of friction, f^{*}, can be determined from a number of tests such as:

1. Direct shear (sliding shear) tests between soil and reinforcing material for either a model or a prototype RSRW constructed to any predetermined scale.

2. Reinforcing strip pullout from a reinforced soil wall for a model, prototype or a full-scale RSRW.

3. Reinforcing strip pullout from embankments.

4. Reinforcing strip pullout from a rigid moving wall conducted on a scale model RSRW.

5. Reinforcing strip pullout tests during vibration conducted on a scale model RSRW.

Research done by numerous investigators (Schlosser and Vidal, 1969; Ponce and Bell, 1971; Almi et al., 1973; Chang and Forsyth, 1977; Bolton et al., 1978) has led to correlations between the direct shear test and "cohesion" values. This work has been summarized by McKittrick (1978) and is as follows:

For smooth reinforcement strips:

> The value of f^* obtained from direct shear tests performed at strain conditions consistent with anticipated structural performance should be used. In most cases, this value will be equal to the residual sliding shear value (Tan ω).

For reinforcements with deformations or transverse ribs:

> The values of f^* consistent with soil parameters adjusted for the effects of the plane compression, dilatancy, and overburden pressure can be used with confidence.

In the case of smooth strips, the soil-strip friction characteristics will control behavior. In the case of ribbed or roughened strips, the soil-soil characteristics will most often control (i.e., the frictional "resistance" developed between the soil and the strip will exceed the shear strength of the backfill soil).

The effective reinforcement length can be determined by first locating the locus of the points of maximum tension. This locus defines two zones within the structure: an active zone in which the shearing stresses exerted by the earth on the reinforcement are directed outward, towards the facing, and a resistant zone in which the shearing stresses are directed towards the free end of the reinforcement. The boundary of this "active zone" varies with the type of structure, the foundation soil, and the location and magnitude of applied external loading. The boundaries have been found by experimental work (Schlosser, 1978), and are depicted in Fig. 2.3. Thus, the effective length will be the combined length of the active zone and the resistant zone.

3. Selection of Soils for Use in Reinforced Soil Construction. The three principal considerations which influence the selection of soils for use in reinforced earth structures are, according to McKittrick (1978):

1. Long-term stability of the completed structure

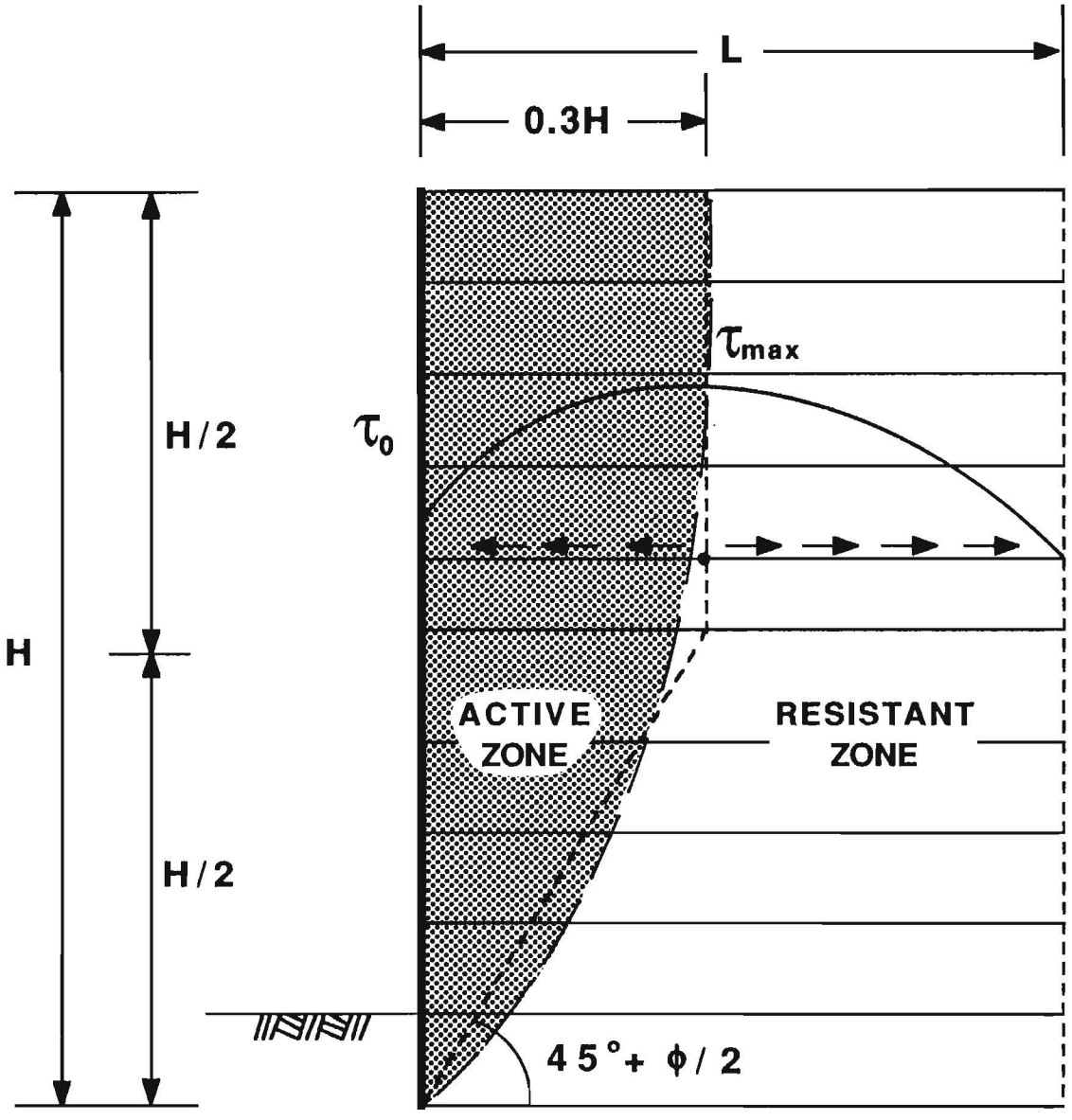

Fig. 2.3. Tensile forces distribution along the reinforcements, separating the backfill soil into an active zone and a resistant zone (after Schlosser and Elias, 1978).

2. Short-term (construction phase) stability

3. Physico-chemical properties of the materials

According to McKittrick (1978):

> Granular soils compacted to densities that result in volumetric expansion during shear are ideally suited for use in reinforced earth structures. Where these soils are well drained, effective normal stress transfer between the strips and soil backfill will be immediate as each lift of backfill is placed, and shear strength increase will not lag behind the vertical loading. In the range of loading normally associated with reinforced earth structures, granular soils behave as elastic materials. Therefore, for structures designed at working stress levels, no post construction movements associated with yielding or readjustments should be anticipated.

Fine grained soils, due to their low permeability and delayed effective stress transfer, which is not immediate if saturated or nearly saturated, are not good for reinforced volumes. The slow effective stress transfer will slow construction and, due to the plastic behavior of these fine grained soils, post-construction movement could be induced. Generally, fine grain soils should not be used. Specifications for select backfill material are given in the current Federal Highway Administration (FHWA) specifications and the Standard Specification of the Texas State Department of Highways and Public Transportation (1982).

An additional consideration is that as soils become more fine grained, their electrical resistivity generally decreases. Soil resistivity is an important factor in controlling the rate of galvanic corrosion. Low resistivity is often associated with aggressive soils.

4. Durability of Buried Metal Reinforcements. The corrosion process is essentially an electrochemical process. For corrosion to occur, there must be a potential difference between two points that are electrically connected in the presence of an electrolyte. In the case of buried metals, the most favorable corrosion conditions occur when water, rich in oxygen and dissolved salts, wets the soil particles in contact with the metal. Among the factors that govern corrosiveness of a soil are:

1. porosity (aeration)

2. electrical conductivity

3. dissolved salts, including depolarizers or inhibitors

4. moisture

5. acidity or alkalinity (pH)

Romanoff (1957) showed that the rate of corrosion is at its peak in the first few years after burial and then the rate of corrosion decreases (oxygen starvation). Darbin et al. (1978)

showed that even in the most aggressive environment, the galvanized steel strips in use with RSRWs today would last 120 years.

According to McKittrick (1978), the procedure to permit the selection of the cross section and coating weight of the galvanized steel reinforcements to insure a minimum service life is:

1. Calculate the anticipated weight loss, based on laboratory or field measured values of resistivity and pH at saturated conditions.

2. Select the suitable site dependent characteristics for precise calculation according to the Romanoff formula:

$$X = KT^n \qquad (2.10)$$

where X = average loss of thickness with time

K = a site characteristic

T = time in years

n = site dependent and is always less than 1

3. Compare answers found in Step 2 with the upper limits inferred by a broad interpretation of the Romanoff data.

4. Proportion the strip dimensions such that the stresses in the equivalent cross section at the end of the anticipated service life will be less than or equal to the yield stress.

5. Apply whatever factor of safety to the calculation that is required by the site and project characteristics.

5. Lateral Deformations and Failures of Reinforced Earth Retaining Walls. Al-Hussaini and Perry (1978) tested a 12 ft high x 16 ft long x 10 ft wide reinforced soil retaining wall to failure. The select backfill material used was sand classified as SP in the Unified Soil Classification System with density, γ, ranging from 98.2 to 117 pcf and an angle of internal friction $\phi = 36°$. The outward movement of the wall during construction was very small; however, the lateral deformation during surcharge loading was significant. Prior to failure, an audible sound of distress occurred and significant bulging in the skin element located at the first and second rows of the reinforcing strips from the bottom was observed. No movement between the interface of the reinforced earth volume and the in situ soil was reported, however.

Baquelin (1978) reported on the performance of 13 instrumented reinforced earth walls constructed in France between the years 1968-1976. These walls ranged in height from

5 m to 22 m (16 - 72 ft) and had lengths of reinforcing strips in the range of 7 - 40 m (23-131 ft). Some of these walls were instrumented with pressure and strain gages. Some of the wall settled en masse by 6 - 35 cm (2.4 - 13.8 in.) without any structural failure. (This supports the coherent gravity structure theory.) No lateral displacement of the walls or rotation of the facing elements about its base was observed. Baquelin notes that the pavement sections supported by the reinforced earth did not show any signs of distress. He also notes that if a reinforced soil structure is designed adequately, it would sufficiently support a pavement.

Goughnour and DiMaggio (1978) conducted a study of reinforced soil construction highway embankments in the U.S. Although many types of damage were reported, no instances of longitudinal cracking in the pavements were cited. The authors concluded that pavement structures constructed over reinforced earth structures performed adequately.

Juran et al. (1978) conducted a study on a fully instrumented bridge abutment in France. The test section was well instrumented and observations and measurements were taken frequently. The authors did not report any rotation of the facing element about its base. They did, however, note that the apparent failure plane was similar to the plane derived from the coherent gravity structure hypothesis.

Walkinshaw (1975) reports on eight reinforced soil structures built in locations spread throughout the continental U.S. Of these eight reinforced earth structures only one structure is similar to the embankments showing distress in SDHPT District 16. Walkinshaw's report contained no references to any of the eight reinforced earth structures exhibiting any type of pavement distress.

Naresh et al. (1988) built and instrumented a 4.5 m (14.8 ft) high reinforced soil retaining wall. The authors mentioned that after construction the wall had a lateral deflection of 23 mm (0.91 in.) at a height of 2.25 m (6.8 ft) which increased with height, peaking at a lateral deflection of 11 mm (0.43 in.). The maximum lateral deflection of 11 mm is equivalent to 0.23 percent of the wall height. With a 104.62 ton load, the maximum deflection was 15 mm (0.59 in. and 0.5 percent of wall height). They stated, however, that the lateral displacement was due to not providing temporary supports to maintain a vertical alignment. The Reinforced Earth Company recommends building the facing element with a slight tilt inward, so that after completion of compaction, the facing elements would maintain a vertical alignment (Schick, 1988).

Cheng and Shi (1988) conducted a model test of a reinforced soil retaining wall. The select granular backfill material had an angle of friction of 38 degrees and a density, γ, of 15 tons/meter^3. The maximum lateral displacement was 1.28 mm (0.05 in.), which was

equivalent to 0.16 percent of the wall height, but reduced to 0.5 mm (0.02 in.) and 0.06 percent of the wall height when the number of reinforcing strips was increased. The failure surface coincided with the failure plane associated with the coherent gravity structure theory.

C. DIFFERENTIAL SETTLEMENT OF THE EMBANKMENT AND SELECT BACKFILL

Consolidation theory is applicable to saturated cohesive (clay) soils. However, compacted embankments virtually never reach saturation and typically are satisfactorily completed with a degree of saturation of less than 90 percent. The division between "saturated" soils and "unsaturated" soils is not well defined and, practically, will vary with the type of cohesive soil, its clay content, and mineralogical composition. A soil that has a degree of saturation in the mid- to upper-90 percent is obviously not completely saturated. However, with an application of load, this soil most likely will undergo immediate compression of its soil structure with an associated reduction of pore spaces containing only air (and if the loading is sufficiently great, some air can be driven into solution in accordance with Boyle's Law) and the soil will subsequently behave as a saturated soil with further compression or settlement being governed by saturated consolidation theory. Thus, the two principal types of settlement--consolidation and immediate--may be applicable to the problem being studied.

1. Consolidation Settlement. The clay embankments constructed by District 16 were comprised of a high plasticity index (PI) material (described in detail in Chapter 3). The high PI soil indicates that it is a soil with a relatively high percentage of clay particles, the principal clay mineral is likely a smectite, and the soil has relatively high shrink/swell potential. Experience has shown that if such a soil must be used in highway or airfield construction, the soil should be compacted a few percentage points wet of the optimum moisture content found in the designated laboratory moisture-density relation test (AASHTO Test T99-86 or T180-86) rather than at the optimum moisture content. Experience has shown that it is better to accept the slightly lower compacted densities achieved at the higher compaction moisture content than to risk the greater pavement damage likely to occur when a drier compacted soil becomes wetter and heaves. Consequently, the construction specifications regarding compacting the soil embankments used by District 16 called for compaction to occur at or "wet of optimum" moisture content.

Laboratory tests performed using soil from the same borrow pit as used in construction of the District 16 embankments showed that the degree of saturation achieved by compacting the soil wet of optimum still did not approach saturation conditions to an extent that overburden pressures would compress the embankment soil to the point where it would act as a saturated

soil with respect to settlement. Thus, consolidation settlement theory was not considered to be applicable to the problem being studied.

2. Immediate Settlement. Immediate settlement occurs "immediately", i.e., within a few hours or a few days after a load is applied to the soil. The load, in the case of an embankment, is the overburden pressure. Immediate settlement analyses are appropriate for all fine grained soils (silts and clays) with a degree of saturation less than about 90 percent. All soils with a large coefficient of permeability (rapid draining under a hydraulic gradient), including all cohesionless soils, undergo immediate settlement (Bowles, 1982). This method of analysis would be applicable to estimating settlement in the free-draining granular select backfill material.

Laboratory tests conducted at Texas Tech University on the select cohesionless backfill material indicates that the material classifies as a fine sand. Therefore, immediate settlement analysis is appropriate. The immediate settlement analysis is based on the theory of elasticity. The settlement can be computed from equations derived from the theory of elasticity (Timoshenko and Goodier, 1970). However it would be necessary to first determine the applied load, since it is this applied load which would cause the deformation leading to soil settlement.

In the particular case of the select backfill material, the load is due to its overburden pressure and, subsequently after the completion of the flexible pavement, to the vehicular load. After the increased load has been determined, it becomes necessary to determine the stress distribution throughout the soil profile. Several methods are currently used to estimate the increased pressure on an element of soil at some depth in the soil strata. According to Bowles (1982) these methods include those of Boussinesq, Westergaard and Newmark.

These methods can be found in most foundation design textbooks. Knowing the increase in stress, the settlement can be estimated from the Steinbrenner equation:

$$\Delta H = qB\frac{1-\mu^2}{E_s} I_w \qquad (2.11)$$

where ΔH = settlement

q = intensity of contact pressure, in units of E_s

B = least lateral dimension of area under consideration, in units of ΔH

I_w = influence factor which depends on shape of area and its rigidity

μ = Poisson's ratio

E_s = modulus of elasticity of soil

The two problems in evaluating Eq. (2.11) are:

1. Obtaining the depth of influence, L

2. Determining the stress-strain modulus, E_s

These are formidable problems, since the depth of influence will depend on the soil properties, in particular density, stratification, and Poisson's ratio for each underlying stratum. The modulus of elasticity also depends on density, stress history, and stratification. Considerable evidence (Gibson, 1967) indicates E_s varies with depth. Thus, load stresses decrease at the same time that E_s increases with depth. This means that most settlement will occur in the upper zone.

There are several methods available for estimating the modulus of elasticity, E_s:

1. Laboratory Tests
    a. Unconfined Compression Test
    b. Triaxial Compression Test
2. In Situ Tests
    a. Standard Penetration Test (SPT)
    b. Cone Penetration Test (CPT)
    c. Pressure Meter Test
    d. Plate Loading Test

Researchers such as D'Appolonia et al. (1968), Schmertmann (1970), Vesic (1970), and Mitchell and Gardner (1975) give recommendations for computing the modulus of elasticity. Schmertmann (1970) proposed that the change in the Boussinesq pressure bulb could be interpreted as being related to the strain. Since the shape of the pressure bulb changes more rapidly from about 0.4B to 0.6B, where B is the minimum dimension of the load application, this depth is interpreted to have the largest strains. Schmertmann then proposed using a triangular relative strain diagram to model this strain distribution with ordinates of 0, 0.6, and 0 at 0B, 0.5B, and 2B, respectively. The area of the diagram is related to the settlement; and for constant E_s, which is the same assumption used to develop the strain profile, the settlement may be computed directly as the product of the area of the triangle and strain to obtain:

$$\Delta H = 0.6B \frac{\Delta q}{E_s} = 0.6B\epsilon \qquad (2.12)$$

where ϵ is the strain.

This equation does not greatly differ from Eq. (2.11). Schmertmann also proposed a correction factor for time:

$$C = 1 = 0.2 \log \frac{t}{0.1} \quad (2.13)$$

where t = time of interest > 0.1 year (in years).

With the correction factors, Eq. (2.12) becomes

$$\Delta H = C(0.6)B\varepsilon \quad (2.14)$$

If E_s is not constant, a method of plotting the strain profile and obtaining average influence factors, I_z, at the center of each change in E_s over a depth increment ΔZ can be used:

$$\Delta H = C\,\Delta q \sum \frac{I_z \Delta Z}{E_s} \quad (2.15)$$

Equation (2.15) obviously gives a conservative value for ΔH if E_s is a constant or increases with depth. If the lower layers have a much smaller E_s, the solution would yield a ΔH value that is underpredicted (Bowles, 1982). With the correction factor and $E_s = 2.5$ to $3.5q_c$, where q_c is the resistance of the soil to penetration by the CPT, Schmertmann obtained rather good correlation with selected settlement data. The strain profile can be obtained from triaxial tests using a procedure suggested by Lambe (1964). There are disadvantages, such as duplicating the original soil condition (stress history, cementation, density, etc.,) but, if overcome, the deviator stress from one or more tests used to profile the soil strata may be plotted and the secant (or tangent) modulus used at the corresponding deviator stress levels produced by the load to estimate strain.

D. SHRINKAGE OF HIGH-PI EMBANKMENT

1. General. Jones and Holtz reported in 1973 that the estimated damage due to expansive soil activity to streets and highways was $1.14 billion of the total estimated damage to structures and facilities of $2.225 billion. Krohn and Slosson reported total damages to pavements resulting from expansive soils had probably increased to $2.0 billion by 1980. Since expansive clays have demonstrated a capacity to cause tremendous property losses due to their shrink and swell nature, it becomes necessary to look at the mechanisms that cause this behavior.

2. The Mineralogical Composition of Clay. Clays are defined as particles having a diameter equal to or less than two microns (0.002 mm). However, it is the mineralogical composition which is more important, not the particle size, in identifying soil with high volume change potential. Due to the nature of the mineralogical composition of clay particles, they develop a net negative surface electrical charge. This surface charge causes the electrical forces

of the surface to be greater than the gravitational forces. These particles are then in the colloidal state.

The three most common groups of clay minerals encountered in civil engineering are:

1. Kaolinite
2. Illite
3. Smectites (Montmorillonite belongs to this group)

These are crystalline hydrous alumina silicates. Smectitic clays are those most commonly exhibiting extremely high shrinking and swelling when their soil moisture content changes. The other clays and silts exhibit lesser volumetric change with a change in soil moisture content. Sands do not exhibit shrinking and swelling and the pressures associated with that behavior.

Smectitic clays swell upon the adsorption of water and shrink with moisture loss. The principal factors affecting swell/shrink are (Gromko, 1974; Holtz and Gibbs, 1954):

1. Crystal lattice structure
2. The structure of the clay mass
3. Cation exchange capacity of the minerals
4. Kind and amount of clay minerals present
5. Electrolyte content of the aqueous phase

Clays have the capability to attract and retain free cations and, to a much lesser extent, anions These ions are exchangeable and are retained on the periphery of the clay particle. Depending on the valence and concentration levels, other ions can displace the held ions. This capability is called cation exchange.

There are two molecular structures which are the basic building blocks of the lattice structure of clays. These are the silica tetrahedron and the alumina octahedron. The silica tetrahedron consists of a silicon atom surrounded tetrahedrally by four oxygen ions. The alumina octahedron consists of an aluminum atom surrounded octahedrally by six oxygen ions. When each oxygen atom is shared by two tetrahedra, a plate shaped layer is formed. Similarly, when each aluminum atom is shared by two octahedral, a sheet is formed. The silica sheets and aluminum sheets combine to form the basic structural units of the clay particle. Various clay minerals differ in the stacking configuration (Mitchell, 1976).

Kaolinite is a typical two layer mineral having a single tetrahedral sheet joined by a single octahedral sheet to form a 2 to 1 lattice structure. Montmorillonite is a three layer mineral having a single octahedral sheet sandwiched between two tetrahedral sheets to give a 2 to 1 lattice structure. Illite has a similar structure to that of montmorillonite, but some of the

silicate atoms are replaced by aluminum, and potassium ions are present between the tetrahedral sheet and the adjacent crystals (Dixon and Weed, 1977).

The potassium ion between the illite tetrahedral sheets prevents other cations from attempting to enter between the molecules. Since montmorillonite particles are joined by weak oxygen bonds and not strongly held together by a cation such as potassium, dipolar water molecules penetrate between the molecules readily and become electrically attached to the negatively charged surface of the montmorillonite particle. This causes the particle to effectively increase in volume, thus bringing about the swelling phenomenon.

Yong and Warkentin (1966) reported that soils containing montmorillonite show an almost reversible swelling and shrinkage on rewetting and redrying. Uzan et al. (1973) measured swelling forces and shrinkage forces of remolded heavy clay and concluded that the swelling force and shrinkage force are similar when compared on the basis of similar conditions. Chen and Lu (1984) state that the same factors that affect swelling also control the mechanics of shrinkage, but to different degrees.

Thus, it is accepted that swelling and shrinkage are the result of the same mechanism. The same mechanism that causes swelling will initiate shrinkage when there is a loss of soil moisture. It is, therefore, logical to investigate next the forces that permit moisture movement through the clay mass which creates the conditions of swelling and shrinkage.

3. Soil Suction Theory. An increase in the water content of a high PI soil will cause that soil to swell while a reduction in the moisture content will bring about a decrease in volume. For expansive soils to expand or swell, three conditions must be satisfied (Snethen et al., 1977):

1. An available source/sink of water
2. A mechanism or group of mechanisms which actually cause volume change in expansive soils
3. A driving force adequate to move the adsorbed water

The first of these conditions simply says that for soil moisture conditions to change, there must be an adjacent soil moisture condition that differs from that at the location under consideration; i.e., the adjacent location must have a soil moisture condition that is either drier or wetter. The second condition has been addressed to some extent in the previous section and will be discussed further, below. Thus, it is appropriate to now address the mechanism by which a driving force can cause soil water to move from one location to another.

(a) Forces Causing Water Movement in Unsaturated Soils. The concept of soil water potential was first conceptualized and reported by Buckingham (1907) in his now classical paper on the nature of capillary potential, which is yet pertinent in today's context. Gardner (1920) further developed Buckingham's ideas by demonstrating the relationship between the soil water potential and the soil moisture content. In his paper, he expounded that soil water, like other bodies in nature, can contain energy in different quantities and forms. Two of the classical forms of energy are kinetic and potential energy.

Kinetic energy is proportional to the velocity of the matter squared, which could be considered negligible since water movement in clay soil is slow (typically in the range of 10^{-6} - 10^{-8} cm/sec). Potential energy, which is due to its position or internal condition, is important in determining the state and movement of water in the soil. Hillel (1982) states:

> The spontaneous and universal tendency of all matter in nature is to come to that elusive state of equilibrium, where all particles surrounding the particle in question have the same energy as the particle. Differences in potential energy of the water cause the water to flow in the soil. Water will always move from an area of high potential to an area of low potential. The rate of decrease of potential energy with distance is in fact the moving force behind causing the flow. A knowledge of the relative potential energy state of the soil water at each point within the soil can allow us to evaluate the forces acting on soil water in all directions and to determine how far the water in the soil is from equilibrium.

An energy increment can be viewed as the product of a force and a distance increment, so the ratio of a potential energy increment to a distance increment can be viewed as constituting a force. Therefore, a force acting on soil water directed from a zone of higher potential to a zone of lower potential is represented by the negative potential gradient $\left(-\frac{d\phi}{dx}\right)$ which is the change of potential energy, ϕ, over a distance, x. The negative sign shows that the force acts in the direction of decreasing potential.

When the soil is saturated and its water is at a hydrostatic pressure greater than that of the atmospheric pressure (such as under a water table), the potential energy level of that water will be greater than that of free water and the soil water will move from the soil into an area of a lower potential. If, on the other hand, the soil is moist but unsaturated, its water will no longer be free to move towards a reservoir at atmospheric pressure. On the contrary, the spontaneous tendency will be for the soil to draw water from such a reservoir if placed in contact with it, much as a blotter draws ink.

Under hydrostatic pressure greater than atmospheric, the potential of soil water is greater than that of free water and is considered positive. In unsaturated soils, the water is restricted from freely moving by capillary and adsorptive forces. Hence, its energy is considered negative, since its equivalent hydrostatic pressure is less than that of free water, which is the reference state.

Energy potential can be regarded in thermodynamic terms as the difference in partial specific free energy between soil water and a reference water condition. A soil physics terminology committee of the International Soil Science Society (Aslyng, 1963) defined the *total potential of soil water* as "the amount of work that must be done per unit quantity of pure water, in order to transport reversibly and isothermally an infinitesimal quantity of water from a pool of pure water at a specific evaluation at atmospheric pressure to the soil water (at the point under consideration)."

Total potential is defined as the sum of at least five component potentials:

$$\phi_t = \phi_m + \phi_p + \phi_o + \phi_g + \phi_\Omega \qquad (2.16)$$

where ϕ_t = total potential

ϕ_m = matric potential

ϕ_p = pneumatic potential

ϕ_o = osmotic potential

ϕ_g = gravitational potential

ϕ_Ω = overburden pressure (Lytton, 1969)

(1) Gravitational Potential. Every body on the earth's surface is attracted towards the earth's center by a gravitational force equal to the weight of the body, that weight being the product of the mass of the body and gravitational acceleration. To raise a body against this attraction, work must be expended, and this work is stored by the raised body in the form of "gravitational potential energy." This amount of energy depends on the body's position in the gravitational force field. The gravitational potential of soil water at each point is determined by the elevation of the point relative to some arbitrary reference level.

$$\phi_g = z\rho_w g \qquad (2.17)$$

where ϕ_g = gravitational potential in terms of potential energy per unit volume

z = elevation above a reference level

ρ_w = density of water at that temperature

g = acceleration of gravity

The gravitational potential is independent of the chemical and pressure conditions of soil water and dependent only on the relevant elevation (Hillel, 1982).

(2) Matric Potential ϕ_m. When soil water is at a pressure lower than atmospheric, the matric potential is considered negative. Matric potential is due to two physical phenomena:

1. Capillarity, which depends on pore size
2. Attractive forces, due to the negative surface electrical charge of the clay particle, attracting dipole soil water

Capillarity: Capillarity arises due to the surface tension forces generated between the water molecules and soil solids. The magnitude of the force depends on the pore size and radius of meniscus curvature (Richards, 1967; Hillel, 1982). This force could be conceptualized by the rise of water within a very narrow tube when one end of the tube is in a reservoir of water freely interfacing with the atmosphere.

Attractive forces: The attractive force is mainly due to the negatively charged surface of the smectitic clay (Evans, 1965). In an effort to become electrically neutral, the clay particles attract water molecules which are dipolar. The water molecules flock around the clay particle forming a hydration cloud (Snethen et al., 1977; Hillel, 1982). The attractive forces are composed of at least the following:

1. Van der Waal forces
2. London forces
3. Hydrogen bonding
4. Clay particle attraction
5. Cation hydration

Van der Waal forces, London forces, and hydrogen bonding are weak attractive electrical forces which form on clay mineral surfaces. The surfaces of two or more adjacent clay minerals are bonded by these forces. An example of this kind of bonding is where thin sheets can be shaved from course grained micas. These forces occur in all materials, but due to the small particle size (low weight) and large surface areas of the clay minerals, these forces become magnified and play a larger role. According to Ingles (1962, 1968), and Low (1968), van der Waal forces, London forces, and hydrogen bonding act in both wet and dry conditions (saturated and unsaturated), and control the sorption of water. After sorption begins, these forces play a diminutive role in bonding the water molecules to the clay surfaces. Van der Waal forces include the types of weak attractive forces described below (Snethen et al., 1977):

Dipole-Dipole Attraction: These forces develop between polar molecules having permanent moments and are at least partly responsible for the orientation of water molecules and their bonding to the clay mineral surface.

Induction Effects: These forces are similar to dipole-dipole attraction and occur between polar molecules. However, the induction effects occur between unoriented molecules by the interaction between one dipole and the polarized electrons of another dipole.

London Forces: These forces, which are also termed "dispersive" forces, occur in all molecules or extremely small particles including non-polar (zero dipole moment) varieties. The forces originate from the development of an instantaneous, non-permanent dipole moment between two particles as they come into close proximity to each other, under conditions where the water is attracted to the clay mineral. The force of the van der Waal force is rapidly overcome by the development of the double layer water. In addition, this phenomenon is hard to measure and interpret physically, and in cases where it can be evaluated, provides little or no practical information for the engineer. Therefore, this phenomenon is often neglected (Snethen et al., 1977).

Elastic release could be considered a special type of volume change rather than a cause of it, since it is particle reorientation resulting from swelling or unloading (Snethen et al., 1977). Snethen et al. also mentioned that factors such as divalent bonding and cementation significantly influence elastic release, generally on the reduction side of volume change. However, elastic release will influence capillary imbibition, which is one of the modes of moisture transfer. Particle reorientation will generally result in increased pore sizes.

Clay particle attraction (surface attraction) relationships exist between clay minerals, between clay minerals and water, and between clay minerals and cations as a result of the shape and internal crystallographic structure of the clay minerals. Clay minerals occur as tiny platelets having two types of exposed surfaces - edges and faces. The edges exhibit a smaller surface area and possess both positive and negative charges which are primarily due to broken bonds. The faces are flat and consist of the major part of the particle's surface area, and possess an electron-rich surface and negative charge, due to the presence of oxygen atoms in the tetrahedral layer. The forces are largely due to the small size of the smectites. In montmorillonite, the substitution of divalent magnesium, or the monovalent sodium for trivalent aluminum (isomorphous substitution) results in a net negative charge. This negative charge has to be electrically neutralized by either cations, hydrated cations, or dipolar water molecules (Snethen et al., 1977; Ingles, 1968). Ladd (1960) reports that when a clay particle is immersed in pure water, exchangeable cations are attracted to it by the net negative

charge of the clay particle and will form a "cloud" around it. This system, which is termed the "clay micelle," is electrically neutral. The ions and water within the clay micelle form the well known "double layer." If two such systems are close to each other or if they overlap, they are termed the "diffuse double layer." Ladd further states that if the particles were immersed in a salt solution instead of pure water, then anions would be present in the double layer, but the number of cations would be increased accordingly in order that the micelle would remain electrically neutral. Thus, the double layer includes that portion of the water surrounding the particle in which there is a negative electric field requiring an excess of positive charges relative to negative charges.

Cation hydration is a mechanism by which the water molecules around a cation flow with or are attracted along with the cation towards the negatively charged clay particles. Snethen et al. (1977) report that the influence of cation hydration involves both attractive forces for water molecules and a physical increase in size (ionic radii) following hydration. They state that there is no purely clay-water or clay-cation system but rather a clay-water-cation combination.

(3) Osmotic Potential. The presence of solutes in soil water affects its thermodynamic properties and lowers its potential energy. Solutes lower the vapor pressure of soil water. This phenomenon may not affect liquid flow significantly, but it does become important whenever a membrane or diffusion barrier is present which transmits water more readily than salts.

Fig. 2.4 is a schematic representation of a pure solvent (pure water) separated from a solution by a semipermeable membrane. Solute particles will not pass through the membrane, but solvent will pass through with the result being an increase in the solution level in the tube on the left until the hydrostatic pressure of the column of dilute solution is sufficient to counter the diffusion pressure of the solvent molecules drawn into the solution through the membrane. The hydrostatic pressure at equilibrium, i.e., when solvent molecules are crossing the membrane in both directions at equal rates, is the osmotic pressure of the solution. The pressure which would balance the levels of water in both the left and right columns is equal to the osmotic pressure of the solution. The pressure that must be applied to the solution in order to prevent the flow of water into the solution through the semipermeable membrane is called the "osmotic pressure potential."

Ladd (1960) and Snethen et al. (1977) report that electrostatic attractive forces for water molecules and ions are at their maximum value at the clay mineral surface, and decrease with distance from the surface. When the soil-water-cation combination is exposed to a pore

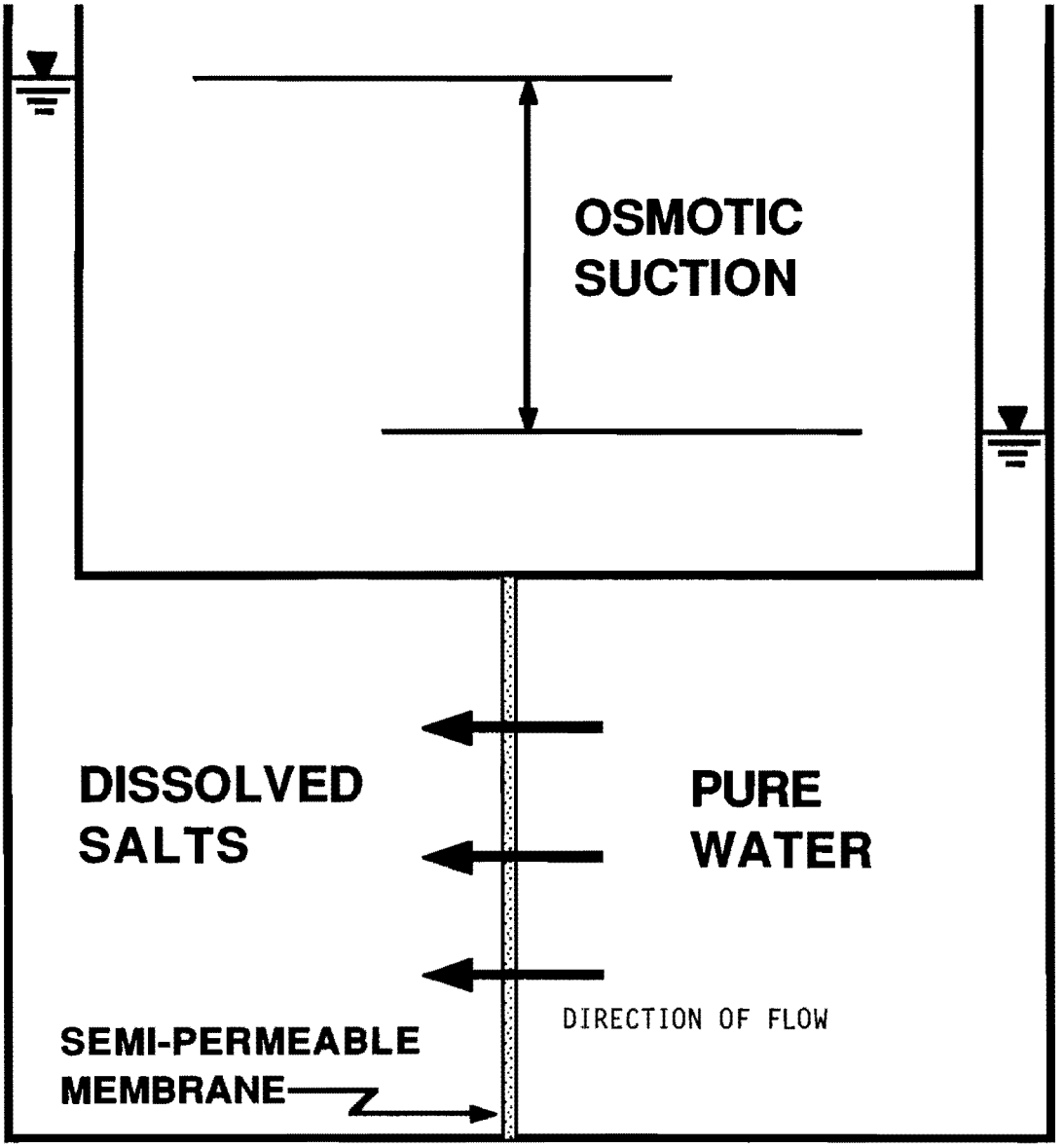

Fig. 2.4. Schematic representation of osmotic suction pressure.

fluid having a different (lesser) ion concentration, the double layer water acts as a semipermeable membrane allowing water to enter in order to bring the differing ion concentrations into balance. This is denoted as osmotic attraction. The result of the osmotic attraction is an increase of double layer water. The subsequent result of the increase in double layer water will be an increase in the volume (swelling) of the soil mass. The precise influence of osmotic repulsion on volume change is not well understood. However, it is accepted that the mechanism has its greatest influence at higher moisture contents (greater the optimum moisture content for compaction).

(4) Pneumatic Potential ϕ_p. Usually, the gas or pneumatic pressure within an unsaturated soil is at atmospheric pressure. If the air void is not completely sealed when pressure is applied, then the excess air pressure will dissipate quickly and come back to its equilibrium state. So for all practical purposes pneumatic potential is equal to atmospheric pressure and is typically neglected in practical applications (Wray, 1984).

(5) Overburden Potential ϕ_Ω. This potential is due to pressure of all the soil (overburden) and structures (permanent surcharge) above the soil at the point of consideration (Richards, 1967; Lytton, 1969).

Clay particle attraction, ion hydration and osmotic repulsion are interdependent and are mutually varying functions of each other. For example, the sorption process cannot begin without clay particle attraction. Ion hydration cannot be significant without clay particle attraction, and osmotic repulsion cannot influence volume change without the particle attraction for water and cations and the variations of cations within close proximity to the clay mineral (Snethen et al., 1977).

Wray (1984) describes soil suction in layman's terms as a measure of a soil's affinity for water. That is, the greater the soil suction, the greater the soil's attraction for water, or the drier the soil, the greater is its attraction for water. The soil will, therefore, crave moisture with a greater force.

Water potential has units of pressure. Potential is also often expressed in units of length as in a column of water of a certain height; this unit is convenient because a column of water 1,000 cm high, for example, exerts a pressure of 1,000 g_f/cm^2 at the bottom of the water column (at 3.9°C). Since partly saturated clays possess water potentials equal to an equivalent height of several thousands of cm of water (and often tens of thousands and sometimes hundreds of thousands of cm of water), and since the elevation or position potential is typically measured with respect to a groundwater table that often is but 10-30 ft (300-900 cm) below

the surface, the elevation potential is often neglected without serious practical error. Additionally, if the pneumatic potential is in reality atmospheric (which it typically is in partly saturated clay soils), then this potential is essentially zero and can also be neglected from the total potential equation. The overburden potential is often also neglected by using the same argument as that for elevation potential. (In swelling considerations, the position potential and the overburden potential often have a canceling effect.) Thus, when the gravitational, pneumatical, and overburden potential terms are neglected in the total potential equation, the result is termed *total soil suction.* The remaining terms from the total potential equation (Eq. 2.16) which now comprise the total suction equation are termed *matrix suction* and *osmotic suction.* In equation form, total suction is stated as:

$$h = -(\phi_m + \phi_o) \qquad (2.18a)$$

or $$h = h_m + h_o \qquad (2.18b)$$

where h = total suction

h_m = matrix suction

h_o = osmotic suction

When the pneumatic overburden and gravitational potentials are neglected, the total suction is still a negative value with respect to the reference pool of pure water. The negative sign in Eq. 2.18a is included to report soil suction as a positive value.

Soil suction, according to Olson and Langfelder (1965), Statement of Review Panel (1960), and Johnson (1973), is a quantity that can be used to characterize the effect of moisture on the volume and strength properties of soils; that is, soil suction quantitatively describes the interaction between the soil particles and water, which determines the physical behavior of the soil mass. Total soil suction is the force which is responsible for soil water retention. Suction is a pressure term which is a measure of the pulling force (tension) exerted on the water. Tension is also a term used to indicate the force of the soil water retention and can be used interchangeably with suction; however, soil suction (or simply suction) is the preferred term.

Expansive soils can have very high soil suction values when partially saturated. Kassif et al. (1969) and Goode (1982) report that oven dry specimens have attained suction values of 10^5 and 10^6 cm of water. An easier way of expressing suction magnitude is by the use of the term "pF" (Schofield, 1935). Here pF is represented as:

pF = Log_{10} (suction expressed as a height of water column measured in centimeters)

(b) Swell/Shrink Prediction Methods.. According to Baker et al. (1973), there are two approaches currently being used for the description of the effects of water in soil: mechanistic and energy.

(1) Mechanistic Approach. The mechanistic approach is based on the measurements of negative pore pressures in specimens using different apparatuses, such as the pressure plate apparatus, special consolidometers, etc. Johnson (1973) writes in great detail about this approach and the equipment used. In general, positive pressure is applied on the soil specimen through membranes with pores sufficiently small enough to prevent cavitation. When the pressure, applied on the soil specimen, is at its bubbling pressure (the pressure that causes the soil to release its adsorbed water molecules) a small bead of moisture will appear in an outlet tube. This pressure is then taken as the suction of the soil. In the consolidometer, a dry soil specimen is permitted to imbibe water and the volume change of the specimen is measured as a change in height (heave) since the consolidometer does not permit expansion in the lateral directions. Alternatively, the soil specimen is not permitted to swell and the pressure necessary to prevent swelling is measured. This pressure is termed swelling pressure. Unfortunately, it is not mechanistically possible to measure the shrinking pressure.

Snethen et al. (1977) state that the evaluation of soil suction by the mechanistic approach has conceptual and measurement problems. Olson and Langfelder (1965) report that "the force fields of clay minerals, which are responsible for the microscale mechanisms that cause swell, very likely cause the actual pore pressure to be positive near the surfaces of the clay mineral particles." The mechanistic approach evaluates an equivalent negative pore water pressure or soil suction that is needed to pull the pore water out of the soil. When the equivalent pore pressure measurement is performed on the soil specimen, the water content of the soil is changed, due to the methodology, whereby water is forced out of or into the specimen. Johnson (1973) states that the equivalent pore pressure neglects much of the contribution to soil suction from the concentration of ions in the pore fluid if the ions are able to pass through the membrane of the apparatus. The ions will pass through membranes made of porous stones or ceramic plates. Hysteresis is also observed in the soil suction-water content relationships determined for a single specimen with the pressure membrane device. Here the equilibrium soil wetness (water content) at a given suction is greater in desorption (drying) than in sorption (wetting) (Haines, 1930; Miller and Miller, 1955; Philip, 1964; Topp and Miller, 1966; Bomba, 1968; Topp, 1969). Desorption depends on the narrow radii of the connecting channels, whereas sorption depends on the size of the maximum pore diameter (Hillel, 1982).

Johnson (1973) states that soil suction determination by the mechanistic approach needs to be corrected with various calibration factors.

(2) Energy Approach. The evaluation of soil suction using the energy approach is based on the principles of thermodynamics. The soil suction is evaluated by measuring the relative humidity of soils, typically determined with thermocouple psychrometers. The two approaches can lead to similar magnitudes on similar specimens (Johnson, 1973). Snethen et al. (1977) state:

> The most fundamental expression of the state of water in soil is the relative free energy of soil water. The force that causes available water to move into the soil is expressed qualitatively in terms of the free energy of the soil water relative to the available water outside of the soil.

The Statement of the Review Panel (1960) that the free energy needed to move free pure water into the pores of soil containing the soil water is as follows:

$$\Delta f = RT \, Log_e \frac{p}{p_o} \tag{2.19}$$

where Δf = free energy

R = ideal gas constant, 82.06 $cm^3 atm/^oK$

T = absolute temperature, ^oK

p = vapor pressure of the pore water in the soil, atm

p_o = vapor pressure of free pure water, atm

$\frac{p}{p_o}$ = relative humidity

The change in pure energy due to movement of the free pure water into the pore water is usually given in terms of an equivalent total soil suction.

$$h = \frac{1.058RT}{V} Log_e \frac{p}{p_o} \tag{2.20}$$

where h = total soil suction, tsf

V = volume of a mole of liquid water, 18.02 cm^3/mole

Osmotic suction

$$h_s = \frac{1.058RT}{V} Log_e \frac{p_s}{p_o} \tag{2.21}$$

where h_s = osmotic soil suction

p_s = vapor pressure of the free pore water solution, atm

Osmotic suction increases as water evaporates due to the increase in concentration. A change of confining pressure, however, does not change the osmotic suction.

The matrix suction (due to capillarity, clay particle attraction, and cation hydration) is expressed as:

$$h_m = \frac{1.058RT}{V} \text{Log}_e \frac{p}{p_o} \qquad (2.22)$$

If the pore water has no solute which can cause osmotic suction, total suction and matrix suction are equivalent. The following instruments can be used to measure total suction, matrix suction, or osmotic suction:

1. Thermocouple psychrometer
2. Resistance blocks
3. Tensiometers
4. Heat dissipation blocks
5. Calibrated filter paper

Chapter 3 examines these instruments in detail.

(c) Prediction Methods of Heave. A number of methods to predict the total amount of shrink or heave have been proposed over the years. Some methods are based on the mechanistic approach while others are based on the energy approach. McKeen (1981) and Austin (1987) have evaluated many of these methods. One method will be presented in some detail since it has been shown to provide reasonable estimates of shrink or heave over an extended period (Wray, 1989): the Gardner-Lytton-McKeen method.

The Gardner-Lytton-McKeen method was devised by Lytton in a series of papers (Lytton, 1969; Lytton and Nachlinger, 1969; Lytton and Kher, 1970). This method was based on earlier moisture flow findings by Gardner (1958) and is an energy approach method since the method is predicated on changes in soil suction. McKeen (1977) improved Lytton's model by providing a refined method for evaluating Lytton's coefficient of suction change compressibility.

Lytton's basic equation for predicting shrink or heave, ΔH, over some depth, H, is

$$\Delta H = H\gamma_h (h_f - h_i) \qquad (2.23)$$

where γ_h = coefficient of suction change compressibility

h_f = final suction value, in pF

h_i = initial suction value, in pF

From Gardner's work (1958), Lytton proposed that for static (steady flux) conditions, the change in soil conductivity (permeability) due to a change in soil suction could be estimated

$$\text{from} \quad k_l = \frac{k_o}{1 + a\,|h_l|^n} \tag{2.24}$$

where k_o = saturated permeability of the soil

k_l = new permeability at location or position l

h_l = soil suction at location or position i

a = a soil property constant = 1×10^{-9}

n = a soil property determined from testing or from trial–and–error back–solution, with a value between 1 and 3 (Lytton, 1977; Wray, 1989)

The change in soil suction in the vertical direction, Δh_l, as a result of the change in soil conductivity estimated from Eq. (2.24) can be estimated from

$$\Delta h_l = \Delta x_3 + \Delta x_3 \frac{v_3}{k_l} \tag{2.25}$$

where v_3 = velocity of vertical moisture flow in the soil

Δh_l = change in soil suction

Δx_3 = change in gravitational potential

The suction at the new position h_{l+1} can be estimated from

$$h_{l+1} = \Delta h_l + h_l \tag{2.26}$$

The new soil permeability obtained from Eq. (2.24) is substituted into Eq. (2.25) to determine the change in soil suction. The change in suction calculated from Eq. (2.25) is substituted into Eq. (2.26) to obtain the suction at position i+1. If the initial suction condition is known, i.e., the soil suction before a change in soil moisture content, then the heave or shrink can be estimated from Eq. (2.23).

McKeen provided equations relating the amount of clay present in the soil and the predominant type of clay mineral to calculate the coefficient of suction compressibility (a rate of strain coefficient):

Kaolinite: $g_h = 0.00018$ (% of Clay) - 0.000098 (2.27)

Illite: $g_h = 0.00047$ (% of Clay) - 0.00351 (2.28)

Smectite $g_h = 0.00056$ (% of Clay) - 0.00433 (2.29)

Wray (1987, 1989) showed that if climate is the only factor affecting the shrink or swell of a soil (static conditions), then using the Gardner-Lytton-McKeen method, wet and dry moisture condition boundaries with depth can be predicted which will describe the maximum amount of shrink or swell that could be expected at a particular site if soil suction conditions are known at any given time.

However, Eqs. (2.23) - (2.26) are applicable to predicting *vertical* shrink or heave. It is likely that *horizontal* shrinkage is involved in the problem being studied herein. Thus, an equation to predict lateral heave or shrink is required.

If Eq. (2.23) is written in more general form:

$$\frac{\Delta V}{V} = -\gamma_h \log_{10}\left(\frac{h_f}{h_i}\right) + \gamma_\sigma \log_{10}\left(\frac{\sigma_f}{\sigma_i}\right) \qquad (2.30)$$

where $\Delta V/V$ refers to the change in soil volume with respect to the initial volume. Since the embankment was constructed under controlled compaction conditions, it can be assumed that the soil mass is initially without significant soil cracking. However, Lytton (1987) has shown that for non-intact soils (i.e., cracked soils), the change in volume attributed to lateral cracking (vertical cracks) in shrinking soil is given by $\left(\frac{1-f}{2}\right)\frac{\Delta V}{V}$ where f is a crack factor. He also showed that the lateral strain due to shrinkais te amount of lateral shrinkage (the sume of the crack widths) divided by the distance over which the shrinkage was measured and is equal to

$$\left(\frac{1-f}{2}\right)\frac{\Delta V}{V} = \frac{\Delta \ell_3}{x_3} = v \qquad (2.31)$$

where $\Delta \ell_3$ is the total lateral shrinkage and x_3 is tha lateral distance over which the shrinkage occurred. Thus, Eq. (2.30) should be written in the following form for shrinking soils:

$$v = -\gamma_h \log_{10}\left(\frac{h_f}{h_i}\right) + \gamma_\sigma \log_{10}\left(\frac{\sigma_f}{\sigma_i}\right) \qquad (2.32)$$

In Eq. (2.32) γ_σ is analogous to γ_h, the coefficient of suction compressibility, and is termed the coefficient of stress compressibility. Picornell (1985) reports γ_σ to typically be larger than γ_h by a factor of 1.15 to 1.20. The σ_f and σ_i terms represent compressive stresses in the soil mass resulting from overburden or surcharge loadings. If the soil is experiencing swelling conditions, then $|h_f| > |h_i|$ and $|\sigma_f| < |\sigma_i|$; the reverse will be true for shrinking conditions.

Solving Eq. (2.32) for σ_f results in

$$\sigma_i [10^{\alpha}] [m^{\beta}] = \sigma_f \tag{2.33}$$

where $\alpha = v/\gamma_h$, $\beta = \gamma_\sigma/\gamma_h$, and $m = h_f/h_i$.

The final stress can also be written as

$$\sigma_f = \frac{1}{3} (1 + 2 K_o) \sigma_v \tag{2.34}$$

where σ_v is the vertical pressure.

Substituting Eq. (2.33) into Eq. (2.32) produces a relationship for estimating horizontal pressure resulting from changes in soil moisture conditions (changes in soil suction):

$$K_o\sigma_v = \frac{3}{2} \sigma_i [10^{\alpha}] [m^{\beta}] - \frac{\sigma_v}{2} \tag{2.35}$$

where K_o = coefficient of at rest earth pressure.

3. LABORATORY AND FIELD INVESTIGATION

A. GENERAL

1. Extent of the Problem. At the inception of the study, it was not known how widespread the cracking problem was throughout the state. Thus, the first objective of the study was to attempt to define the extent of the problem. This was accomplished by surveying each SDHPT district. Two questions in the survey were of particular importance: (1) Has your district experienced the same longitudinal cracking observed in District 16? and (2) What are the compaction specifications employed in your district in association with constructing RSRW walls?

The survey revealed that by 1988 only 9 of the 24 SDHPT districts had constructed or were constructing RSRWs. Of these 9 districts with RSRWs in their inventory, only District 16 had experienced the longitudinal cracking problem. Thus, the problem was not as extensive as initially feared.

Table 3.1 summarizes the principal embankment construction criteria set forth in each district's embankment construction specifications. Interestingly, three of the districts did not have any special specifications while five of the remaining six districts required the embankment soil to have a liquid limit (LL) of 45 percent or less and all six required that the soil be compacted at the laboratory-determined optimum moisture content if the PI of the soil was 15 percent or less. For those soils with a PI of 15 or less, the soil was permitted to be compacted to a value of 100 percent or greater than the maximum dry density determined in the laboratory. A curious feature of these specifications was that the compaction density criteria were applicable to swelling soils with a PI of 20 or less, but the PI criteria did not permit the soil to be used if the PI exceeded 15. For those soils with a PI greater than 15 but less than 30, the dry density achieved during field compaction was permitted to range between 98 and 102 percent of the laboratory maximum value; these soils were also required to be compacted at a moisture content of not less than the optimum.

Thus, it was clear that any field monitoring should be conducted in District 16 since that was where the problem seemed to be concentrated.

TABLE 3.1. SUMMARY OF CONSTRUCTION SPECIFICATIONS FOR EACH SDHPT DISTRICT WITH REINFORCED SOIL WALL-RETAINED EMBANKMENTS

District No.	Plasticity Index (PI) Range (%)	Maximum Liquid Limit (%)	Optimum Moisture Content Limits (%)	Dry Density Limits, γ_d*
11[b]	- -	- -	$\leq w_{opt}$	$\gamma_d \geq 100\%$ (PI < 20) $98\% \leq \gamma_d \leq 102\%$ (PI ≥ 20)
14[b]	- -	- -	$\leq w_{opt}$	$\gamma_d \geq 100\%$ (PI < 20) $98\% \leq g_d \leq 102\%$ (PI ≥ 20)
15	- -	- -	w_{opt}	$\gamma_d \geq 100\%$ (PI < 20) $98\% \leq \gamma_d \leq 102\%$ (PI ≥ 20)
16	$4 \leq PI \leq 15$	≤ 45	w_{opt}	$\gamma_d \geq 100\%$ (PI < 20) $98\% \leq \gamma_d \leq 102\%$ (PI ≥ 20)
18	$4 \leq PI \leq 15$ $4 \leq PI \leq 30$	≤ 45	w_{opt}	$\gamma_d \geq 100\%$ (PI < 20) $98\% \leq \gamma_d \leq 102\%$ (PI ≥ 20)
20[b]	- -	- -	$\leq w_{opt}$	$\gamma_d \geq 100\%$ (PI < 20) $98\% \leq \gamma_d \leq 102\%$ (PI ≥ 20)
21	$4 \leq PI \leq 15$	≤45	$\leq w_{opt}$	$98\% \leq \gamma_d$ (PI < 20) $98\% \leq \gamma_d \leq 102\%$ (PI ≥ 20)
23	- -	- -	w_{opt}[a]	$98\% \leq \gamma_d \leq 102\%$[a]
24	$4 \leq PI \leq 15$	≤45	w_{opt}	$98\% \leq \gamma_d \leq 102\%$ (PI ≥ 20)

*γ_d = Laboratory maximum dry density

[a]Inferred from field test results

[b]Inferred to be 1982 "SDHPT Standard Specification" Criteria.

2. Method of Constructing Embankments and Pavement Structures. Generally, the clay embankments are constructed by placing suitable and conditioned clay material conforming to SDHPT specifications in 6 to 8 in. loose lifts followed by compacting the placed clay soil to achieve the density and moisture content considered necessary. The SDHPT District 16 specifications required that the embankment be constructed by placing the soil in layers not exceeding 8 in. of loose depth. The moisture of the placement soil was required to be adjusted to approximately the optimum moisture content. For soils with a PI greater than 20, the required moisture content was to be at or more than the optimum moisture content and the density of the soil after compaction could be no less than 98 percent, but not greater than 102 percent of the maximum dry density as determined by Test Method Tex 114-E (SDHPT, 1989).

The embankments were constructed in advance of either the bridge structure or the RSRWs. The slope of the constructed embankment was selected principally for safety and economy in construction since the construction technique employed in District 16's RSRW construction program required the earthwork contractor to construct a sloped embankment and then required the RSRW contractor to remove the slope at the time of RSRW construction. Once construction of the RSRW began, the first step in the procedure was to cut away the slope, leaving a vertical face at the location of the interface between the clay embankment and the granular backfill of the RSRW (Fig. 3.1). Select cohesionless backfill was placed in shallow lifts over the reinforcement grids and against the exposed vertical cut of the clay embankment (Fig. 3.2). The select backfill was granular cohesionless soil having a PI less than 15. Once the embankment and the reinforced soil retaining walls were constructed to approximately the desired grade, the top 8 in. of the clay embankment was lime-treated by mixing a predetermined quantity of lime with the high-PI soil and adding water to the resulting mix prior to being compacted in place. The resulting pozzolonic reaction stabilized the soil. Then a 12 ft wide strip centered on the clay-sand interface was cement treated to a 12 in. depth. (See Appendix C.) A flexible base constructed from compacted crushed stone or caliche was then placed on the treated subgrade. Finally, 10 in. of hot mix asphalt concrete (HMAC) was placed over the flexible base.

B. FIELD MONITORING

1. Objective. The objective of monitoring the field conditions of the constructed clay embankments was to gain a knowledge of the soil moisture condition behavior of both the high-PI clay and the sand of the select cohesionless backfill material of the RSRW under field conditions. It was also important to monitor the interaction of the clay and sand materials in

Fig. 3.1. Photograph of the procedure employed by the RSRW contractor in cutting back the constructed clay embankment to provide a vertical interface between the embankment and the to-be-constructed reinforced soil retaining wall and the cohesionless backfill.

Fig. 3.2. Photograph of placement of the cohesionless backfill and the construction method employed by the contractor in constructing RSRWs on SH 358 overpasses.

order to determine the moisture movement patterns and discern whether two interfacing materials of vastly different plasticity properties could exist side by side without causing problems to the overlying pavement structure.

2. Selection of Field Sites. In consultation with District 16 personnel, it was determined that three embankments should be instrumented. The objective was to choose two field sites whose embankments were not only identically constructed as the embankments exhibiting distress, but also influenced similarly by climatic and environmental conditions. The third site was selected because its soil was very sandy and was a low-PI soil. The two high-PI field sites were chosen along State Highway (SH) 358 in Corpus Christi. The third instrumented location was chosen along Interstate Highway (IH) 37 at Calallen, approximately 7 miles inland of Corpus Christi (Fig. 3.3). The first clay embankment field site was installed at the intersection of SH 358 and Bear Lane, while the second clay embankment field site was located at the intersection of SH 358 and Old Brownsville Road. Thus, these sites are referred to as the Bear Lane, Old Brownsville, and Calallen sites, respectively. These particular field sites were chosen since the clay embankment and reinforced earth retaining walls had already been constructed, but had no pavement structure placed upon the finished embankment. A typical cross section of the pavement structure and embankment is shown in Fig. 3.4 and Appendix C.

The Bear Lane and Old Brownsville embankments are similar to the other embankments built along SH 358 which exhibited longitudinal cracking of their asphalt concrete surface. These two embankments were constructed using soils from the same borrow area as the older embankments exhibiting pavement distress. The Calallen site along IH 37 was chosen as a field site because it has embankment materials different from but climatic conditions similar to those of the other two field sites. Table 3.2 and Fig. 3.5 provide some of the soil properties of the soil being studied.

3. Climatic Conditions. From the technical literature review it was determined that the behavior of high-PI soils can be considerably influenced by climatic conditions. Therefore, it is important to describe the climatic conditions of Corpus Christi in order to determine their influence on the soils used to construct the embankments of SH 358.

Since Corpus Christi is a coastal city on the Gulf of Mexico it has a mild climate throughout the year. The warmest period is from mid-July through mid-August. During this period the temperatures typically fluctuate between 75 and 94 degrees F and it is generally a period of considerable sunshine. The relative humidity is approximately 60 to 90 percent, with the highest value of relative humidity typically being recorded at 6 a.m. and the lowest

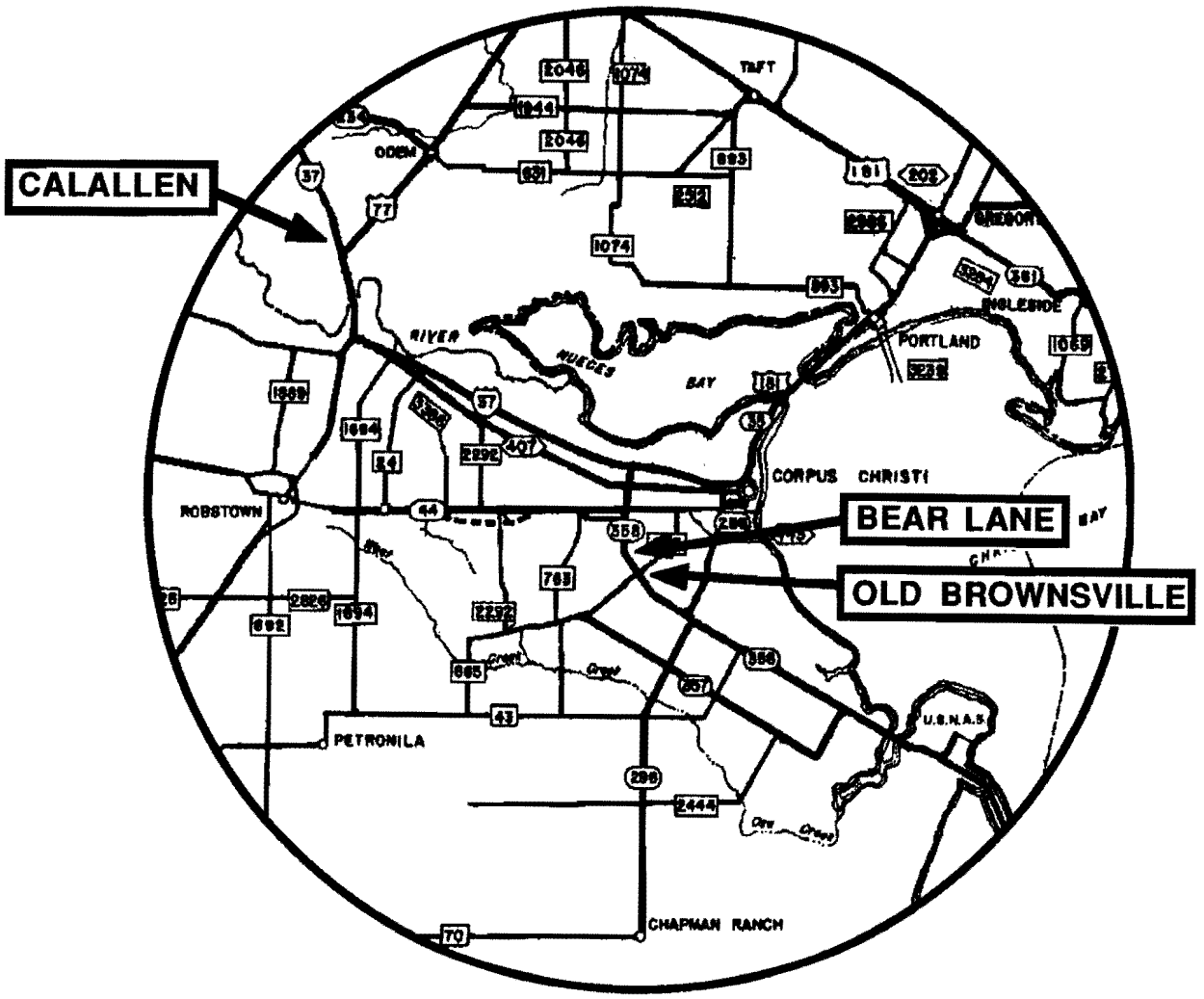

Fig. 3.3. Location of the three instrumented soil moisture condition field monitoring sites: (1) intersection of SH 358 and Old Brownsville Highway, (2) intersection of SH 358 and Bear Lane, and (3) IH-37 at Calallen.

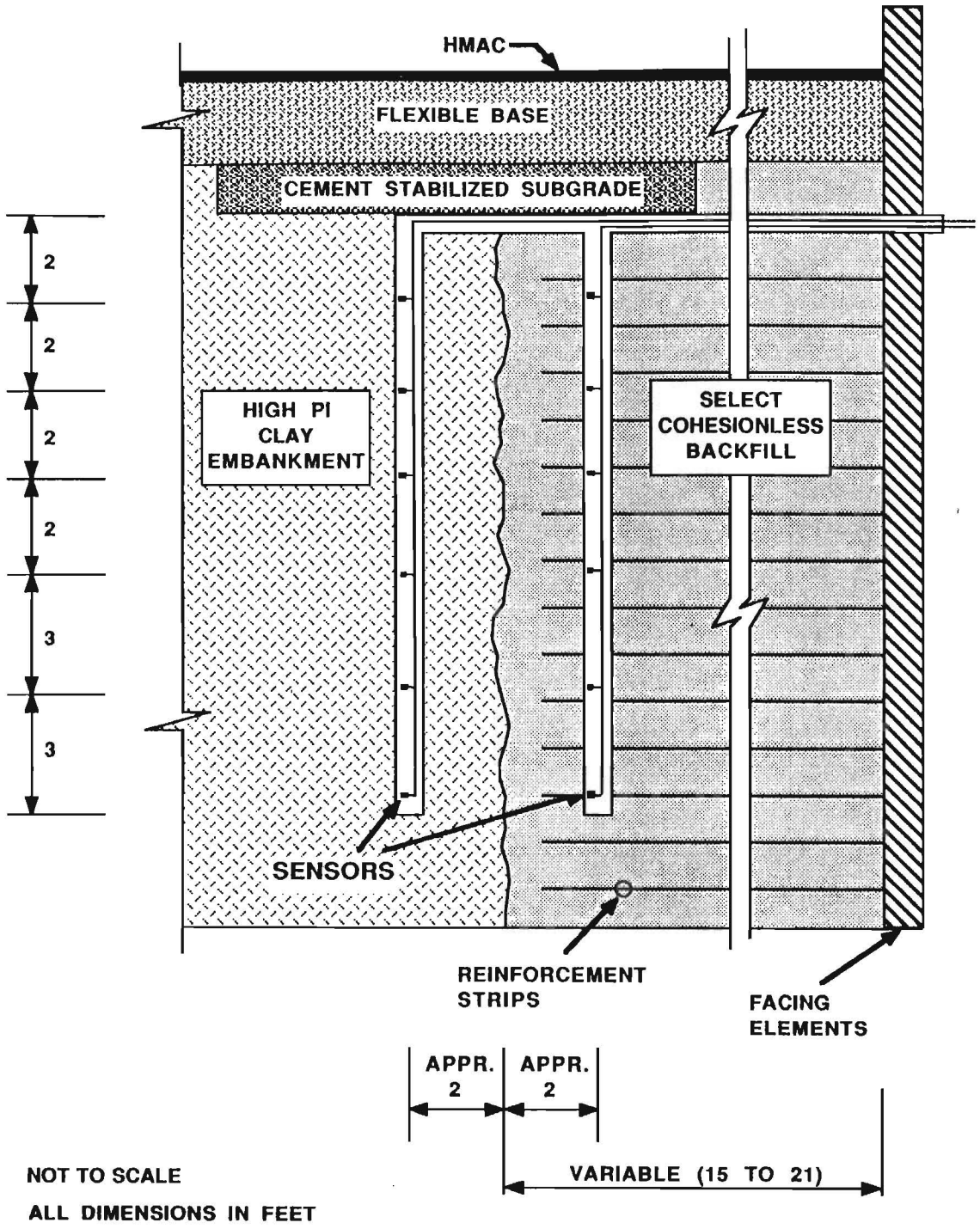

Fig. 3.4. A typical cross-section of the RSRW-clay embankment system. Sensors to monitor changes in soil moisture conditions were installed in two stacks on either side of the clay-sand interface at each field site.

Table 3.2. Physical Properties of Corpus Christi Soils

Soil	Liquid Limit, Range (%)	Plastic Limit, Range (%)	Plasticity Index, Range (%)	Specific Gravity of Soil Solids	Soil Classification	
					USCS	AASHTO
Clay From Big Ditch Borrow Pit	39.5-41.5	18.3-18.5	21-23.2	2.74	CL	A-7-5(14)
Clay From Embankment Cuttings (Old Brownsville)	65.0-70.0	25.7-28.8	44.3-36.2	2.82	CH	A-7-6(20)
Sand Flour Bluff	NP	NP	NP	2.64	SP	A-3

NP: Nonplastic

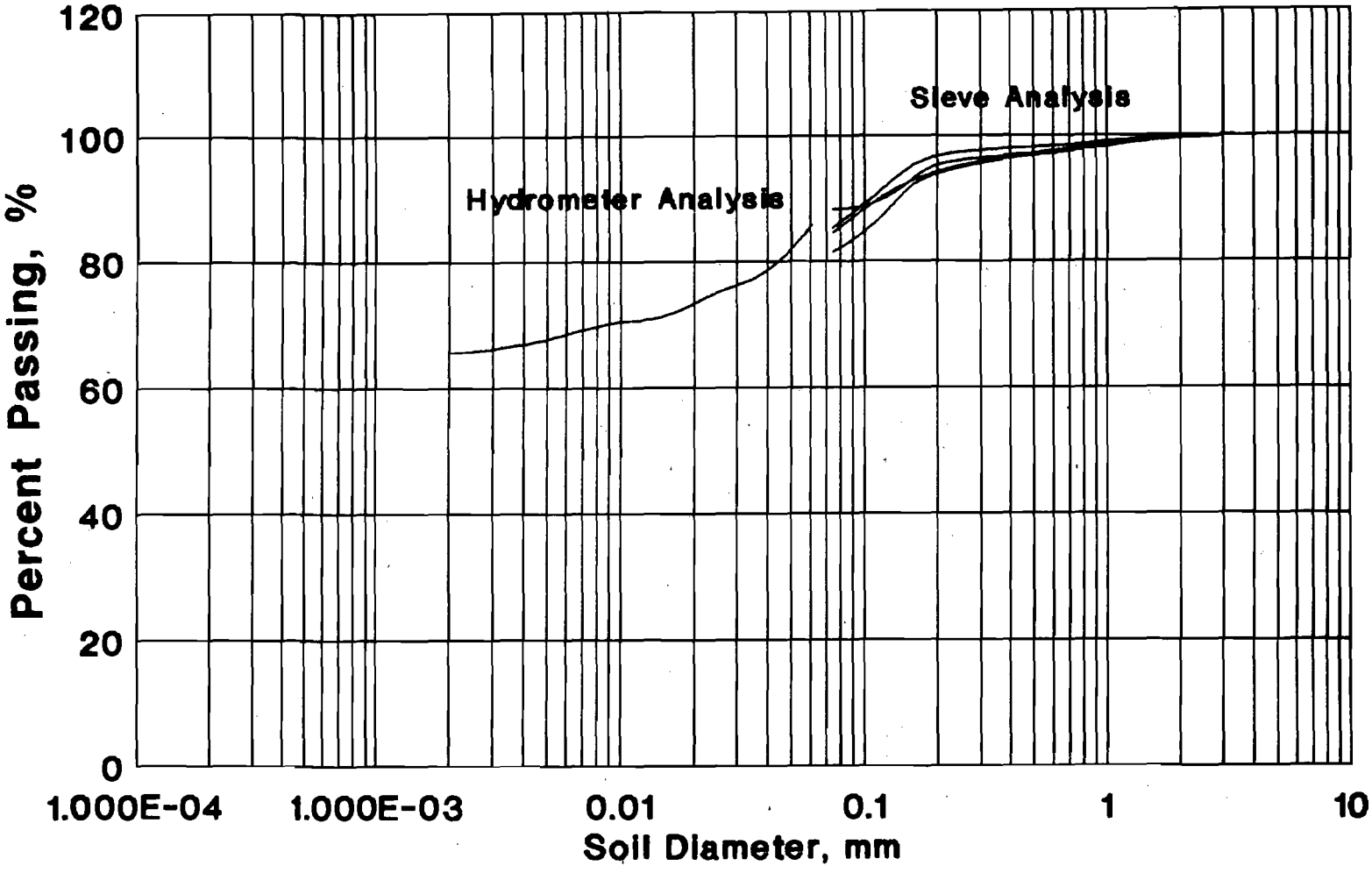

Fig. 3.5. Grain size distribution curve of the clay embankment material recovered from borings taken at the Old Brownsville Highway test site.

value of relative humidity typically being recorded at noon. The average wind speeds during this time are about 10 to 11 mph.

The coldest months are December through February, when the temperatures fluctuates between 45 and 65 degrees F. In 1989, the year in which the field instruments were installed, there were approximately 15 days when the recorded daily low temperature was below 32 degrees F. It is in this period that the most overcast days have been recorded. The relative humidity for this period typically ranges between 60 and 90 percent. The average wind speed is approximately 12 to 14 mph.

Using weather data from the National Climatic Data Center, Asheville, NC, the Thornthwaite Moisture Index (TMI) was determined annually for the 31-year period 1960 - 1990; this is the entire period over which weather data has been officially reported by the U.S. Government for Corpus Christi. The TMI numerically describes the climate of a location using a number, if negative, that represents the number of inches of water annually that could be given up to the atmosphere through evaporation and plant transpiration if that additional amount of water were available in the soil, or, if a positive number, that is excess to the needs of the soil and is lost through surface runoff. The following information at Corpus Christi was provided through the calculation of the TMI for this 31-year period:

1. Climatically, the wettest year was 1968 which was represented by a TMI of +8.5 in./yr.

2. Climatically, the driest year was 1962 which was represented by a TMI of -44.5 in./yr.

3. The historical mean TMI was found to be -21.1 in./yr.

4. The TMIs for the 5 years preceding initiation of the study were -10.2, -32.2, -14.6, -27.4, and -9.0 in./yr (1983-1987).

5. The TMI for the 12 months preceding the sensor installation was -32.9 in./yr.

Analysis of the TMIs revealed the climate to have cycled between a relatively wet and relatively dry year during the five years preceding this study. The climate was relatively wet in the year that the embankments were constructed for that section of SH 358 which was opened to traffic in 1989. Cracks in this newest section of SH 358 were observed even before the final lift of the HMAC pavement was placed. The climate during the entire period of the study (and the period during which the embankments that were instrumented as a part of this study were constructed) was found to be quite dry. TMIs for this 2-year period were -32.9 and -31.5

in./yr (Sept. 1988-Aug. 1989 and Sept. 1989-Aug. 1990, respectively), the fourth and sixth driest 12-month periods over this 31-year climate history.

4. Instrumentation. The soil properties of principal concern in the overall study were PI, grain size distribution, specific gravity, soil suction, and soil moisture content. While the PI, grain size distribution, and specific gravity of the soils can be determined in a soil mechanics laboratory from soil samples obtained through soil sampling operations, the in situ soil moisture conditions of the embankments must be constantly monitored. Therefore, it was necessary to utilize instruments capable of quantitatively measuring or inferring the soil suction and soil temperatures in the field. The instruments used in this study were the thermocouple psychrometer (TCP) and the heat dissipation block (HDB) . The filter paper method was employed to determine the soil suction at the time of sensor installation.

C. THERMOCOUPLE PSYCHROMETERS

1. Theory. Psychrometers are used to infer the water potential of soils and other media by making measurements of equilibrium vapor pressure. The theory of how psychrometers operate has been described by numerous investigators (e.g., Spanner, 1951; Rawlins, 1966; Dalton and Rawlins, 1968; Peck, 1968; Brown, 1970; Wiebe et al., 1971; Brown and Bartos, 1982). The thermocouple psychrometer is basically a thermocouple that makes use of the Peltier effect to measure relative humidity between about 95 and 100 percent corresponding to a water potential ranging between 0 and about 1,000 bars. (Typical units of soil suction and their conversions are reported in Appendix B.) Although a variety of design features has been developed and reported in the technical literature (e.g., Brown and Johnston, 1976; Rawlins and Dalton, 1967; Ingvalson et al., 1970; Brown, 1970), all Peltier thermocouple psychrometers now used have the same basic components (Brown and Bartos, 1982). The basic circuitry of a thermocouple psychrometer is depicted in Fig. 3.6. A photograph of an assembled Merrill-type thermocouple psychrometer is shown in Fig. 3.7. The wiring used in the psychrometer circuitry is a very fine diameter of 0.00254 cm (0.001 in.). The measuring (or sensing) junction is formed by welding together a constantan wire and a chromel wire as shown in Fig. 3.6. Two reference junctions are created slightly behind the sensing junction by attaching each of the constantan and chromel wires to separate copper lead wires of a larger diameter. Thus, the typical thermocouple psychrometer now commercially available consists of one measuring or sensing junction and two reference junctions.

The thermocouple psychrometer operates by passing a current through the measuring junction which cools the junction or tip (i.e., the Peltier effect). This cooling effect is

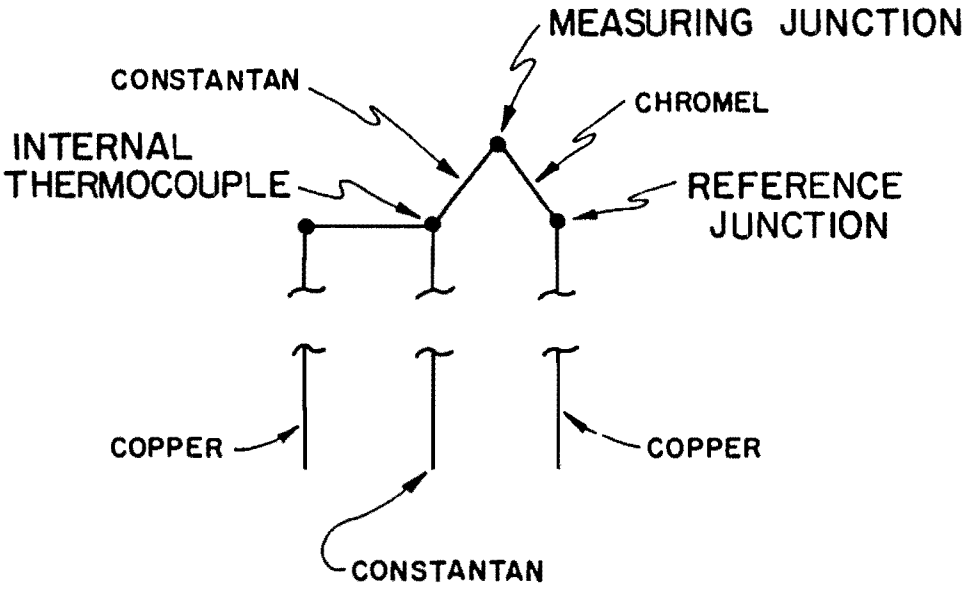

Fig. 3.6. Schematic drawing of the circuitry employed in a J.R.D. Merrill thermocouple psychrometer.

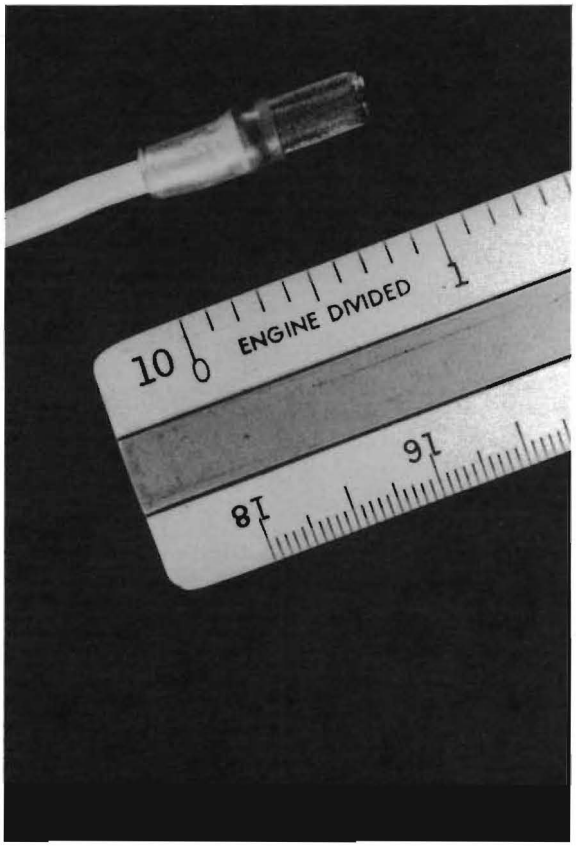

Fig. 3.7. Photograph of a J.R.D. Merrill stainless steel tip thermocouple psychrometer.

continued until a small bead of water condenses on the junction. After the current is switched off, the condensed bead of water begins to evaporate, further cooling the junction (the psychrometric effect). An electronic readout device or meter measures the temperature difference between the measuring and reference junctions during this evaporation process. The psychrometric cooling is a function of the relative humidity (which is a measure of the water potential of the soil). The thermocouple psychrometer also has an internal copper-constantan thermocouple for measuring sensor temperature. Thus, the thermocouple psychrometer does not directly measure water potential or soil suction; it actually measures relative humidity which can be related to soil suction. Since soil suction is dependent upon temperature, each field psychrometric reading must be adjusted to account for the effect of the ambient temperature.

2. Calibration. Each thermocouple psychrometer was individually calibrated. This was accomplished by following the procedure described below:

1. The thermocouple psychrometer was suspended in one end of a closed stainless steel calibration chamber purchased from J.R.D. Merrill Co. that was compatible with its psychrometers. This chamber could be sealed to prevent the exchange of the atmosphere of known relative humidity inside the chamber with that of the ambient laboratory room atmosphere.

2. A piece of #40 Whatman filter paper was saturated in an NaCl solution of known molality and then sealed in the opposite end of the calibration chamber used in Step 1, above.

3. The sealed calibration chamber was then immersed in a large tank of water. The ambient temperature of the room was controlled to remain at 65 ° ± 2° F. (Although not ideal, this represented the limits of temperature control available to the research project.) The water bath prevented sudden changes in room temperature caused by air conditioning/heating equipment starting and stopping and fluctuations caused by doors to the laboratory opening and closing.

4. The relative humidity in the small calibration chamber was permitted to come into equilibrium. This equilibration period typically required approximately 1 hr to reach equilibrium; however, the minimum equilibration period employed was 2 hr to ensure that complete equilibrium had been attained before proceeding to the next step.

5. The microvolt output from the readout device was checked periodically beginning at an elapsed time of approximately 1 hr into the equilibration period. If the microvolt output remained constant, then a calibration reading was taken at the 2 hr elapsed time point.

6. The microvolt reading was then plotted as a function of the water potential corresponding to the molality of the NaCl solution used in each calibration step.

7. The calibration chamber was removed from the water bath, opened, the filter paper removed, and the chamber cleaned and dried. Another piece of filter paper saturated in a different molal NaCl solution was then inserted into the calibration chamber and the procedure repeated until a definite curve was produced. Each calibration curve was developed from 10 to 12 calibration points using NaCl solutions ranging in molality from 0.1 to 2.0 m.

D. HEAT DISSIPATION SENSOR (AGWA-II SENSOR)

1. Theory. The AGWA-II heat dissipation sensor or block (HDB) is designed to infer the soil matrix suction by measuring the heat dissipation within a standard porous ceramic matrix. The heat relation of soil and soil moisture has been studied by many investigators (i.e., Patten, 1909; Shaw and Baver, 1939; Bloodworth and Page, 1957). However, it was not until the work of Phene et al. (1971) that the heat dissipation within a porous matrix was proposed to be used as an index of soil matrix suction. Basically, the AGWA-II sensor is constructed of three major components: a temperature transducer, a mini heater, and a standard porous ceramic matrix embodying the temperature transducer and the heater. A schematic drawing of the AGWA-II sensor is shown in Fig. 3.8. A photograph of the AGWA-II sensor is presented in Fig. 3.9.

To make a suction measurement, the AGWA-II sensor is embedded in the soil to allow the ceramic matrix of the sensor to come into equilibrium with the adjacent soil. Due to a matrix suction gradient, a moisture exchange in the form of liquid flow will occur between the ceramic matrix and the soil. The resulting moisture content of the ceramic matrix is a function of the soil matrix suction and is proportional to the rate of the heat dissipation within the ceramic matrix. To measure the heat dissipation, the mini heater acts as a point heat source and generates a controlled heat pulse within the ceramic matrix. The heat thus generated begins to dissipate and the resulting temperature rise at the heat source after a fixed period is then recorded by the temperature transducer. The magnitude of the temperature rise varies according to the amount of moisture within the ceramic matrix; i.e., the heat dissipates faster in a porous body with higher moisture content and results in a lower temperature rise. The temperature rise is thus inversely related to the moisture content of the ceramic matrix and can be calibrated to infer the soil matrix suction. The temperature rise is measured by the AGWA-II sensor as the current output (or voltage output using Ohm's Law) of the temperature

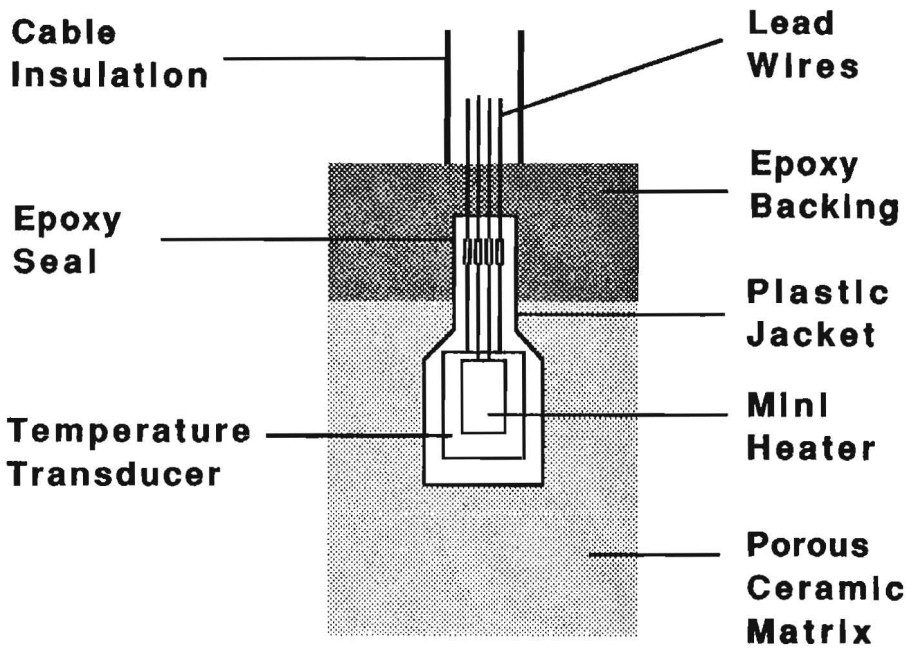

Fig. 3.8. Schematic drawing of an AGWA-II heat dissipation block sensor manufactured by the Agwatronics company (After Sattler and Fredlund, 1989).

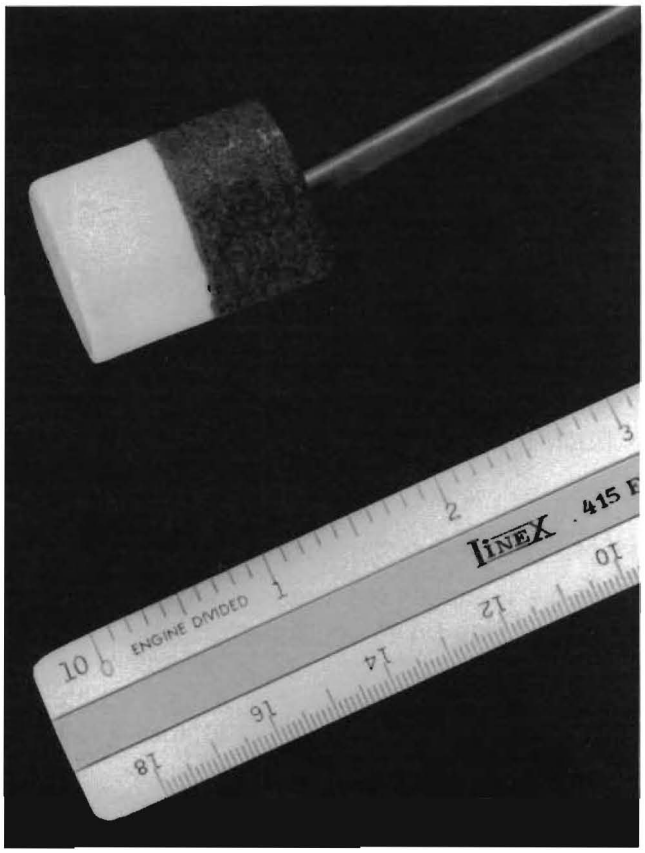

Fig. 3.9. Photograph of an AGWA-II heat dissipation block sensor manufactured by the Agwatronics company.

transducer, which is proportional to the absolute temperature (1 micro-ampere/^{0}K). The soil matrix suction is then calculated as the function of the temperature rise as follows:

$$y = m\,x + b \qquad (3.1)$$

where y = soil matrix suction in bars

x = temperature rise in micro-amperes or milli-volts

m = constant

b = constant

The two constants, m and b, vary among individual AGWA-II sensors and can be determined by calibrating the temperature rise within the ceramic matrix of the AGWA-II sensor against known matrix suction using pressure plate apparatus.

2. Calibration. Each AGWA-II sensor used in this study was individually calibrated by the manufacturer. Described below are the basic procedures in the calibration of the AGWA-II sensor using pressure plate apparatus.

1. The AGWA-II sensor is embedded in a standard calibration soil mixture placed inside a PVC cylinder ring resting on a porous ceramic plate. The sensor, the soil mixture, and the porous ceramic plate were initially saturated. The lead wire of the AGWA-II sensor is allowed to pass through a hole drilled on the wall of an added extension ring on top of the pressure chamber, and is connected to a data logger.

2. The desired air pressure is then applied to the instrumented soil mixture after the pressure chamber is sealed. The outflow of water from the soil mixture, the sensor, and the porous ceramic plate is permitted to drain and is collected in a graduated cylinder. The response of the AGWA-II sensor to the applied pressure (which is assumed to be the soil matrix suction at equilibrium) is monitored and recorded, using the data logger. The response of the sensor at equilibrium is used for the calibration curve.

3. Step 2 is repeated by applying various desired air pressures separately until a definitive calibration curve is produced. Fig. 3.10 is a typical calibration curve of the AGWA-II sensor, reproduced from the calibration data provided by the manufacturer.

E. FILTER PAPER METHOD OF MEASURING IN SITU SOIL SUCTION

1. Theory. Special filter papers were used to measure the in situ soil suction of the sampled embankment soils. A very simple method of measuring soil suction was reported by Gardner (1937) and developed further by McQueen and Miller (1968). Initially termed a "wide-range gravimetric method for measuring moisture stress ," it has subsequently become known as simply "the filter paper method." Using this method, two filter paper disks, treated to

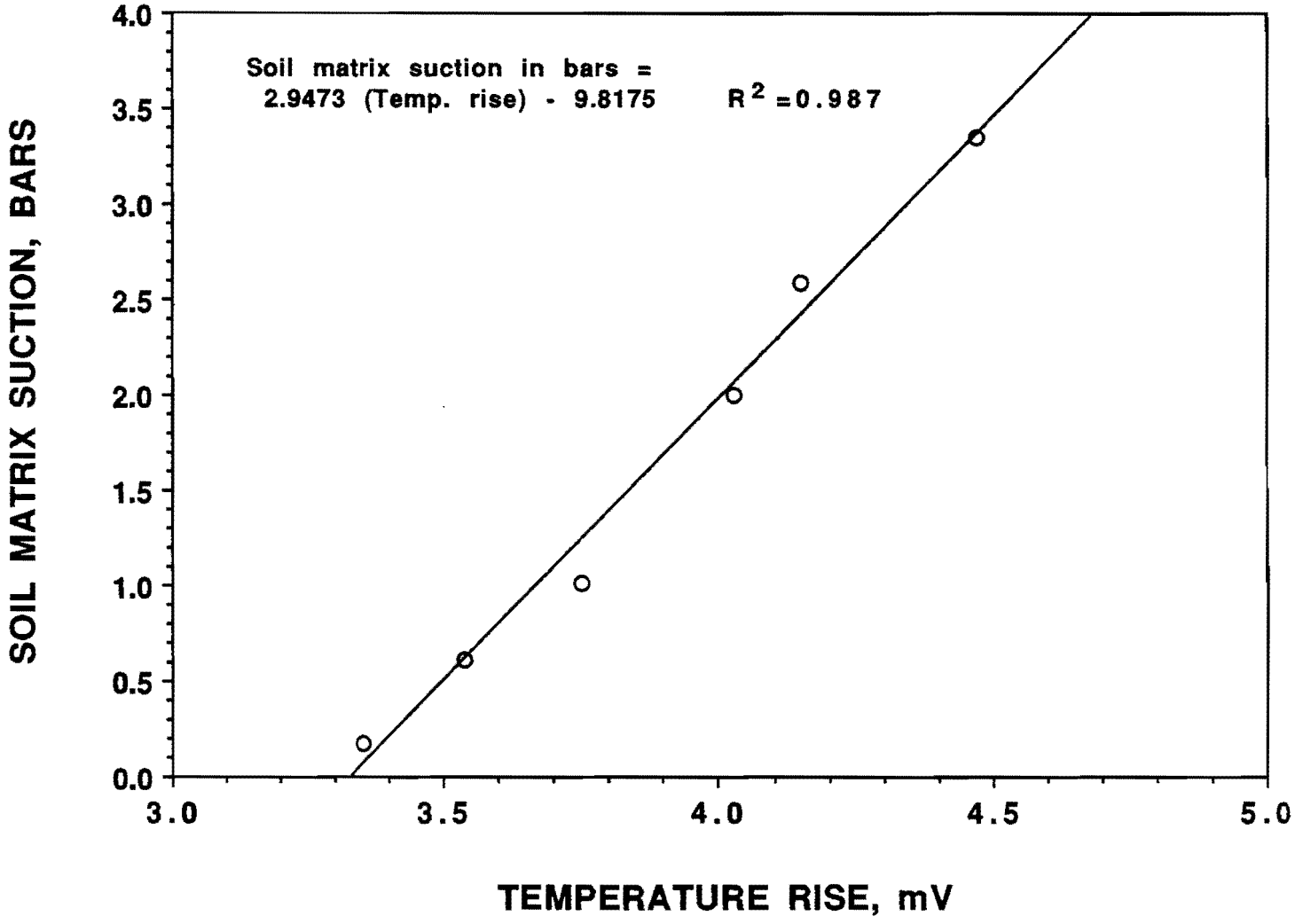

Fig. 3.10. A Typical calibration curve for an AGWA-II heat dissipation block sensor manufactured by the Agwatronics company.

inhibit biological decomposition, are either placed in full contact with the soil sample as it is extracted and sealed, or the soil sample and the filter paper are simply placed together inside a sealed container. In either method, the soil and the filter paper are permitted to come into equilibrium in a temperature controlled environment (usually $\pm$ 20° C). Equilibrium may be reached in a few hours, but typically requires periods of up to 8 days or longer when heavy clays are involved. When equilibrium is attained, the moist filter paper is removed from the sealed container and quickly weighed. Each filter paper is then placed in an oven to dry. Upon removal from the oven, each dried paper is again quickly weighed. The moisture content of the moist filter paper is plotted as a percentage of dry weight on a calibration curve for that particular filter paper and the matrix soil suction can be estimated for low soil moisture contents.

The filter paper method has been found to be accurate to within 2 percent at soil suctions greater than 3.0 pF. Introduced by Schofield (1935), the "pF" nomenclature is used to define soil suction in terms of the common logarithm of the height in centimeters of a column of water needed to give an equivalent suction pressure. Since suction is a negative value, the logarithm is taken of the absolute value of the height of the equivalent column of water. The "p" in the pF term is analogous to Sorensen's acidity scale (i.e., "pH") and the "F" represents Gibb's free energy. The pF scale is convenient to use when measured suctions exceed 10 atmospheres, i.e., 10,000 cm of equivalent water pressure. McQueen and Miller (1968) report the method to be effective over a range of 0 to 6.2 pF; Fawcett and Collis-George (1967) suggest a reliable range of 2.0 to 6.0 pF. McKeen (1981) found that the results of the filter paper method compared quite favorably with those obtained from conventional field and laboratory methods.

2. Data Collection. In situ soil suction was measured at the time of site installation using the filter paper method. At each test site, soil borings were made to a depth of 14 ft. At predetermined depths, a small representative sample of soil was recovered and placed in a wide-mouthed glass jar with two pieces of Schleicher and Schull (S&S) No. 589 "White Ribbon" filter papers placed on top of the soil sample. Each jar was properly labeled and the lid tightly screwed on and then sealed with plastic electrician's tape. Each sample jar was placed in a large, 64-qt insulated beverage container and surrounded with styrofoam shipping materials to provide protection from excessive vibration or damage during transportation back to Texas Tech University and the soil laboratory humid room. Each sample was permitted to remain in the humid room for a minimum of 8 days in accordance with the findings reported by Snethen and Johnson (1980).

Upon removal from the humid room, each filter paper was quickly removed from the sample jar and weighed to the nearest 0.0001 g. Each paper was then placed in a drying oven and permitted to dry overnight at a constant temperature of 110° ± 5° C. The next day, each drying tin was capped, removed from the oven, and the tin and its contained filter paper were weighed within seconds after removal from the oven. By performing calculations described by McKeen (1985) and using the calibration curve developed by McKeen (1981) for S&S No. 589 "White Ribbon" filter paper, the in situ vertical soil suction profile was determined for each boring at each test site.

At high soil suction levels, soil suction values can change greatly with a very small incremental change in moisture content. It is such a small moisture increment, that the present commercially available instruments that measure soil moisture content do not give sufficiently accurate measurements. Therefore, it was decided to use neither the moisture cell nor the neutron probe as moisture measuring instruments but to rely on the soil suction measuring instruments to provide a measure of the change in soil moisture conditions. Thus, the three field test sites were instrumented using only thermocouple psychrometers and heat dissipation blocks.

The TCP data was read using a thermocouple readout meter, while the readings of the AGWA-II instruments were recorded by computerized data loggers. The TCPs were read by the Texas Tech University Civil Engineering Department personnel approximately every three months. During those visits, the daily HDB data stored in the data loggers were down loaded into a laptop computer as ASCII text files.

F. INSTRUMENTATION PROCEDURE

A truck-mounted Faehling 1500 SDHPT-owned drilling rig was used to advance three holes in each embankment after it had been completed, but before the subgrade was lime treated. One boring was advanced in the clay approximately 2 ft from the clay-sand interface and was continuously sampled using undisturbed sampling techniques while a second boring was advanced in the sand approximately 2 ft from the clay-sand interface. A third boring was advanced in the clay embankment, approximately 1 ft away from the first clay boring. Continuous soil samples from this boring were also recovered using undisturbed sampling techniques. The soil from the third boring was transported to the laboratory and was used to determine "site specific" soil characteristics. The boring was then backfilled and compacted using extra embankment material. The first two holes were instrumented and backfilled. The instrumentation sequence was as follows:

1. Each instrumented boring was advanced in 1 ft intervals using a thin-walled Shelby tube sampler in order to cause minimum disturbance to the soil. Each recovered foot of soil was carefully segregated, and placed in a plastic container which was marked with the depth interval from which the soil was recovered. The soil from each depth interval was broken up into small pieces. The soil in the plastic containers was covered with plastic sheeting and placed out of direct sunlight in order to preserve its soil moisture content.

2. A thermocouple psychrometer or AGWA-II sensor was molded inside a ball of soil taken from the desired installation depth (Fig. 3.11). The ball was approximately the size of a small chicken egg (Fig. 3.12).

3. Each instrument was placed with the ball of soil at the predetermined depth which was determined using a steel measuring tape (e.g., Figs. 3.13 and 3.14).

4. The boring was carefully backfilled and hand-compacted with the same soil that came from a particular depth in order to provide a restored soil continuum as nearly duplicating the original soil arrangement as possible.

5. The hole was then continued to be backfilled using the original soil that came from the hole from each depth interval. All soil was compacted by a hand tamper duplicating the in situ density as closely as possible.

6. The compaction-sensor placement-compaction sequence was repeated until all sensors had been installed and each boring completely backfilled.

7. All sensor leads were placed in PVC conduit for protection (Fig. 3.15) and carried to the facing wall of the RSRW (Fig. 3.16).

8. The sensor leads were carried through a 2 in. diameter hole cored in the concrete facing panels of the RSRW (Fig. 3.17) and were terminated in a waterproof termination box fixed to the outside surface of the facing panels (Fig. 3.18).

Two TCPs were placed at depths of 2, 4, 6, 8, 11, and 14 ft below the finished subgrade elevation for redundancy. The more costly AGWA-IIs were placed at depths of 2, 4, 8, and 14 ft; single sensors were installed at each depth. Specimens of the undisturbed soil samples from each borehole were taken at 2, 4, 6, 8, 11, and 14 ft and laboratory tests were run on them to characterize the soil and to determine the in situ soil suction using the filter paper test. The results of the tests run on the soils are reported in Table 3.2 and Fig. 3.5. In situ soil suction values from the filter paper tests are reported in Table 3.3. The clay from the second borehole drilled in the clay embankment was extruded from the tube samplers, wrapped first in plastic Saran wrap and then aluminum foil, labelled, and placed in special cardboard sample boxes.

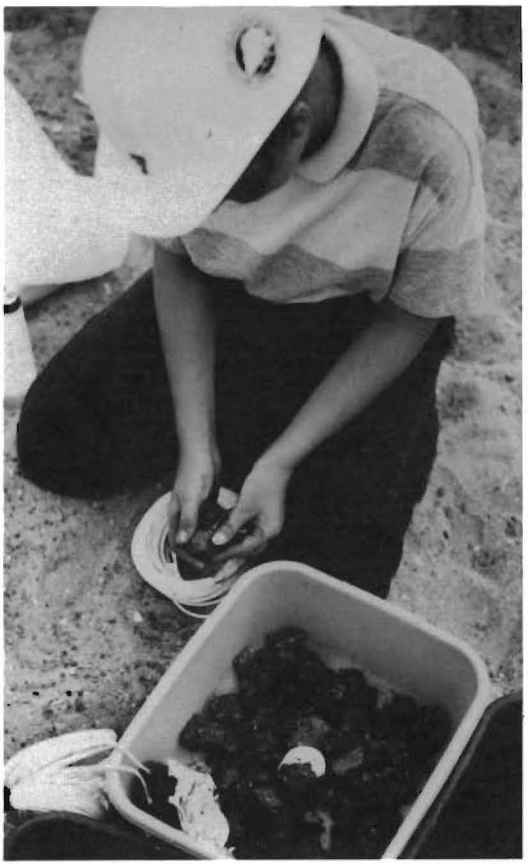

Fig. 3.11. Photograph of the procedure followed in balling clay soil around a thermocouple psychrometer in preparation for installation at some depth below the surface of the clay embankment.

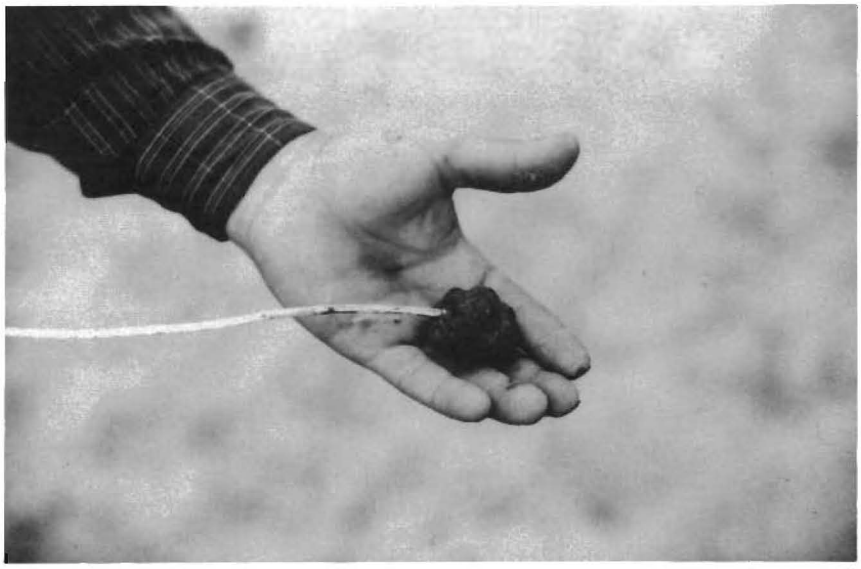

Fig. 3.12. Photograph of a thermocouple psychrometer with clay soil balled around the sensor in preparation for installation at some depth below the surface of the clay embankment.

Fig. 3.13. Clay was compacted in the sensor boring shaft until the depth at which a sensor is to be installed was reached. Shaft depth was checked frequently.

Fig. 3.14. Once the sensor installation depth was reached during the refilling and compaction procedure, a sensor was installed, tested, and backfilling continued until the next sensor installation depth was reached.

Fig. 3.15. Sensor leads were installed in PVC conduit to protect the leads from damage.

Fig. 3.16. The protective sensor lead conduit was carried to the RSRW facing elements.

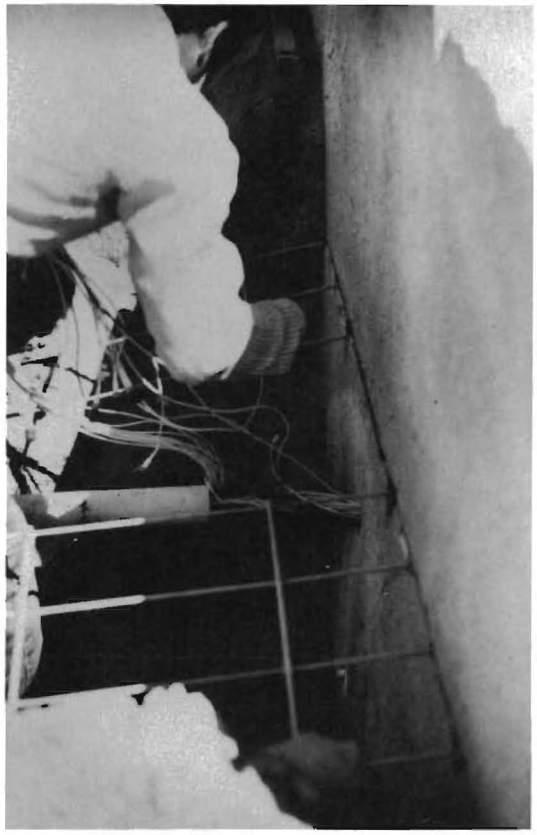

Fig. 3.17. A 2 in. diameter hole was cored through the 11 in. thick concrete wall facing element to permit the sensor leads to be passed through the wall.

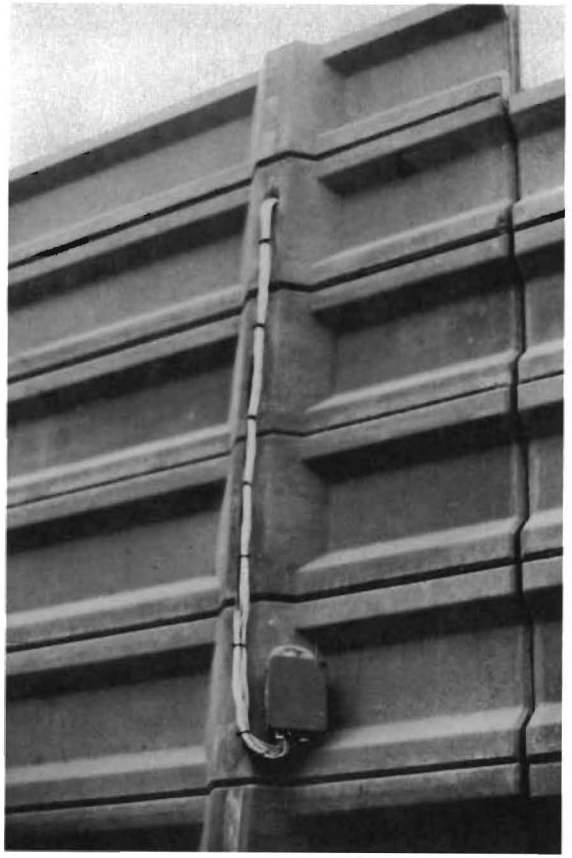

Fig. 3.18. Sensor leads were terminated in a water-proof electrical box attached to the face of the wall elements.

Table 3.3. In Situ Soil Suction Values at Field Test Sites at Time of Instrument Installation

Depth (ft)	Soil Suction, pF					
	Bear Lane Site		Old Brownsville Site		Calallen Site	
	Clay	Sand	Clay	Sand	Clay	Sand
2	4.58	--	4.30	--	4.30	--
4	4.43	3.63	4.49	--	4.33	--
6	4.10	3.27	4.41	--	4.65	--
8	4.20	3.73	4.36	--	4.17	--
11	4.60	--	4.57	--	--	--
14	4.31	4.31	4.09	--	4.10	--

These boxes were then transported to Texas Tech University and kept in the humid room of the Civil Engineering Department Soil Mechanics Laboratory until testing was complete.

G. LABORATORY STUDY

1. Objective. The objective of the laboratory study was to study the behavior of the clay-sand system by duplicating field conditions under laboratory controlled conditions. The objective was to duplicate the longitudinal cracking that had occurred in the HMAC pavements constructed in District 16.

2. Procedure. Laboratory models of the District 16 embankment clay-granular backfill systems were built in order to collect the greatest possible volume of data. In building laboratory models of the system, geometrical scaling was considered, but the full-scale behavior of the two different soil systems at their interface was deemed more important. Therefore, it was decided to model the interface of the clay-sand soils to the largest scale physically possible for the laboratory. Three test boxes having physical dimensions of 36L x 16W x 36D in. (Figs. 3.19 and 3.20) were constructed out of 1/4 in. thick steel plate. The boxes were stiffened using 8 in. vertical and horizontal steel channel stiffeners. The reason for stiffening the steel laboratory boxes was to prevent the dissipation of swell pressure developed in swelling clay due to flexing of the test box walls. Swell pressure in expansive clay dissipates rapidly if the container in which the swelling clay resides is permitted to deform. While it was not anticipated that the soil would swell, it was decided that it would be prudent to consider every possibility.

Each test box has a 3/4 in. thick, 8 in. wide fully tempered plate glass window centered at the clay-sand interface in order to view the behavior of both soils at their interface. Two-thirds of the laboratory-model volume was filled with high-PI Corpus Christi embankment clay, while the remaining volume, except for a small aperture built at the sand end of the box, was filled with fine sand from the Flour Bluff area of Corpus Christi. The soils used were representative samples of the actual soils used in the construction of the embankment-RSRW system; the clay was taken from the same borrow pit as the soil used in constructing the embankment. A 1 in. wide aperture built at the sand end of the test box runs the full height of the box and is separated from the sand by wire mesh and burlap cloth.

The clay was placed in the test box in 6 in. loose lifts and compacted at optimum moisture content using a pneumatic tamper. The select cohesionless backfill material was placed alongside the compacted layer of clay in approximately 6 in. loose lifts, and sufficient water and light tamping were employed to achieve a density of approximately 100% of the laboratory

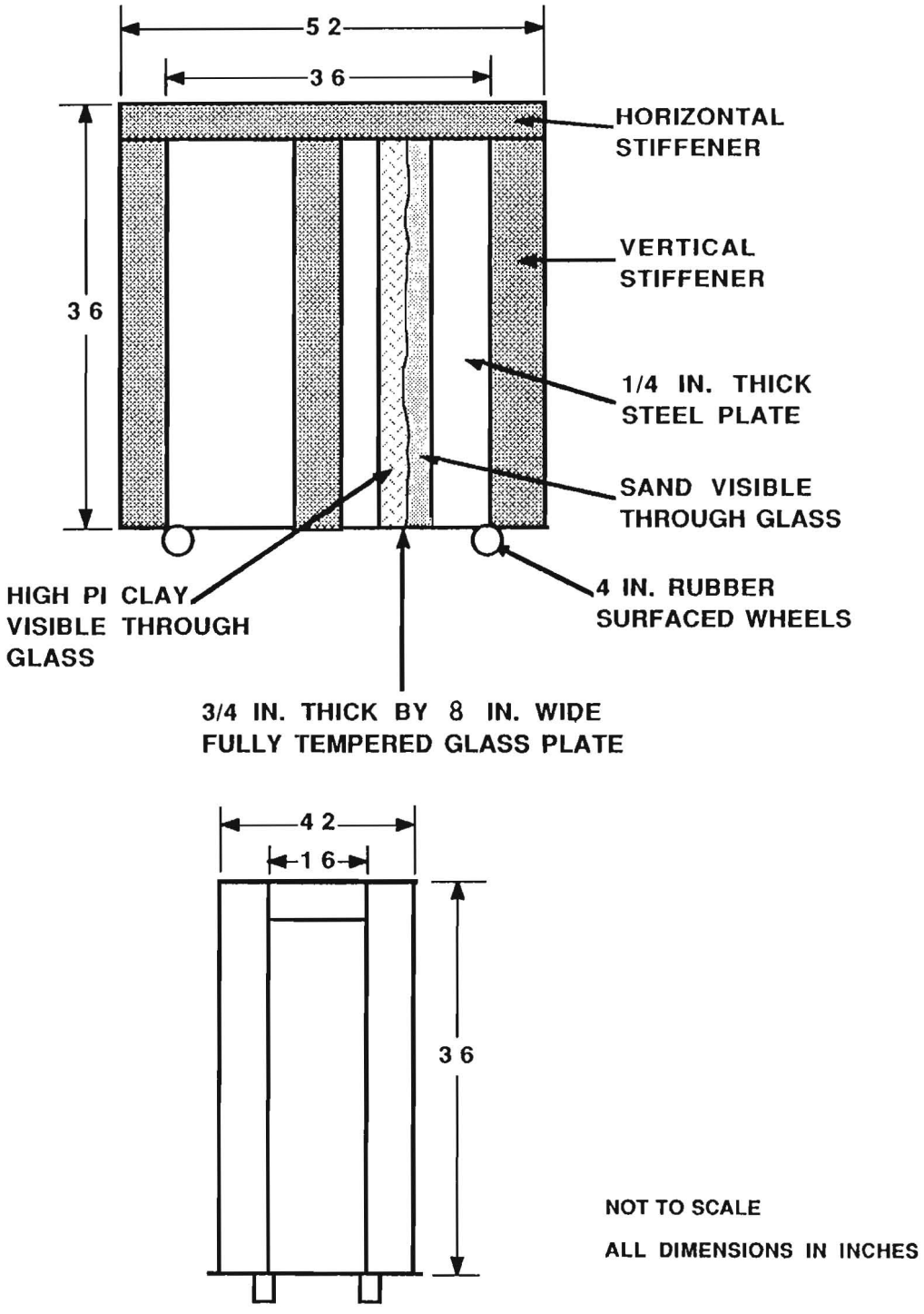

Fig. 3.19. A schematic drawing of a laboratory test box.

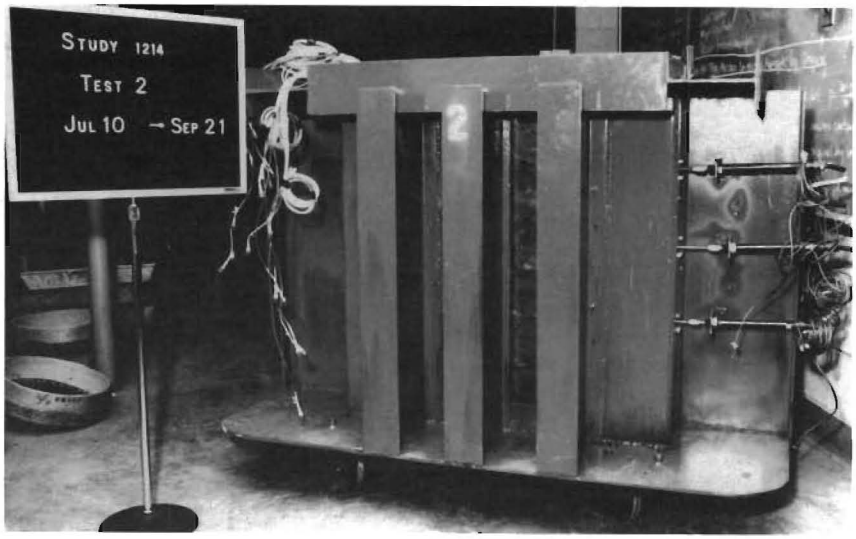

(a)

(b)

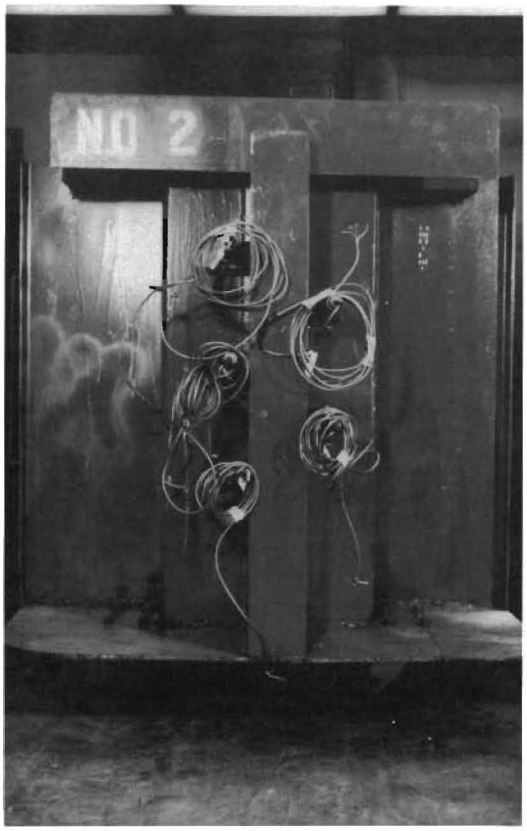

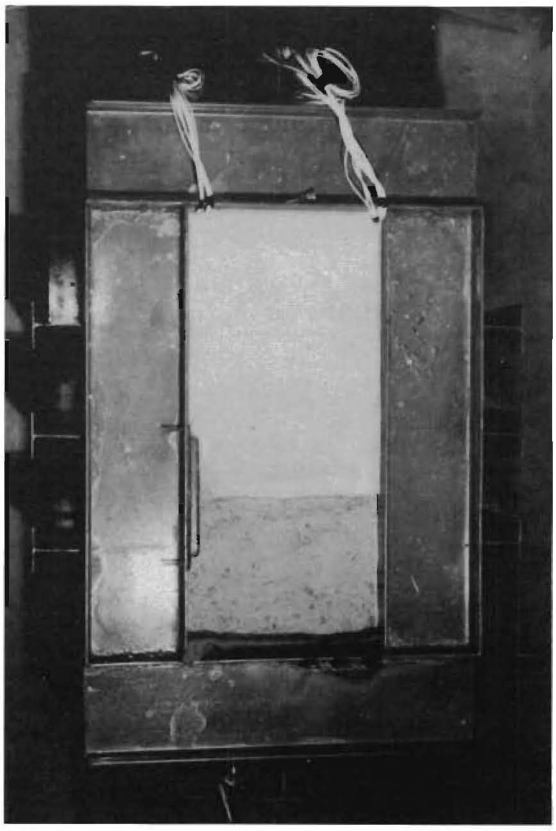

(c)

Fig. 3.20. Photographs of Test Box 2 showing (a) front, (b) side elevations, and (c) top of the test box. Thermocouple psychrometer leads (white wires) were read from one end of the box while the deflection measurement devices (DMDs) were monitored with LVDTs on the opposite end.

maximum dry density as determined by the TEX 115 method. Thus, both soils were compacted as nearly as possible to match SDHPT construction specifications. Pneumatic tamping was not used for compaction of the sand since pneumatic tamping resulted in the sand being scattered.

3. Instrumentation. The soil in the test boxes was instrumented using the thermocouple psychrometers and displacement measuring devices (DMDs). Thermocouple psychrometers were described above in Section 3.C. The DMD is an instrument capable of measuring both the lateral shrinkage of the clay soil and, to an extent, the shrinkage pressure of the clay soil as it shrinks away from the clay-sand interface. Figs. 3.21 and 3.22 show a cross section view and a photograph of the DMD, respectively.

The 3 in. diameter disk of the DMD was embedded in the clay at a distance of approximately 2 in. from the clay-sand interface. As the clay soil lost moisture and began to dry, it shrank away from the sand-clay interface. The embedded disk then moved laterally with the shrinking clay soil. A linear voltage displacement transducer (LVDT) attached to the DMD measured the displacement of the clay soil away from the clay-sand interface. Using a specially engineered precalibrated spring, the lateral force and the lateral stress created by the shrinking clay could be estimated until fracturing of the intact clay mass occurred.

The clay and sand in the test boxes were instrumented at five levels with four TCPs and one DMD in each layer. The bottom most level of instrumentation (Level 1) was placed 12 in. from the bottom of the test box and each succeeding level was placed 6 in. above the next lower level of instrumentation. The first TCP of each layer (Position 1) was placed 2 in. from the clay-sand interface on the sand side while the second TCP was placed 2 in. away from the clay-sand interface on the clay side (Position 2). The third TCP was placed 6 in. from the second TCP on the clay side (12 in. from the interface). The fourth TCP was similarly placed 6 in. from the third TCP on the clay side (18 in. from the interface). The DMD of each instrumentation level was installed at the same elevation as the TCPs with the disk of the DMD firmly fixed in the clay soil approximately 2 in. into the clay from the clay-sand interface. Fig. 3.23 shows the instrumentation arrangement.

4. Data Acquisition. Data from the TCPs was acquired using the TCP readout device. The data generated by each DMD was obtained by reading the voltage output of an LVDT using a voltmeter.

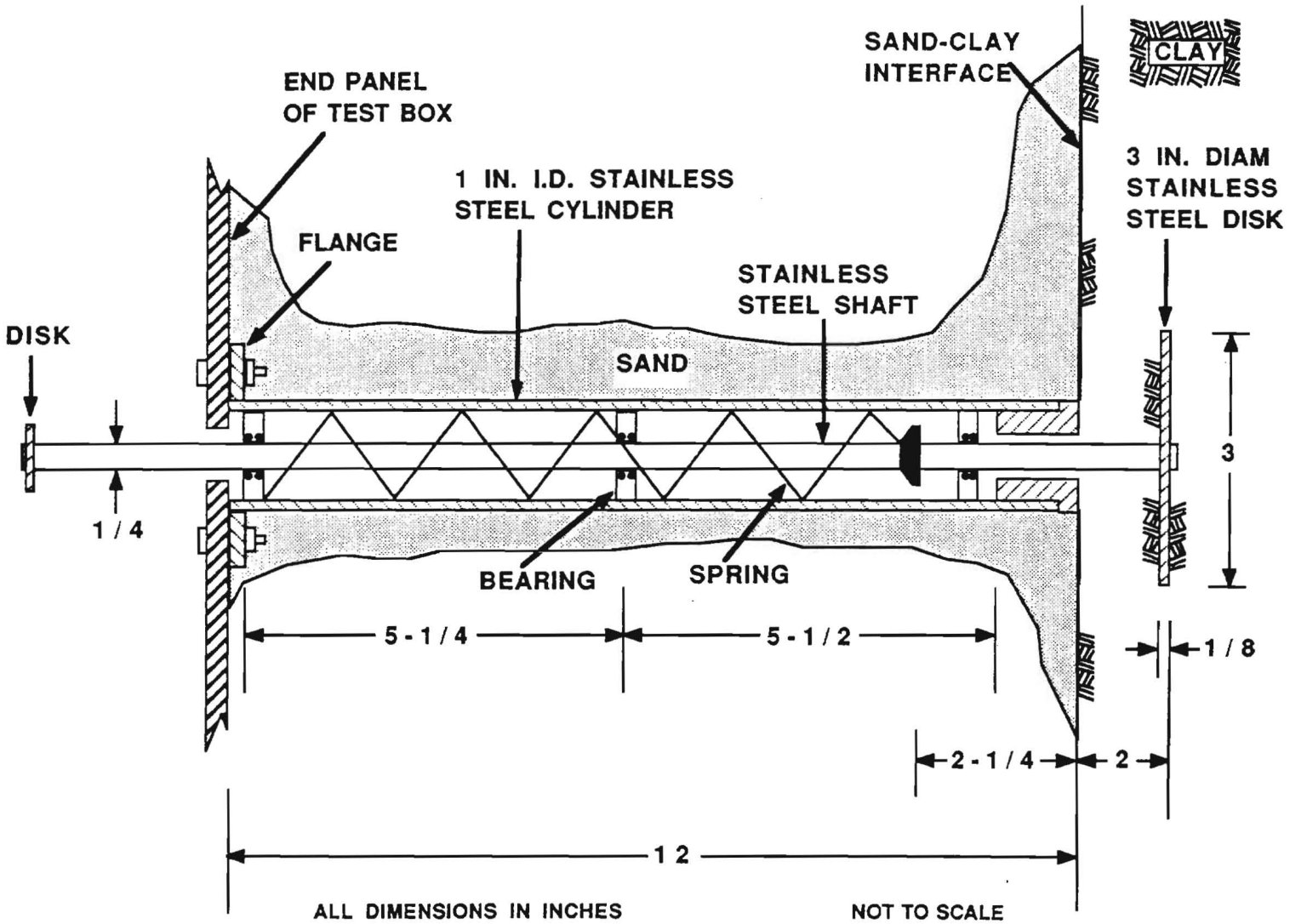

Fig. 3.21. Schematic drawing of deflection measurement device (DMD).

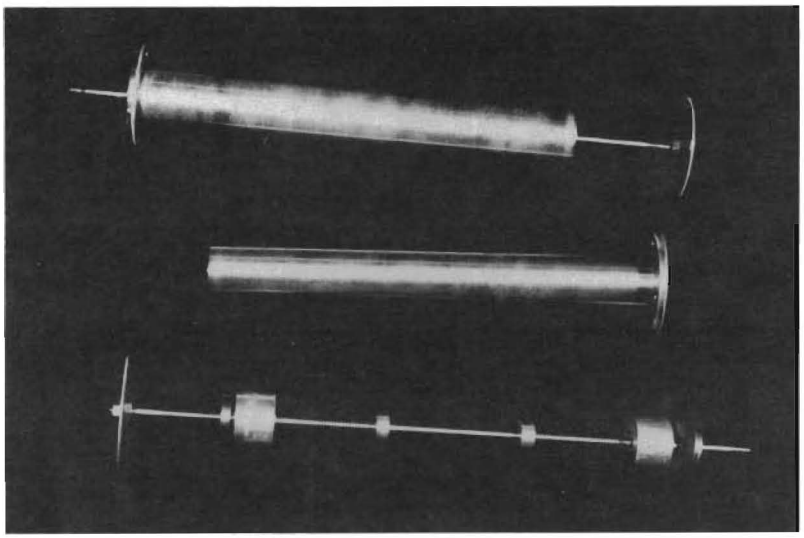

Fig. 3.22. Photograph of deflection measurement device (DMD): internal mechanism, protective stainless steel cylinder, and assembled device, from bottom to top in the photo.

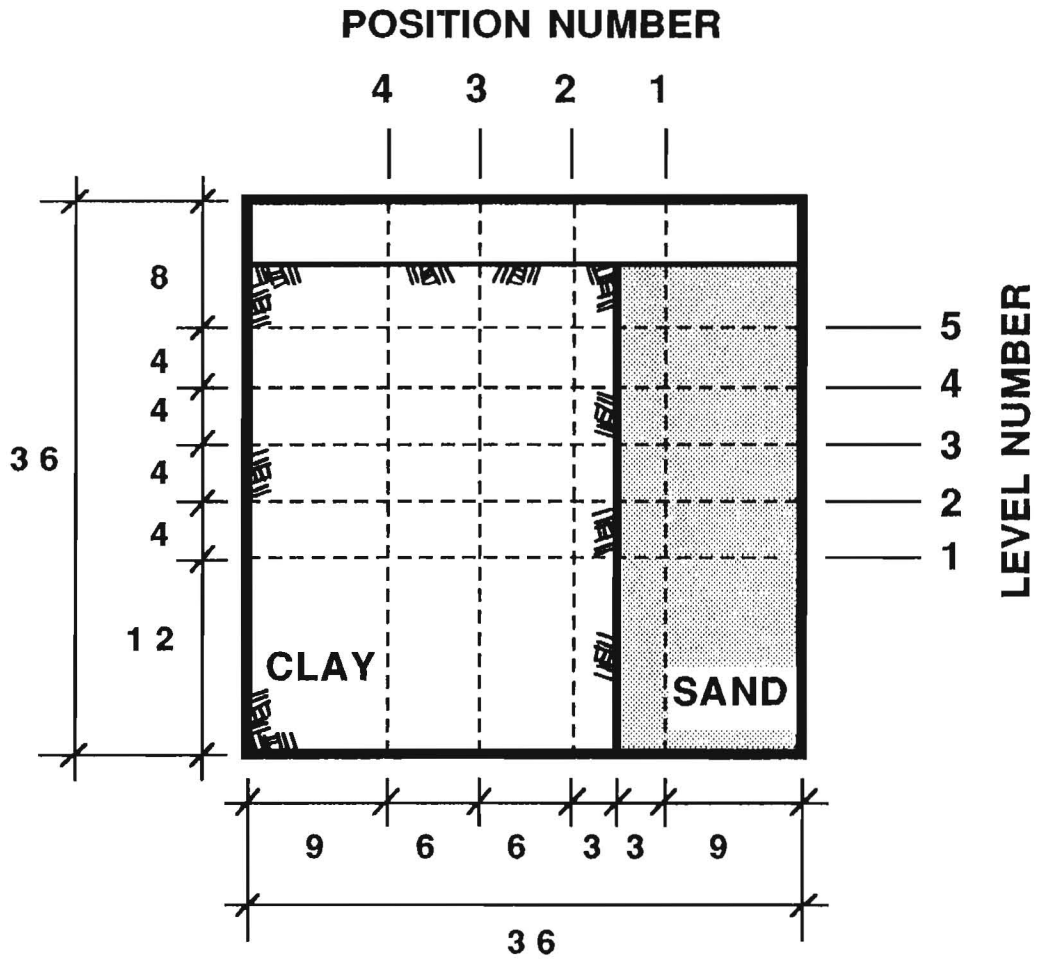

Fig. 3.23. Schematic drawing showing the location of thermocouple psychrometers and deflection measurement devices as they were installed in each test box. Instruments were identified by "level" (vertical reference) and "position" (horizontal reference).

4. RESULTS AND DISCUSSION

A. LABORATORY TESTS

1. Test Plan. The objective of the laboratory tests was to attempt to duplicate in the laboratory the cracking conditions that had been observed in the field. Full-scale modeling was considered impractical but it was believed that a scale model of the embankment-RSRW situation of sufficient mass would be capable of reproducing the field situation. Thus, the steel test boxes described in Section 3.G. were constructed. The climates of Corpus Christi and Lubbock are quite similar (TMI for Lubbock is approximately -20 in./yr vs. Corpus Christi's average TMI of -21.1 in./yr) although Lubbock has a colder winter season than Corpus Christi. Thus, the test boxes were placed in the heated but not air conditioned Structural Engineering Laboratory of the Texas Tech Civil Engineering building which permitted the soil to experience summer temperatures in the summer but not freezing temperatures in the winter.

Clay soil was taken from the same borrow pit used in constructing the SH 358 embankments in Corpus Christi and transported to Lubbock for use in constructing the "embankments" in the test boxes. Sand from Flour Bluff (near Corpus Christi), which was a source for the select cohesionless backfill used with the RSRWs, was also transported to Lubbock for use in constructing the "RSRW backfill" in the test boxes. The method of constructing the embankments was described in Chapter 3. One principal deviation in the method of constructing the laboratory test box embankment-RSRW backfill system from that used in the field is that the test box "embankment" was not constructed first and then "cut back" before placement of the cohesionless backfill. The field sequence of construction was employed in the initial attempts made in constructing the test box systems but was quickly rejected because the confining nature of the stiff box made it extremely difficult to remove ("cut back") the compacted clay; the box had to be suspended nearly upside down by an overhead crane and power digging tools employed to remove the clay a little at a time. Consequently, the clay-sand system was constructed in simultaneous compacted lifts (i.e., a lift of clay was placed and compacted and then a sand lift of the same compacted thickness was placed and tamped). Instrumentation was installed as the compacted thickness increased. Each instrument was tested several times during the compaction process to ensure that each sensor was working and had not been damaged by the compaction effort. A total of 20 TCPs and 5 DMDs were placed in each test box as indicated in Fig. 3.23. Figure 3.20 is a photograph of one of the completed test boxes.

The test plan consisted of four separate tests. Test 1 consisted of clay and sand only. Test 2 consisted of clay and sand with the surface of the clay covered with an impermeable material to prevent surface evaporation. Test 3 consisted of the clay and sand covered with a thickness of caliche (flexible base). Test 4 was identical to Test 3 except the flexible base was surfaced with approximately 1 1/2 in. of hot mix asphalt concrete. The hypothesis to be tested was that the longitudinal cracking observed by District 16 personnel was the result of lateral shrinkage of the clay embankment soil. Thus, each test progressively tested this hypothesis with a sequentially more complete pavement structure.

2. Test 1. Test 1 was designed to test the proposed method of testing, i.e., would the test box provide the expected results? The test was permitted to continue for a total of 125 days. Sensor measurements were made approximately weekly. A surface crack at the interface between the clay and sand was noted very early in the test period. Shrinking of the clay laterally was observed at depth from very early in the test period. The shrinking was observed through the glass window placed at the location of the clay-sand interface. This shrinking was observed to occur in both lateral directions, i.e., away from the sand at the interface and away from the box wall (glass).

Figure 4.1 shows the soil suction changes occurring in Position 1 (sand, 2 in. from the interface) at each level of instrumentation over the entire test period. As shown in Fig. 3.23, Level 5 is the level of instrumentation closest to the surface and Level 1 is the lowest level. The most remarkable aspect of this figure is the steady increase in suction at the Level 5 sensor position over an approximately 6-week period, nearing the upper limit of the TCP's sensitivity before suddenly plummeting (wetting up) followed by an equally quick recovery to a drier condition. The deeper sensors did not exhibit this same dramatic range in measurements but did show a fairly uniform change over time, i.e., the curves were reasonably parallel until the end of the test. Figure 4.2 shows the soil suction changes occurring in Position 2 (clay, 2 in. from the interface) at each level of instrumentation over the entire test period. The Level 5 TCP exhibits the same dramatic increase in suction followed by a sharp wetting with a subsequent sharp return to drier conditions as did the Position 1, Level 5 sensor. Plotting all Level 5 instrumentation readings on the same figure results in Fig. 4.3 which shows that only the two sensors adjacent to the interface exhibited this dramatic change in suction readings. With the exception of the radical changes reported by the Position 2 sensor over the Day 72-Day 91 period, all three TCPs in the clay reported remarkably consistent results.

Figure 4.4 reports the results of the DMDs over the test period. As might have been expected, the Level 5 DMD registered the greatest displacement during the test period. The DMD

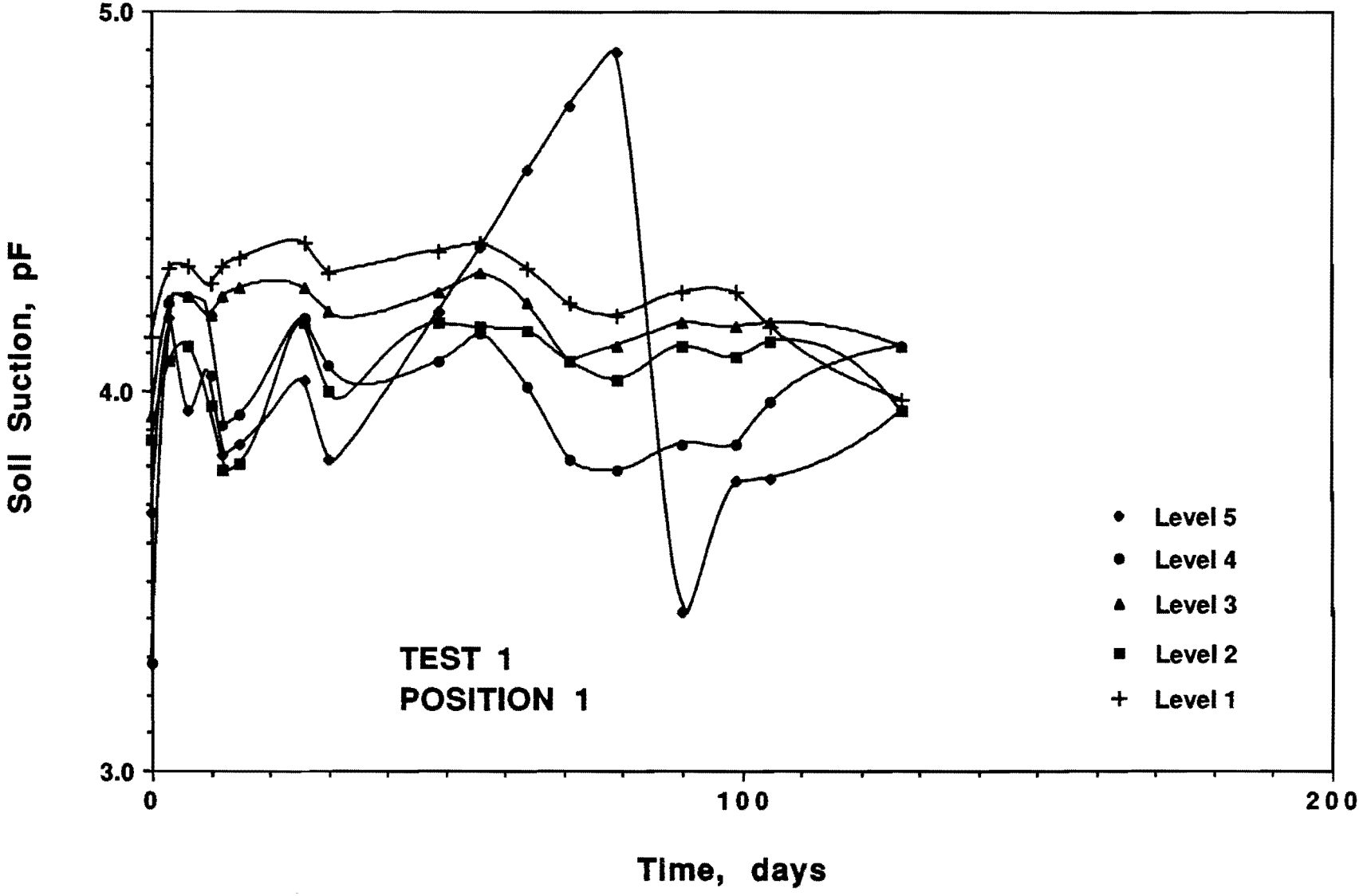

Fig. 4.1. Soil suction vs. time at each sensor level for Position 1 sensors (Test 1).

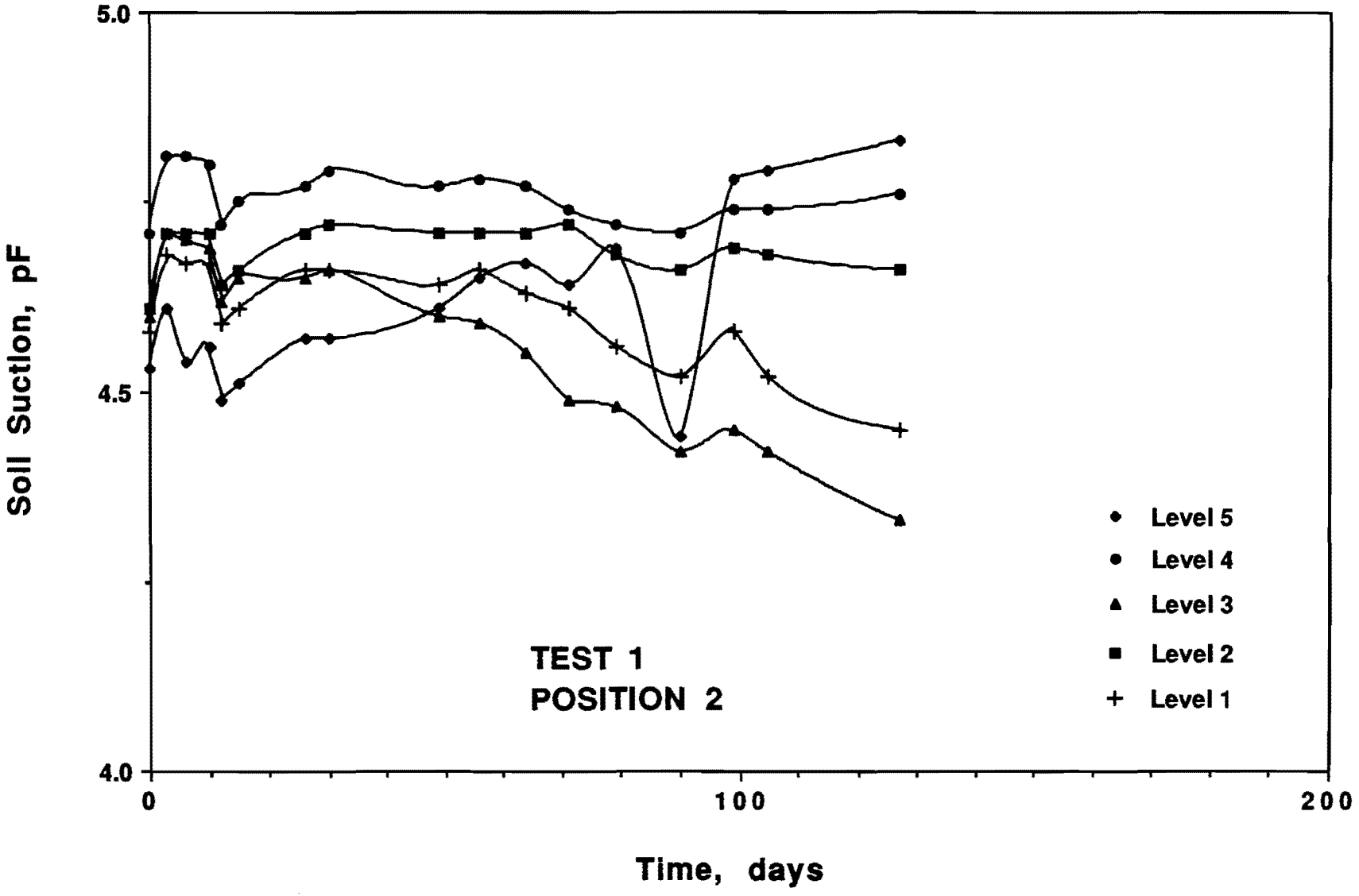

Fig. 4.2. Soil suction vs. time at each sensor level for Position 2 sensors (Test 1).

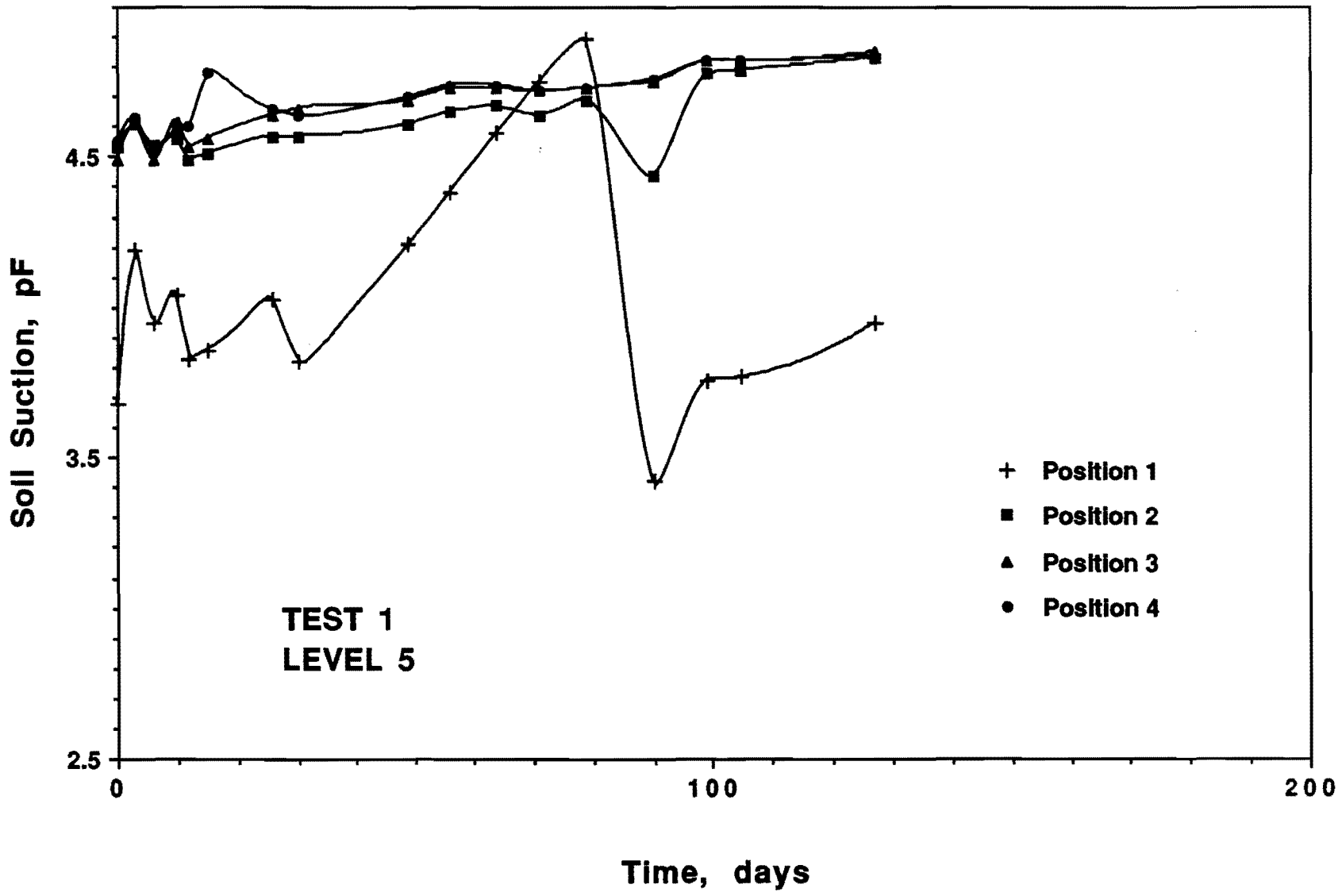

Fig. 4.3. Soil suction vs. time at each sensor position for Level 5 sensors (Test 1).

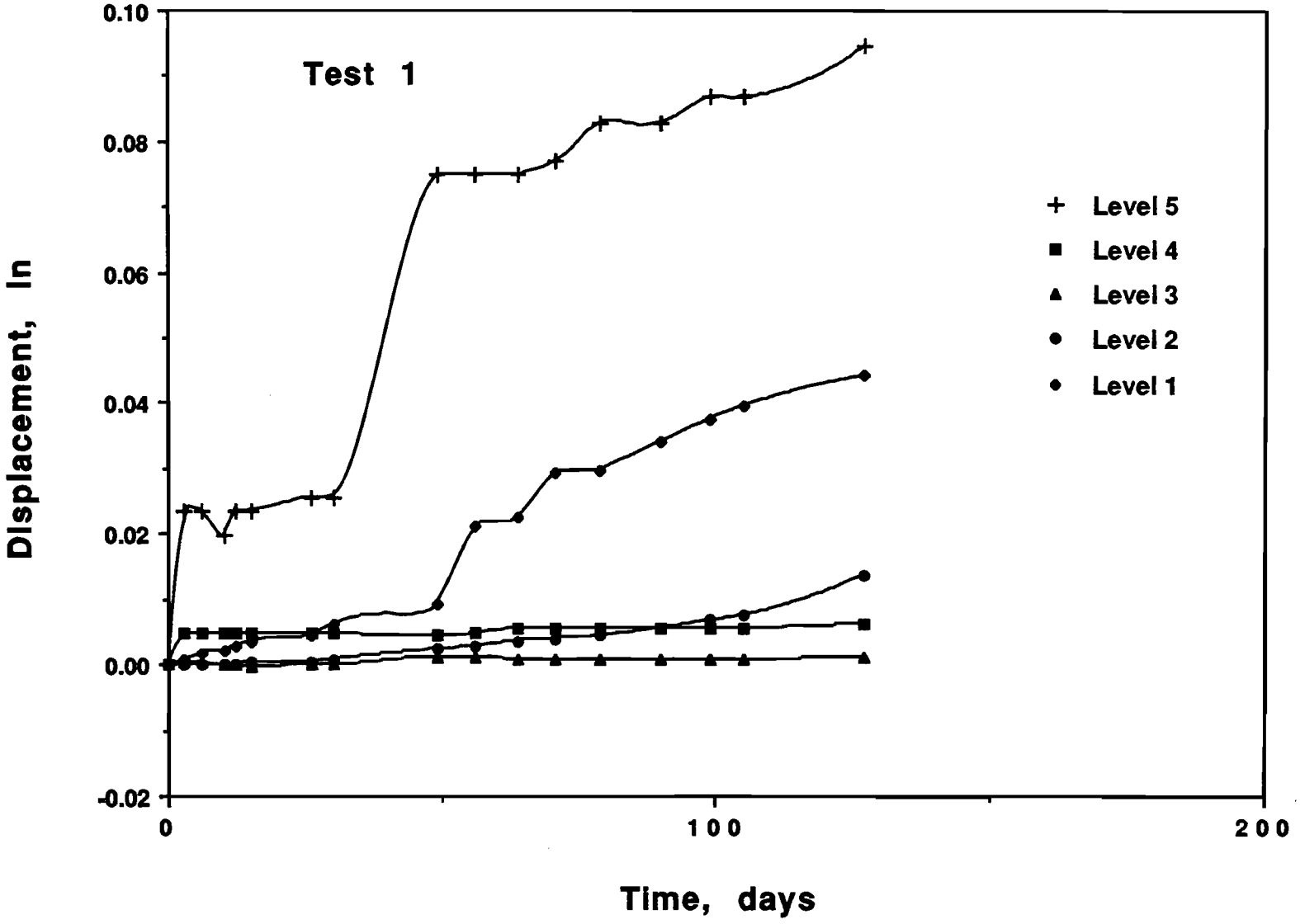

Fig. 4.4. Lateral deflection vs. time as measured by the DMD at each level (Test 1).

at the lowest level measured much smaller displacements but the cumulative displacement curve resembles the Level 5 displacement measurements. The DMDs at the other three levels were oddly nonresponsive. At the termination of Test 1, the soil was removed from the test box. At that time, it was discovered that the 3 in. DMD displacement disk that had been embedded in the clay at levels 2, 3, and 4 had disappeared! Subsequent investigation discovered that the technician that had constructed the stainless steel components of each DMD had run out of stainless steel material and had fabricated several of the disks from aluminum. When embedded in the smectitic soil in the test box, the aluminum chemically reacted with the clay and the aluminum was transferred to the clay particles. Thus, after some period--apparently a fairly short period--there was insufficient disk area to produce displacement measurements. Thus, the valid DMD measurements are consistent with the soil suction measurements, i.e., laterally shrinking soil produced lateral displacements with respect to the clay-sand interface.

Test 1 showed that the test box could adequately duplicate field conditions and produce reasonable results. Consequently, it was concluded that the test sequence should continue.

3. Test 2. Test 2 was designed to ensure that lateral moisture loss and soil shrinkage could be duplicated in the laboratory. Thus, the clay "embankment" was covered with approximately 2 in. of water-impervious wax while the sand was left open to the atmosphere as in Test 1. The test was permitted to continue for a period of 219 days. Sensor measurements were taken approximately every 2 weeks. Like Test 1, a surface crack at the clay-sand interface was noted very early in the test period. Shrinking of the clay laterally was observed at depth through the glass plate at the interface from very early in the test period, similar to Test 1. As in Test 1, this shrinkage was observed to occur in both lateral directions. Figure 4.5 is a photograph of the clay-sand interface at the start of the test. Figure 4.6 is a photograph of the interface at the conclusion of the test. Although not taken at exactly the same location, it is still apparent from comparing the two photographs that considerable lateral shrinkage had occurred over the duration of the test.

Figure 4.7 shows the soil suction changes occurring in Position 2 (clay, 2 in. from interface). This figure is similar to Figs. 4.1 and 4.2 in that a dramatic dip and recovery is noted in the soil suction values over a short period (22 days). In this test, however, four of the five sensors registered these changes simultaneously (with the fifth sensor lagging by about 2 weeks). However, during this test, it was noted that the vertical crack became visible shortly after the dip/recovery changes in soil suction. Inspection of Test 1 notes showed this same sequence, i.e., visible observation of a crack some 3 weeks after the sensor dip. Thus, the

Fig. 4.5 Photograph of the clay-sand interface at the start of Test 1. Note the smooth appearance of both the clay (left side of window) and sand (right side of window) through the observation window.

Fig. 4.6. Photograph of the clay-sand interface at the conclusion of Test 1. It can be seen that a crack has appeared between the clay-sand interface and that the clay has shrunk away from the glass window while the sand has remained in full contact with the glass.

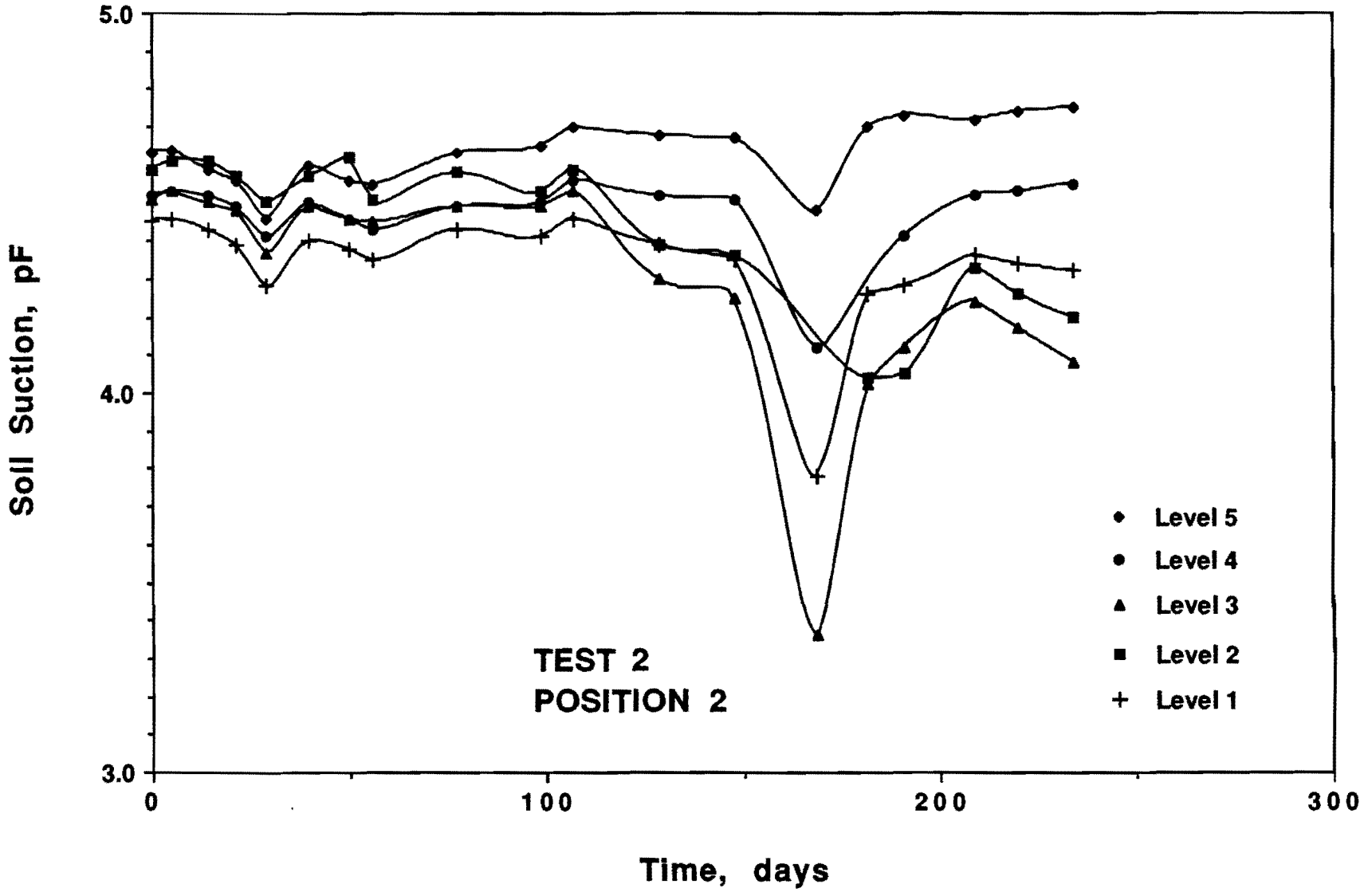

Fig. 4.7. Soil suction vs. time at each sensor level for Position 2 sensors (Test 2.).

change in soil suction actually indicated the inception of the cracking despite the crack being sufficiently small that it could not be seen by the human eye at that time.

Figure 4.8 compares all of the Level 4 instruments. All of the clay sensors exhibited the dip/recovery trend (the Position 4 sensor lagged the others by approximately 2 weeks). The Position 1 (sand) sensor failed after the Day 107 reading. Figure 4.9, showing measurements from mid-depth, shows the sensors at this depth to measure similar dips/recoveries in soil suction as measured at the other levels at the same time. The TCP in the sand at this level also failed following the Day 129 reading; however, the measurements up until failure appeared to be duplicating the now-familiar rapid rise in soil suction followed by the dramatic decline and subsequent dramatic recovery that the other sensors in the sand have recorded.

Figure 4.10 shows the displacements measured by the DMDs (all of which now had stainless steel displacement disks!) in this test. As expected, the level nearest the surface exhibited the greatest displacement (approaching 1/8 in.) with each deeper DMD measuring decreasingly smaller displacements. The two bottommost DMDs registered negligible movement. Fig. 4.11 shows the sand-clay interface at the start of the test and Fig. 4.12 shows the interface at the conclusion of the test. As with Test 1, shrinkage of the clay in both lateral directions can be observed through the window.

Test 2 thus showed that considerable lateral shrinkage could occur beneath a covered surface if permitted to occur. Therefore, commencing Test 3 in the sequence appeared to be warranted.

4. Test 3. The first objective of Test 3 was to determine if lateral shrinkage could occur despite both the clay and the sand being covered. The second objective was to determine if a crack occurred at the clay-sand interface due to lateral shrinkage of the clay, would that crack propagate through the flexible pavement base. Test 2 was not initiated until Test 1 had conclusively proved that the box tests would provide acceptable results. It was planned to wait until the conclusion of Test 2 before commencing Test 3. However, it became apparent that Test 2 was requiring considerably longer time than had been anticipated at the start of the study. Thus, Test 3 was begun prior to completing Test 2. Test 3 was constructed in the same manner as Tests 1 and 2, except that the clay-sand system was stopped a few inches below the level of the system in the first two tests. After the clay-sand system had been constructed and instrumentation installed, approximately 6 in. of caliche was placed and compacted over the top of both the clay and the sand. Test 3 required an even longer period than Test 2; Test 3 was permitted to continue to the end of the study, a period of 265 days.

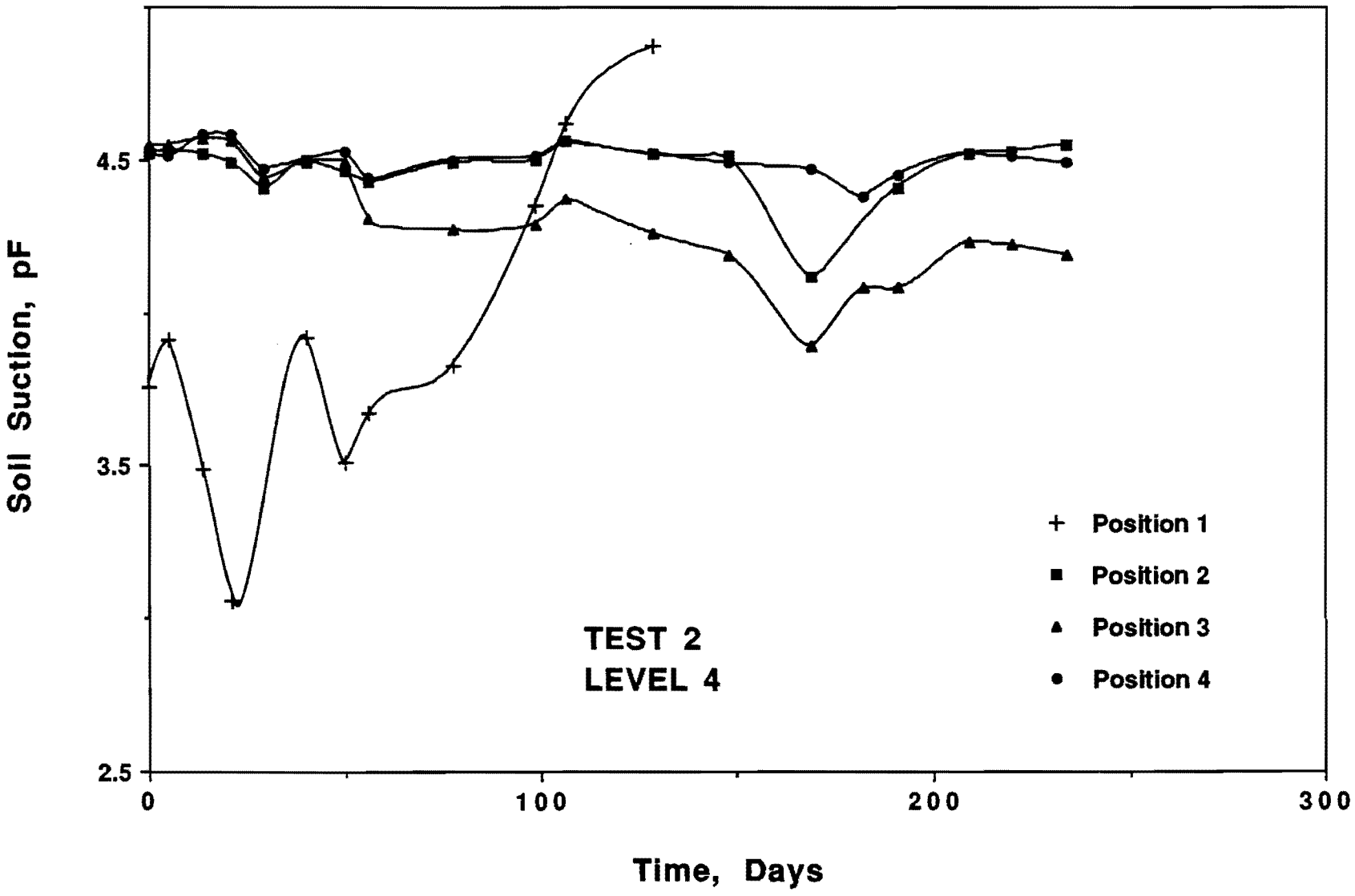

Fig. 4.8. Soil suction vs. time at each sensor position for Level 4 sensors (Test 2).

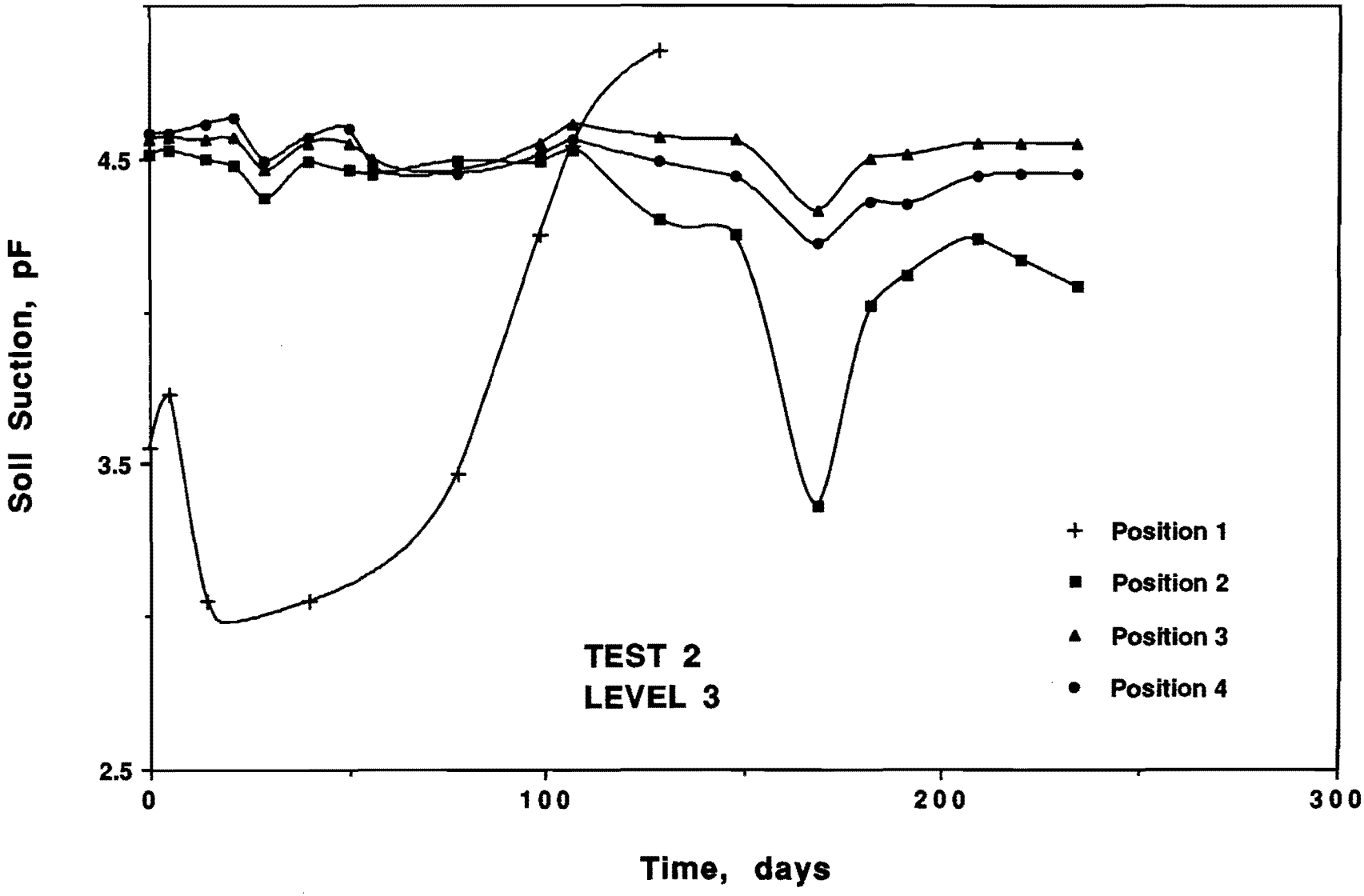

Fig. 4.9. Soil suction vs. time at each sensor position for Level 3 sensors (Test 2).

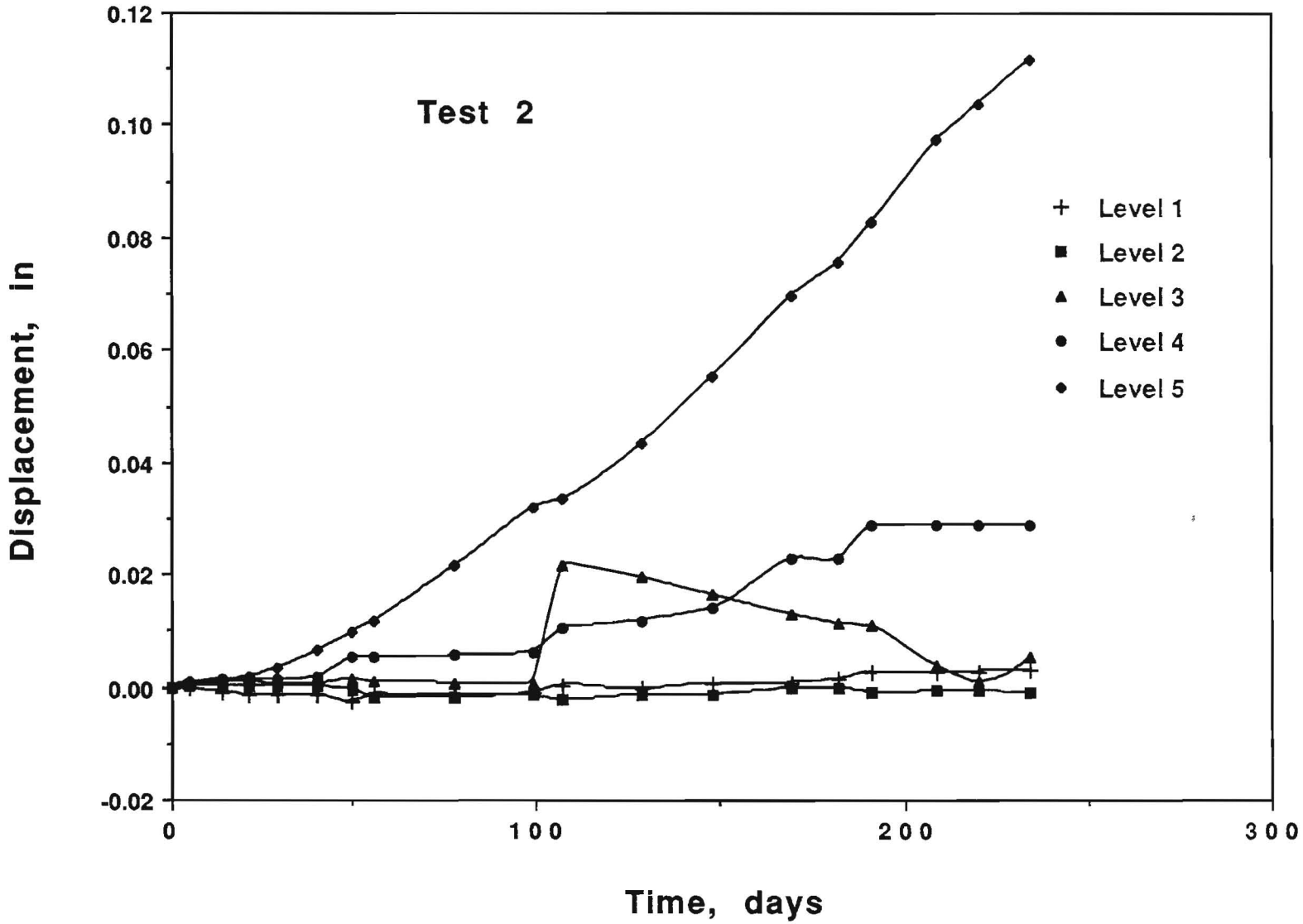

Fig. 4.10. Lateral deflection vs. time as measured by the DMD at each level (Test 2).

Fig. 4.11. Photograph of the clay-sand interface at the start of Test 2.

Fig. 4.12. Photograph of the clay-sand interface at the conclusion of Test 2 showing shrinkage of the clay soil away from the glass window as well as from the sand backfill.

Two events of possible significance occurred during Test 3. At the outset, it was estimated that a certain period would be required to complete the four box tests. However, by the time the end of that period arrived, Tests 3 and 4 were still far from being completed. Demands on the structural test lab floor space are always at a premium and another research project required the space occupied by the three test boxes. Test 2 had been completed and could be unloaded but Tests 3 and 4 needed more time to complete their respective tests. As a result, the Test 3 and Test 4 boxes were carefully lifted by overhead crane and lowered to a level below that of the test deck. Although the moving was done very carefully and no jolting, shaking, or other shocks were observed during the moving operation, it is not certain that none occurred. Such jolting, shaking, or shocking could alter the test in progress, modify cracking patterns, or otherwise affect the test. Sensor readings made following the moving showed no particular change in soil suction measurements; however, DMD measurements following the moving were illogical and unexplainable, with the measurement on one date indicating shrinkage and the next measurement implying swelling. These erratic readings were recorded for the remainder of the test period. It was subsequently concluded that the soil mass surrounding the DMD disks had in some manner fractured as a result of the moving process with the result being that the displacement disks were no longer responding to a coherent soil mass attempting to shrink. Thus, DMD measurements were disregarded in analyzing the results from Tests 3 and 4.

The second event of possible significance occurred following the measurements taken on Day 104 of the test period. The TCP readout device malfunctioned and had to be returned to the manufacturer for repairs. This entire period took 65 days and no measurements were able to be acquired over this time. Thus, it is uncertain what might have happened during this period but if the acquired data is reviewed while remembering the trends observed in Tests 1 and 2, it is probable that little significant data was lost despite the lengthy period of no monitoring.

Figure 4.13 shows the measurements at Position 2 (clay, 2 in. from interface) at each instrumentation level. The two uppermost levels showed the same trend as in the two earlier tests: an increase in soil suction followed by a dramatic dip in suction with a subsequent quick recovery to a higher suction value. The TCP at Level 3 exhibited this same trend. A crack was observed in both the caliche surface and at the clay-sand interface approximately a month following the dip/recovery measurements, an event consistent with that noted in Tests 1 and 2.

Figure 4.14 compares the suction readings over the test period from each of the Level 5 TCPs. The sensor in the clay closest to the clay-sand interface (Position 2) suggests that a crack probably occurred between Day 187 and Day 204. The Position 3 sensor (9 in. from the clay-sand interface) data indicates that a cracking event probably occurred after Day 195. The

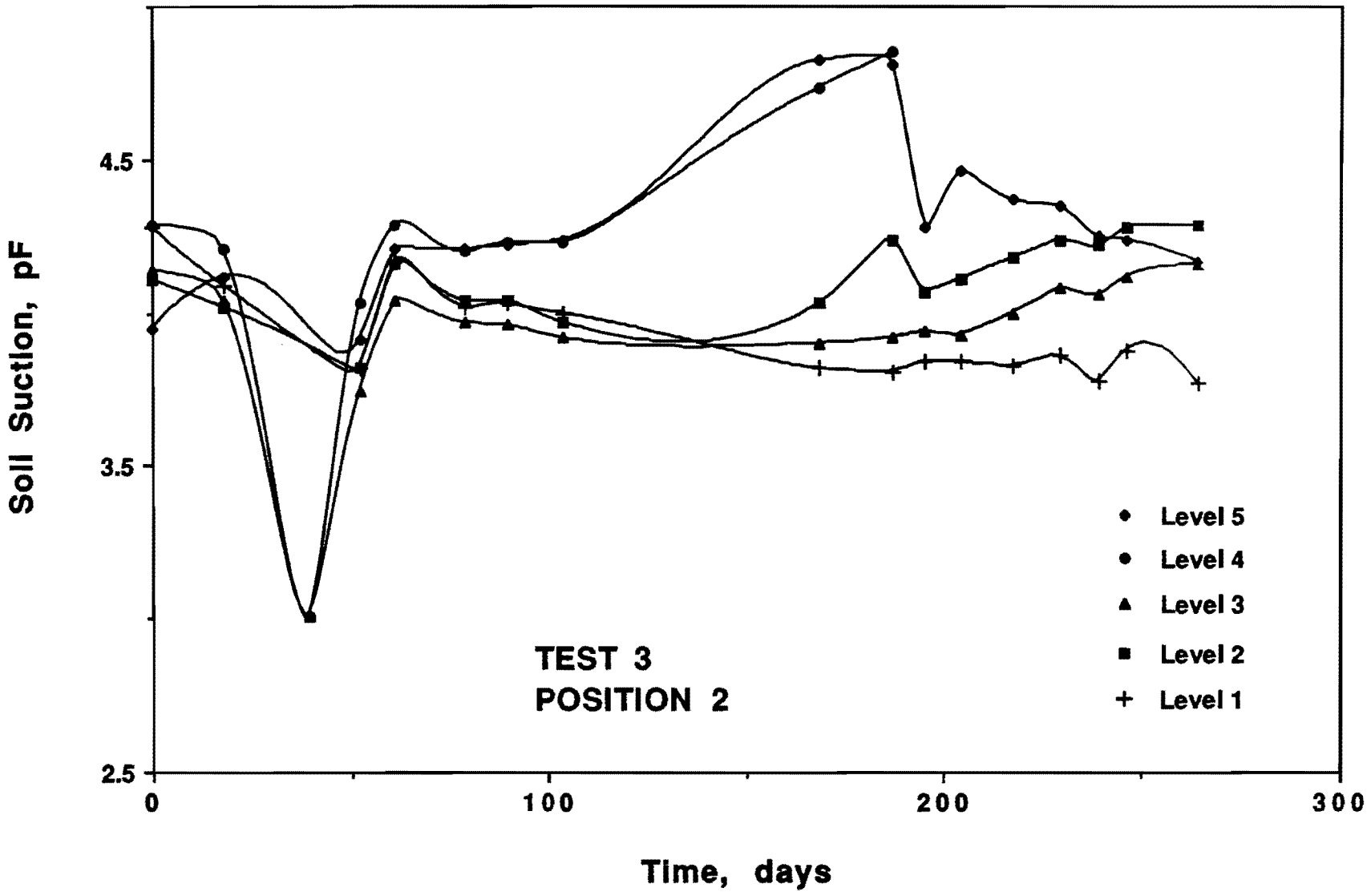

Fig. 4.13. Soil suction vs. time at each sensor level for Position 2 sensors (Test 3).

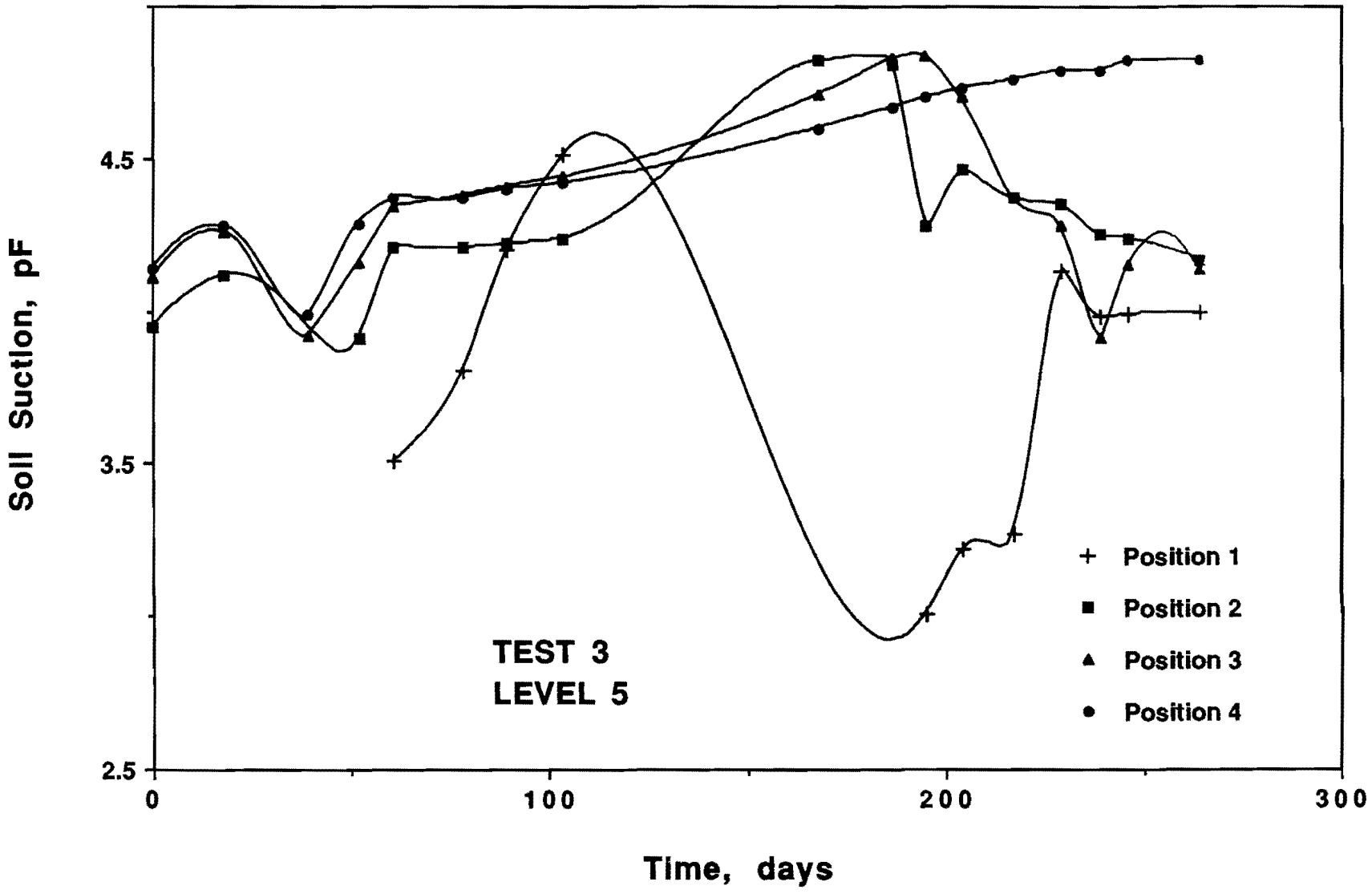

Fig. 4.14. Soil suction vs. time at each sensor position for Level 5 sensors (Test 3).

Position 4 sensor (15 in. from interface) data shows the clay to be getting steadily drier through the end of the study. The TCP in the sand (Position 1, 2 in. from the interface) yields inconclusive data. The sensor refused to provide readings at the beginning of the test (despite yielding readings during the test box construction). The sensor, however, began providing data on Day 63. However, no data was acquired during the period the readout device was being repaired. Once the readout device was back in operation, the psychrometer did not yield a reading until Day 195. All data acquired after the Day 195 reading suggests that the cracking event had already occurred and the data being captured after Day 195 was on the "recovery" part of the dip/recovery curve.

Fig. 4.15 shows the interface separation and shrinkage at the end of Test 3. The crack produced in this test conforms with the crack observed by the District 16 personnel who cored the SH 358 pavement described in Chapter 3. Thus, based on the results from Test 3, progression to Test 4 was warranted.

5. Test 4. The objective of Test 4 was to see if the laterally shrinking soil could induce a tension crack to occur through both the flexible base and asphaltic concrete surface. As described above, Test 4 was initiated prior to Test 3 being completed because of the time expected to be required to complete the test. Test 4 began approximately 6 weeks after Test 3 was started.

The Test 4 system was constructed in the same manner as the Test 3 system with approximately 1 1/2 in. of hot mix asphalt concrete (HMAC) applied to the surface of the caliche base. Compaction was obtained by using a pneumatic tamper which did not produce a conventional smooth surface. However, the proper compaction of the hot mix was considered to be more important than an attractive appearance of the finished surface in this instance. The duration of this test was 234 days and was only discontinued at the end of the study period.

As was discovered from Test 3, the DMD results were illogical. As in Test 3, it was concluded that during the moving of the boxes from the structural test deck level to a subbasement level, the soil mass was somehow disturbed and the DMDs no longer yielded valid measurements. As a result, the Test 4 DMD results were disregarded as being invalid.

Test 4, for some reason, seemed to have acquired all of the sensors that were doomed to malfunction. As a result, the data acquired from Test 4 is not as conclusive as that obtained from the three prior tests. Figure 4.16 shows the soil suction data acquired from the TCPs embedded in the sand backfill. As can be seen, this data has virtually no value. Figure 4.17 presents the soil suction changes occurring at Position 2 (clay, 2 in. from interface) over the test period. The TCP at the Level 5 position apparently malfunctioned and ceased to yield results

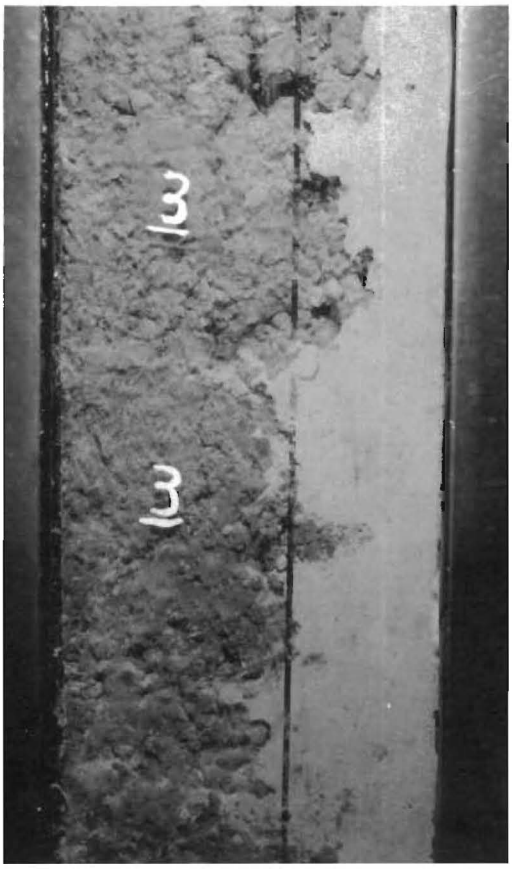

Fig. 4.15. Photograph of the clay-sand interface at the conclusion of Test 3.

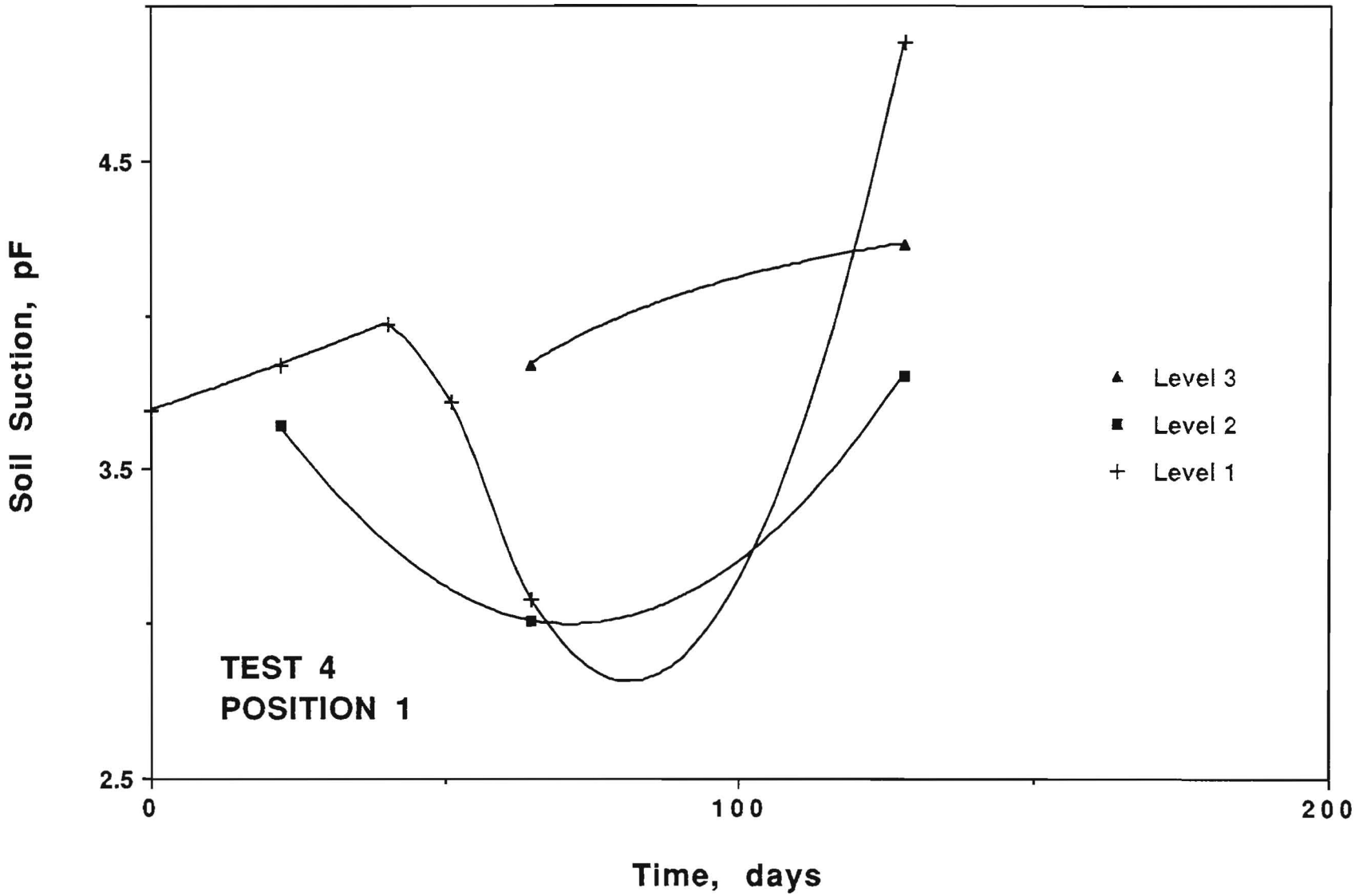

Fig. 4.16. Soil suction vs. time at each sensor level for Position 1 sensors (Test 4).

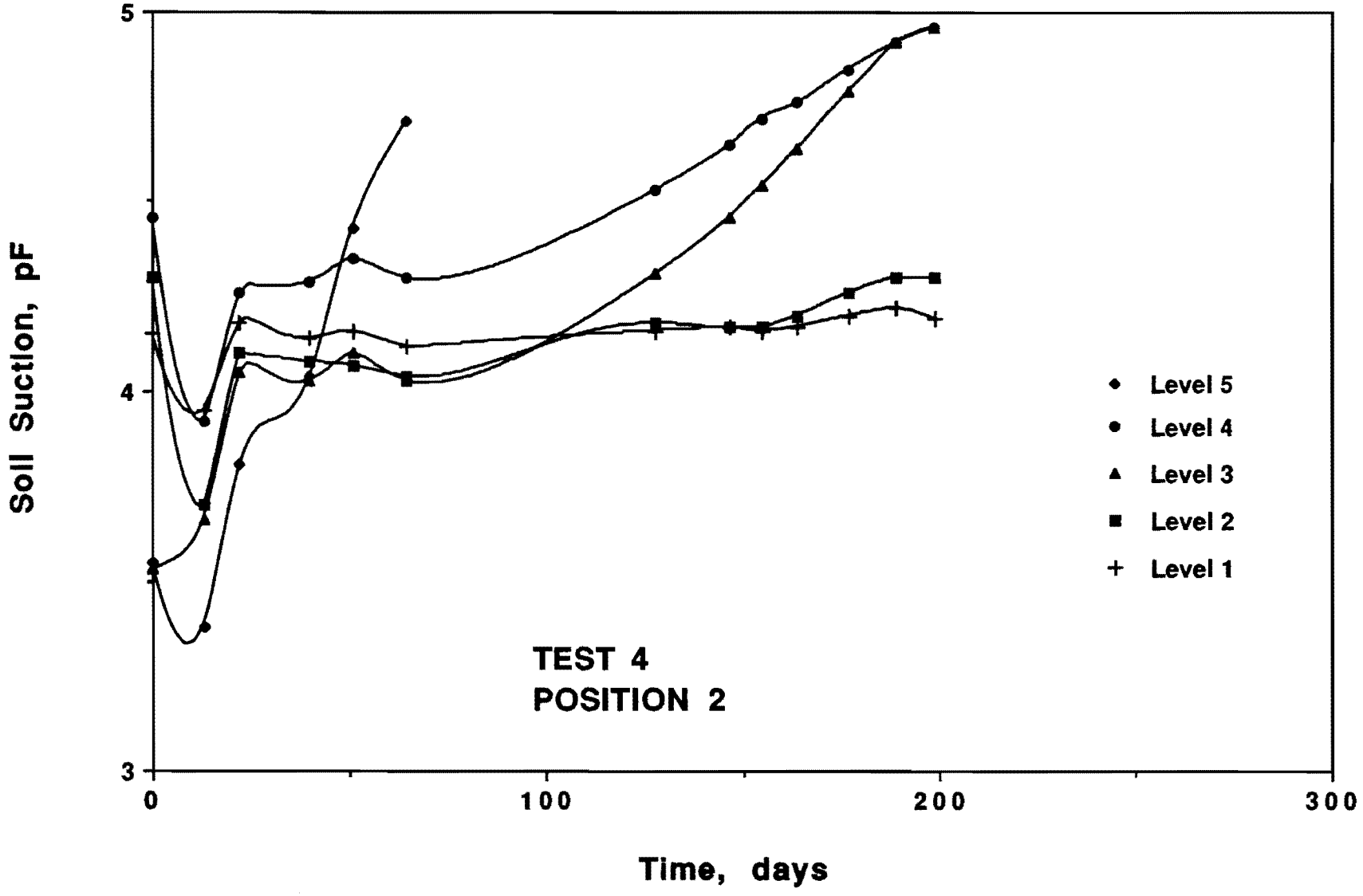

Fig. 4.17. Soil suction vs. time at each sensor level for Position 2 sensors (Test 4).

after Day 65. The TCPs at each of the next two lower levels produced results that suggested that the soil was approaching the dip/recovery event at the end of the study. The data from the two bottommost sensors could be interpreted as supporting the approaching dip/recovery event but the increase in soil suction measured by either instrument is not particularly significant when compared to that measured at the other levels. Figures 4.18 through 4.21 report the changes in soil suction occurring at each level, Level 5-Level 1. All of the Level 5 psychrometers ceased to work after Day 196. Thus, the data reported in Fig. 4.18 is of little use in evaluating what is occurring with respect to changes in soil moisture conditions and the formation of shrinkage cracks. Figure 4.19 reports the data from Level 4.

Although the TCP embedded in the sand failed, the three sensors in the clay continued to respond through the termination of the project. The sensor closest to the interface shows more drying than the sensors more removed from the interface. All show a continued drying trend through the end of the study. The Position 2 psychrometer in Fig. 4.20 shows the same drying trend as the Position 2 sensor in the level above it. Although the increase in soil suction measured by the Position 3 and Position 4 sensors in Fig. 4.20 is nearly negligible, the trend by all three sensors is to suggest that a maximum value has been reached and a reduction in suction value is about to occur. However, by the time the sensors at Level 1 (neglecting the Position 1 sensor) are evaluated (Fig. 4.21), the clay suction values have changed very little since early in the life of the test.

No crack was observed in the surface of the HMAC in Test 4 by the termination of the study. However, a gap of approximately 1/16 in. between the bottom of the HMAC and the top of the caliche could be observed through the side window. An obvious shrinkage crack could also be seen between the clay and the sand, and the clay had shrunk away from the glass surface as seen in Fig. 4.22. The gap between the HMAC and caliche that could be seen through the glass window could not be captured in a photograph; however, Fig. 4.23, taken from the top of the test box after part of the HMAC had been removed after the conclusion of the test, shows that the gap extended across nearly the whole width of the box.

The separation between the clay and the sand had propagated through the depth of the caliche above the clay-sand interface. This could be observed through the window. Thus, the HMAC had adhered to the steel walls of the test box and, even when contact was lost between the HMAC and the underlying caliche, the bond between the HMAC and the steel walls was sufficiently great such that the weight of the HMAC did not shear the bond and permit it to drop and remain in contact with the flexible base. Consequently, because the bond created between the HMAC and

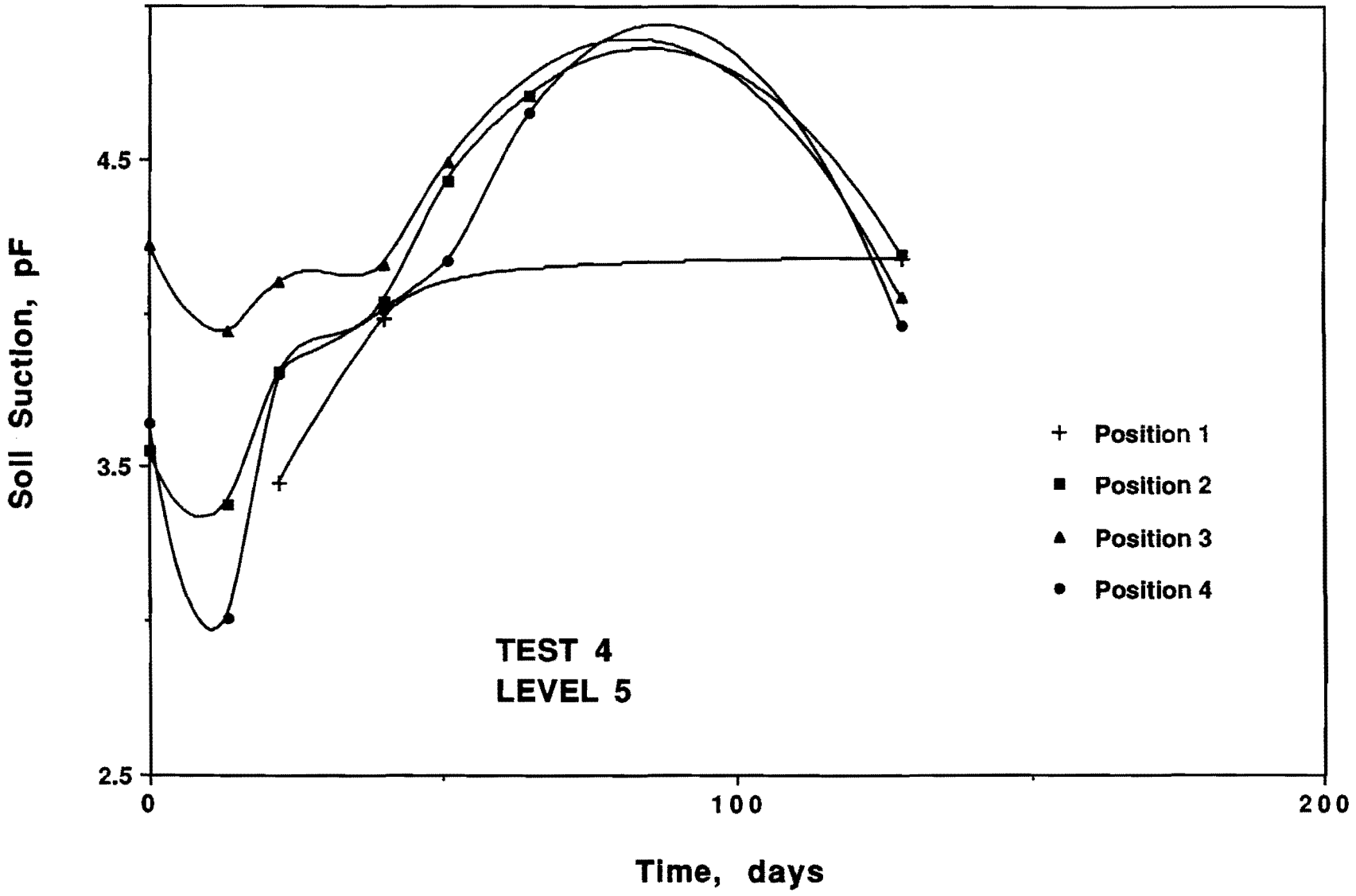

Fig. 4.18. Soil suction vs. time at each sensor position for Level 5 sensors (Test 4).

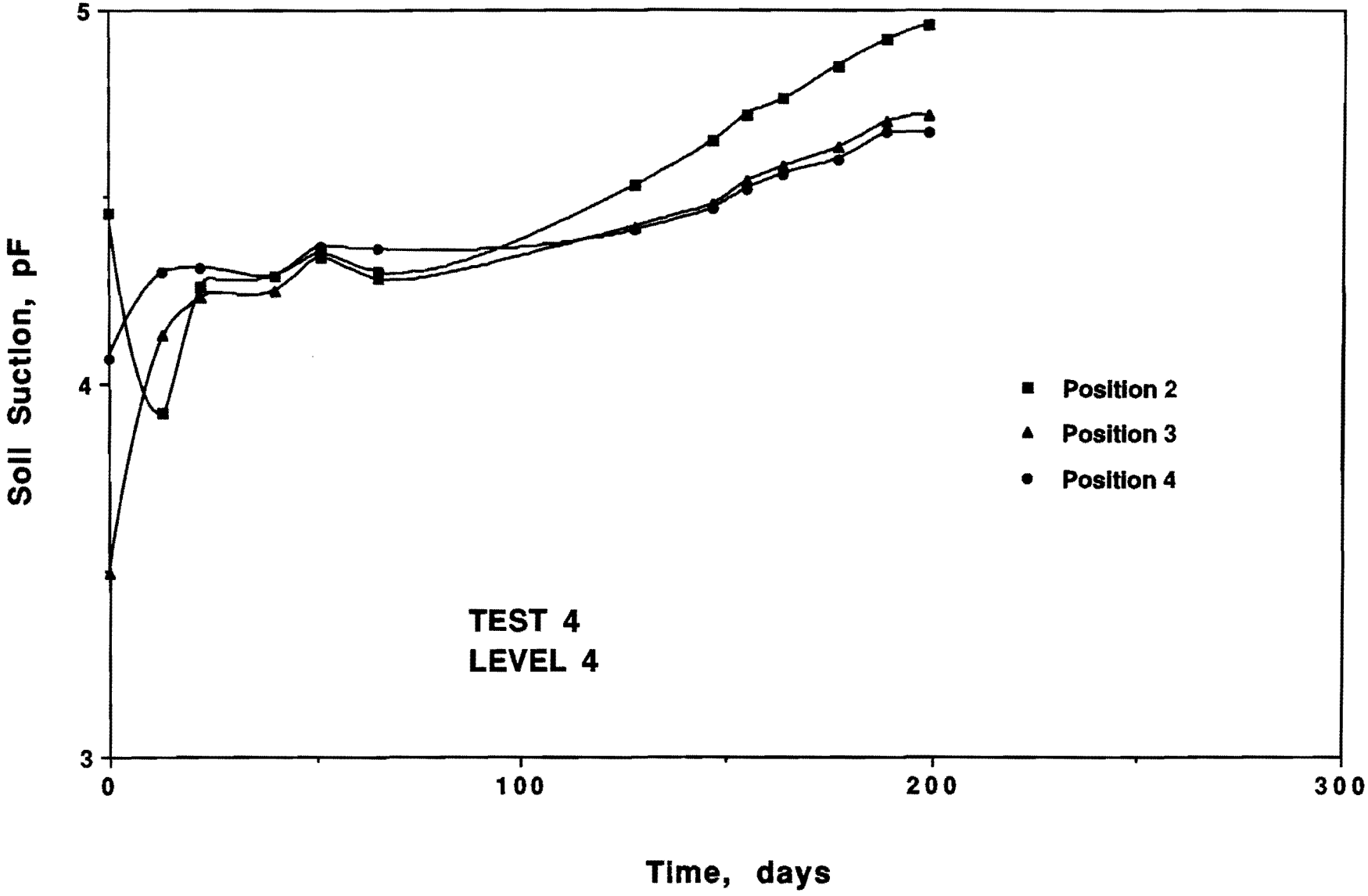

Fig. 4.19. Soil suction vs. time at each sensor position for Level 4 sensors (Test 4).

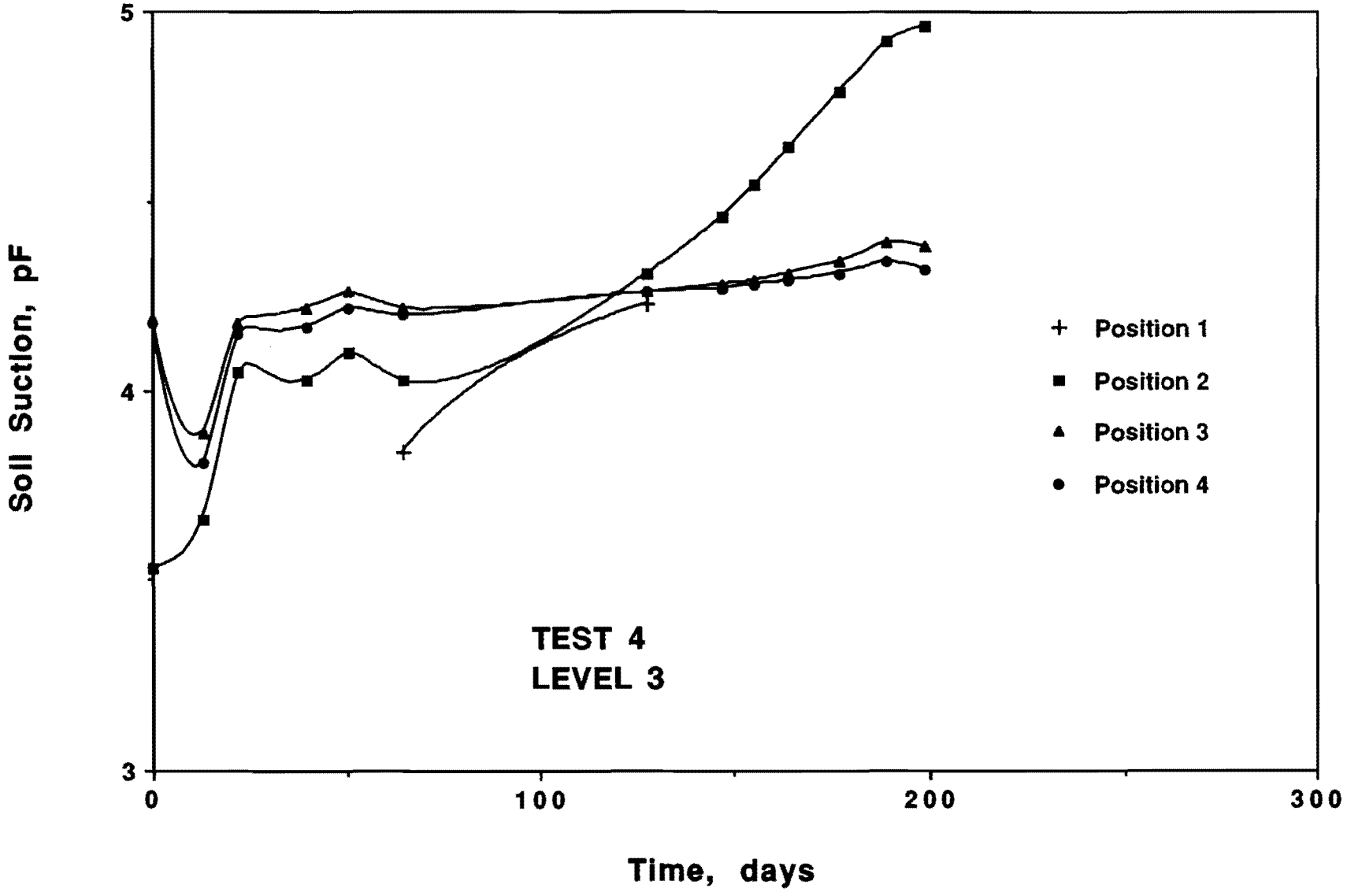

Fig. 4.20. Soil suction vs. time at each sensor position for Level 3 sensors (Test 4).

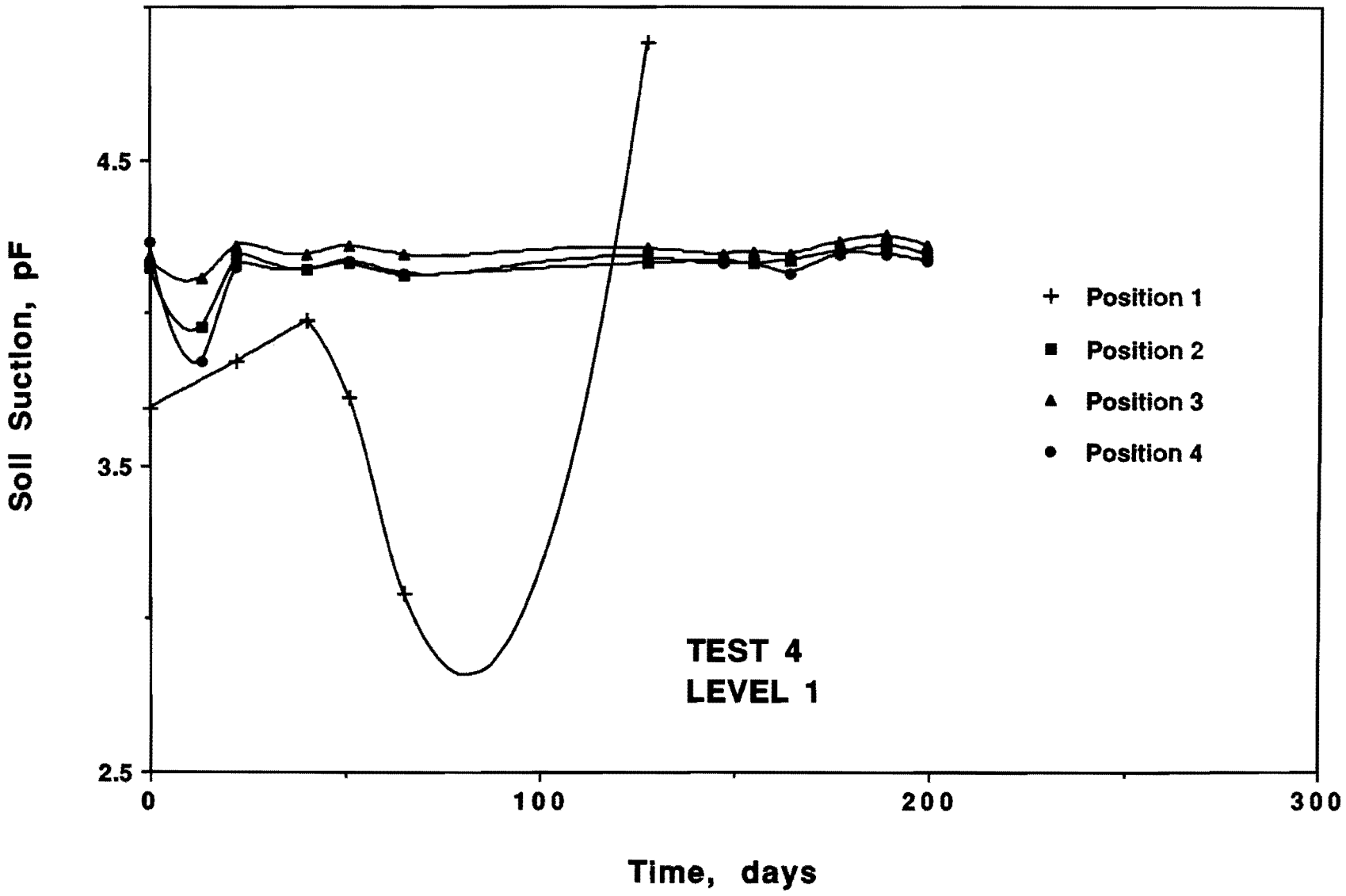

Fig. 4.21. Soil suction vs. time at each sensor position for Level 1 sensors (Test 4).

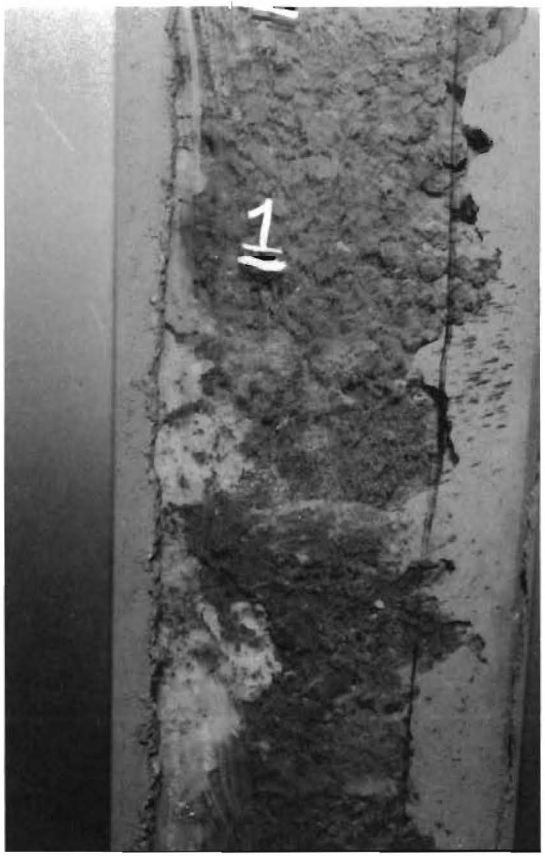

Fig. 4.22. Photograph of clay-sand interface at the conclusion of Test 4. (The number "1" on the window glass refers to Text Box 1, not Test 4.)

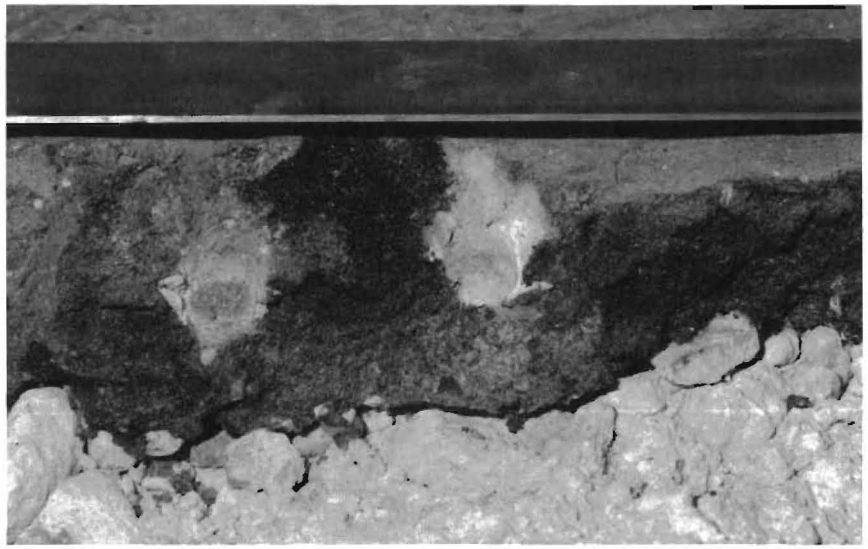

Fig. 4.23. Photograph of gap between the HMAC and the caliche base (Test 4).

the caliche was lost during the shrinking of the clay mass, no crack was able to propagate through the asphaltic concrete despite a crack occurring in the caliche.

6. Discussion. The laboratory test sequence showed that (1) a crack could occur between the clay and sand due to lateral shrinkage of the clay, and (2) this crack could propagate through the flexible pavement base. Thus, if the process which created the cracks in the laboratory is also responsible for the cracks observed in the field, the mechanism which actually creates the crack in the asphalt concrete is frictional force between the asphaltic concrete and the underlying flexible base. This hypothesis is predicated on good bonding between the clay and the flexible base and between the flexible base and the asphalt concrete.

As reported by Wimsatt and McCullough (1989), the tensile strength of asphaltic concrete is in the range of 90-100 psi (others have reported tensile strengths to range from 70-150 psi, depending on aggregate type, size, and shape as well as other factors). Thus, temporarily setting aside the question of the method of transfer between materials and courses, the question first needing to be addressed is the one of whether or not the shrinking soil can produce lateral stresses that can exceed the tensile strength of asphalt concrete.

From Chapter 2, an equation for estimating the lateral pressure developed in a shrinking soil was developed:

$$K_o\sigma_v = \frac{3}{2}\,\sigma_l\,[10^{\alpha}]\,[m^{\beta}] - \frac{\sigma_v}{2} \qquad (2.35)$$

From laboratory tests, the percentage of clay in the soil recovered from the embankments during instrumentation installation was found to be approximately 66 percent and the PI of the embankment soil was found to be approximately 40. From McKeen (1980), the suction comp-compressibility index can be estimated as 0.163 x 0.66 = 0.108. From Picornell (1985), γ_σ typically is 1.15 - 1.20 times greater than γ_h; thus, γ_σ is estimated to be 0.126. From Appendix C, the pressure due to the weight of the pavement structure acting on the subgrade can be calculated to be 2.138 psi. If field compaction specifications are met, a minimum of 78.12 psi of compaction energy is imposed on the compacted soil. Using the initial equilibrium soil suction pressure of 3.92 pF (8,300 cm water) and final suction pressure measured at Position 2, Level 4 from Test 4 (Fig. 4.19), which was measured to be 4.96 pF (91,200 cm water), the shrinkage lateral stress generated by the embankment soil in arriving at its final soil moisture condition was approximately 25,700 cm water or 366 psi. Thus, the lateral pressure generated by the shrinking soil exceeds the tensile strength of the HMAC by a considerable amount.

B. FIELD INSTRUMENTATION

The purpose of the field instrumentation was to install soil moisture condition sensors in newly constructed embankments and monitor the changes in soil moisture conditions over a period after the embankment and RSRW backfill were covered with pavement. The exact hoped for situation for the installation of the instrumentation was not able to be achieved during the study period. The sensors were installed in June, 1989. At that time, there were no roadway sections ready for paving; the instrumented sections were paved in June and July, 1990. Thus, although the instrumentation had an opportunity to measure changes in soil moisture conditions for a full year prior to paving, the funded study was concluded in August, 1990.

Despite not being able to acquire a comparison of the measured changes in soil moisture conditions before and after paving and the appearance or nonappearance of cracking in the asphaltic concrete pavement during the study period, the instrumentation was, nonetheless, able to provide valuable and interesting data regarding changes in soil moisture conditions occurring in the embankment between the time of its construction completion and the time of being paved.

1. Old Brownsville Road Site. Figure 4.24 shows the suction measurements made in the cohesionless backfill, approximately 2 ft from the clay-sand interface. Readings were taken over a 15-month period. All readings were taken before the site was paved. The November, 1989 reading still reflected the effect of rainfall which had occurred a few days before the measurement visit. With the exception of the November reading, the measurements indicate a fairly narrow range of change in soil moisture conditions, varying between about 3.3 pF and 3.8 pF. Figure 4.25 shows the soil moisture condition changes with depth in the adjacent clay embankment (approximately 2 ft from the clay-sand interface). The readings in the clay show an obviously less variable soil moisture condition; suction measurements differed over only an approximately 0.3 pF range from a depth of 4 ft and deeper. The more variable readings recorded at the 2 ft depth reflect the effect of climate. The November, 1989 readings also reflect the effect of the rainfall preceding the measurement visit.

2. Bear Lane Site. Taken as a whole, the cohesionless backfill instrument readings for this site differ considerably from those in the sand at the Old Brownsville Road site (Fig. 4.26). However, if the August, 1989 and January, 1990 readings are neglected, the readings show close agreement with those taken at the Old Brownsville site, with suction measurements varying between approximately 3.4 pF and 3.9 pF. The August, 1989 reading at the 6 ft depth was too wet to provide a measurement; the January, 1990 readings were also too wet to yield readings. No rainfall had occurred in the several days immediately preceding the January,

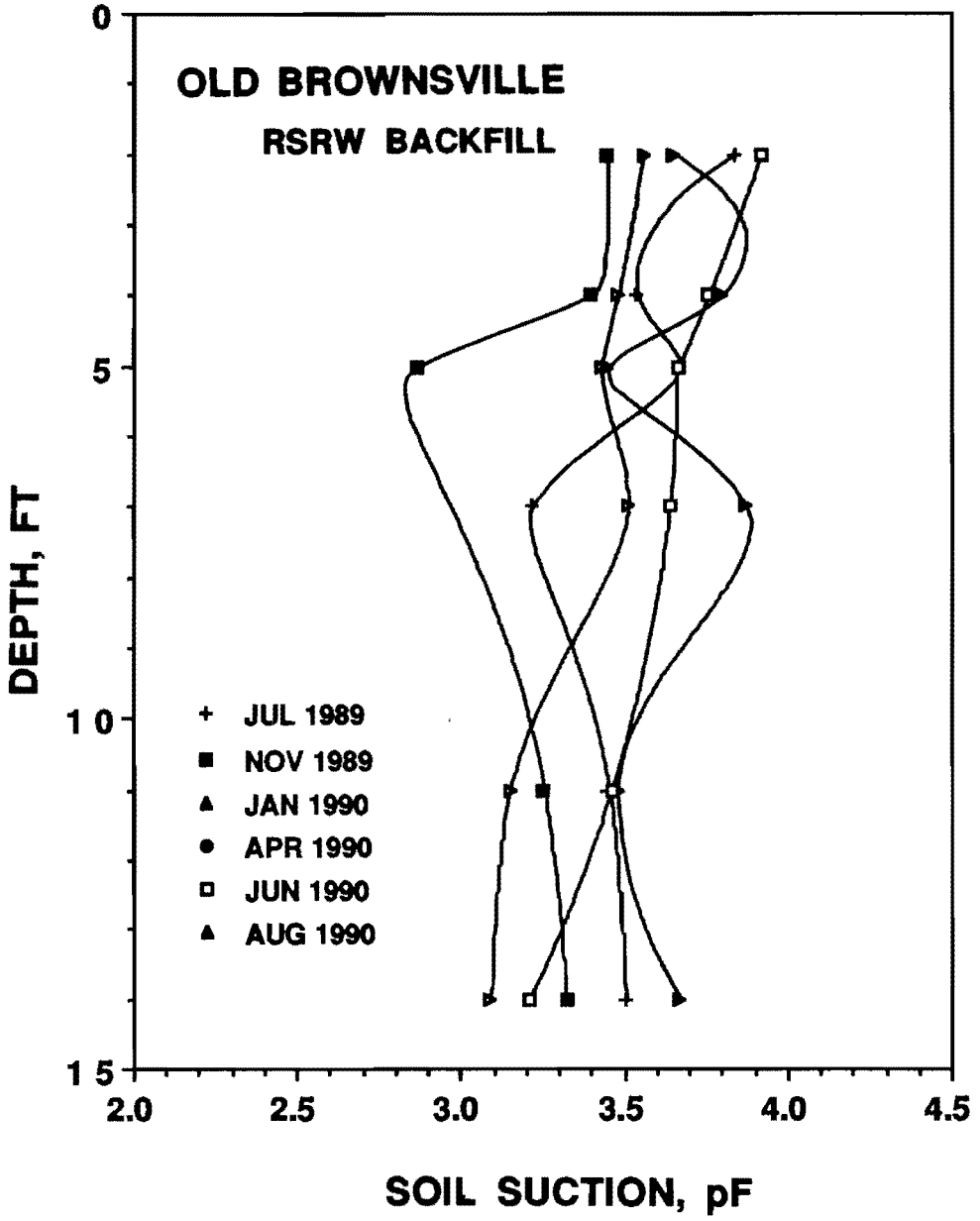

Fig. 4.24. Soil suction vs. time for field measurements obtained from sensors installed in the cohesionless backfill at the Old Brownsville Highway test site.

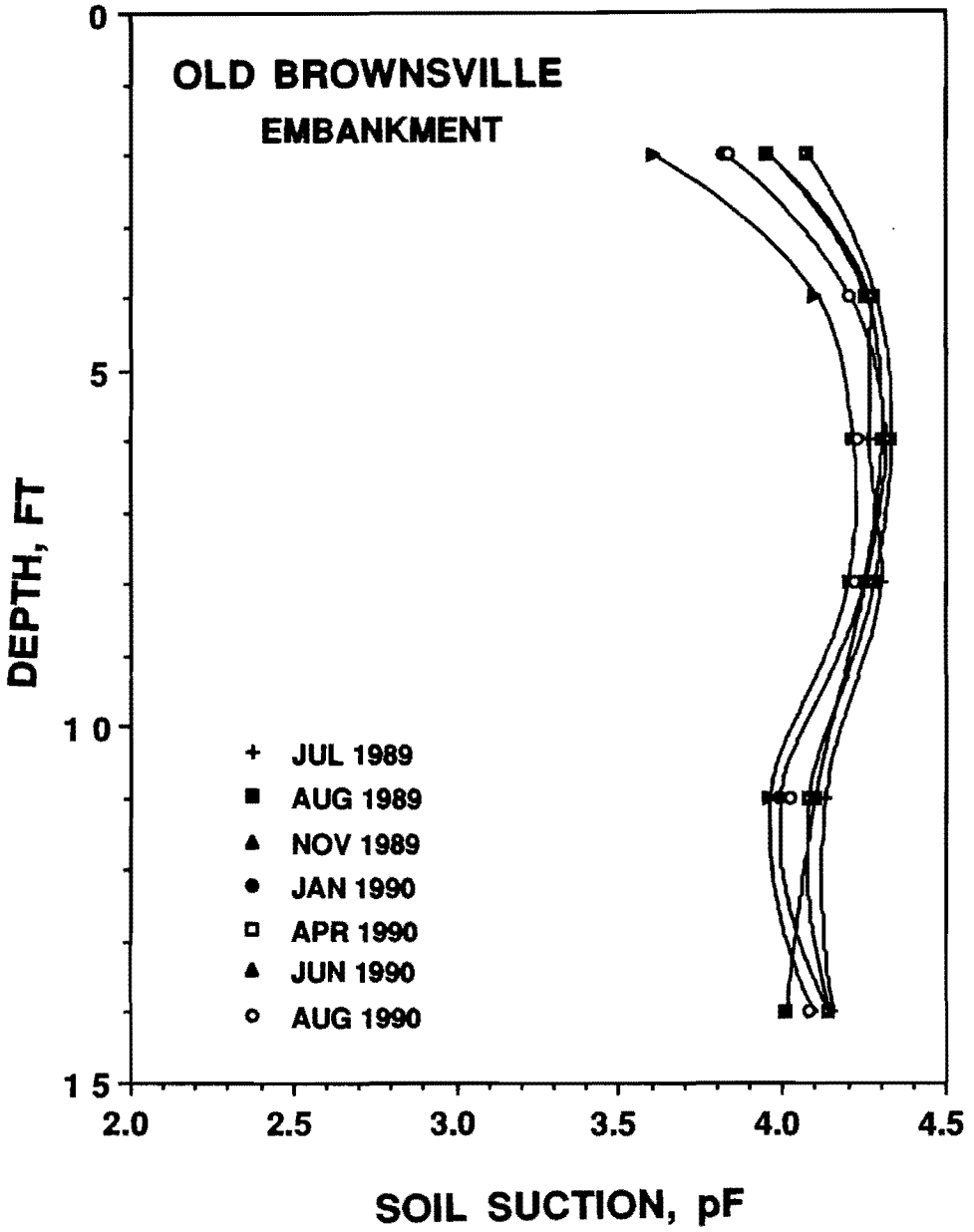

Fig. 4.25. Soil suction vs. time for field measurements obtained from sensors installed in the clay embankment at the Old Brownsville Highway test site.

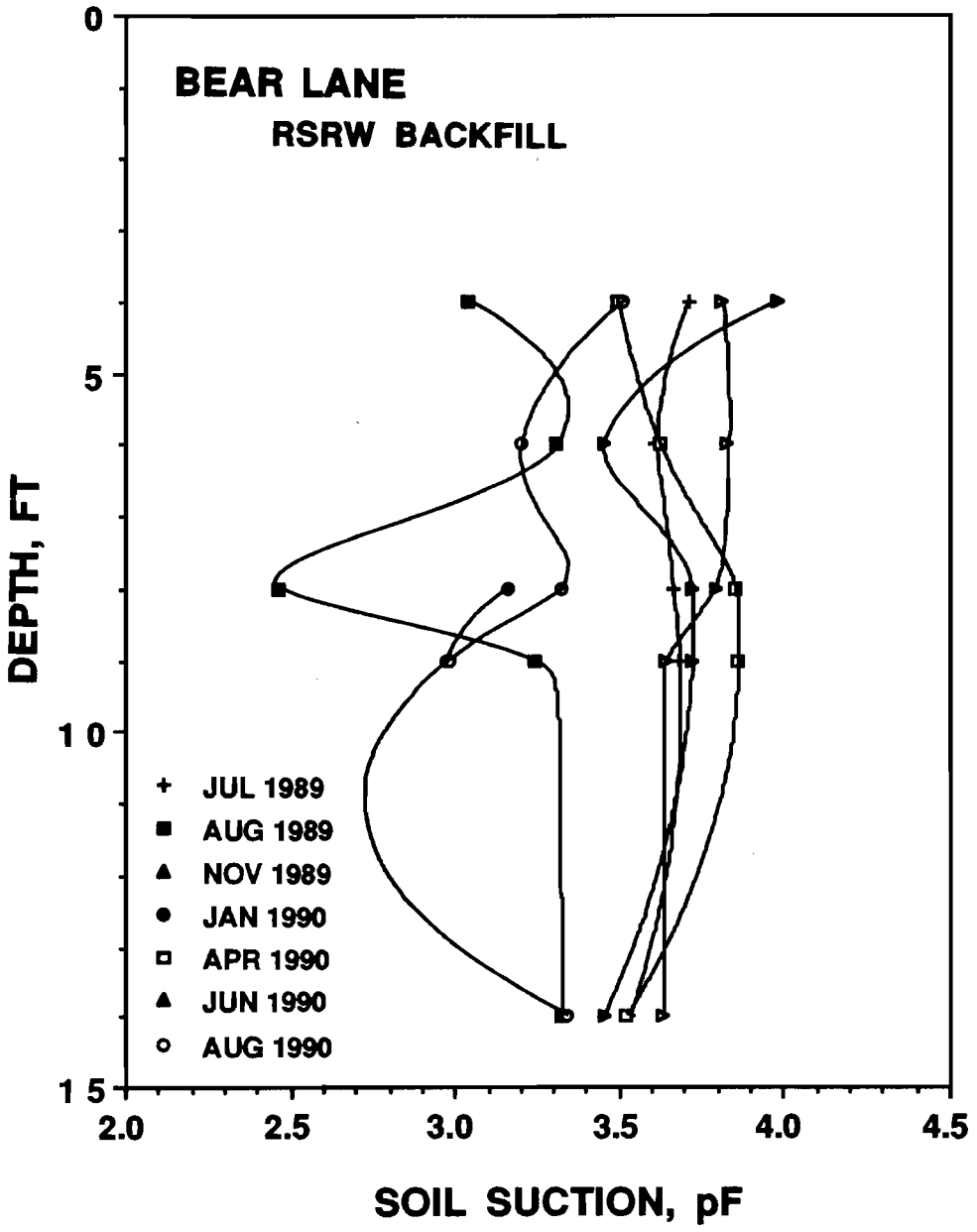

Fig. 4.26. Soil suction vs. time for field measurements obtained from sensors installed in the cohesionless backfill at the Bear Lane test site.

1990 reading visit. Thus, no explanation is available for the strange measurements acquired at this site during the August, 1989 and January, 1990 readings.

The clay at this site, however, does not indicate the wet conditions that the sand showed in August, 1989. The clay did indicate wet conditions for the January, 1990 visit as the sand measurements had indicated. The clay showed a tendency to be responsive to climatic condition changes as can be seen in the 2 and 4 and, to a lesser extent, the 6 ft sensor readings in Fig. 4.27. Below the 8 ft depth, the clay did not show much variation in suction measurements over the period of readings with variation ranging approximately from 4.0 pF to 4.35 pF.

3. Calallen Site. Figures 4.28 and 4.29 represent the changes in the RSRW backfill sand and the embankment material, respectively. This site provided "control" information in that the embankment material was not a high-PI imported clay but was a cut section of sandy clay. Comparing the suction measurements at the two sensor locations at this site, it can be seen that there is not a great deal of difference in response between the two backfill materials. Neglecting the readings above the 6 ft depth--which were most likely affected by changes in climate--the sensors in the backfill material measured changes ranging approximately from 3.3 pF to 3.9 pF. The embankment sensors recorded similar variances with readings ranging approximately from 3.3 pF to 4.0 pF.

4. Discussion. All three cohesionless backfill sites reflect similar soil moisture condition changes over the monitoring period with average minimum suction value (wetter condition) of approximately 3.3 pF and an average maximum suction value (drier condition) of 3.8 pF. The two imported clay embankments reflected considerably higher suction values than the RSRW backfill experienced; the average minimum suction value was 3.8 pF and the average maximum suction value was 4.25 pF. The naturally-occurring sandy clay that was used for the embankment material at the Calallen site exhibited soil moisture conditions similar to those of the sand backfills with a range of suction change of 3.3 to 3.8 pF.

There is little to evaluate in the field data since all but the last measurement readings were taken while the soils were exposed to the atmosphere (and subject to the change in climate). Both sets of sensors at each of the sites reflected an obvious response to changes in climate, indicating that the climate can affect soil moisture conditions to a depth of between 4 and 6 ft (and deeper in the sand backfill during precipitation events since it is free draining). The climate during the duration of this study was one of drought. At the inception of the study, work had just begun on constructing the Bear Lane and Old Brownsville highway overpass embankments. Both had stood completed for a considerable time by the date of the sensor installation although the RSRWs had been completed at these locations for a much lesser period.

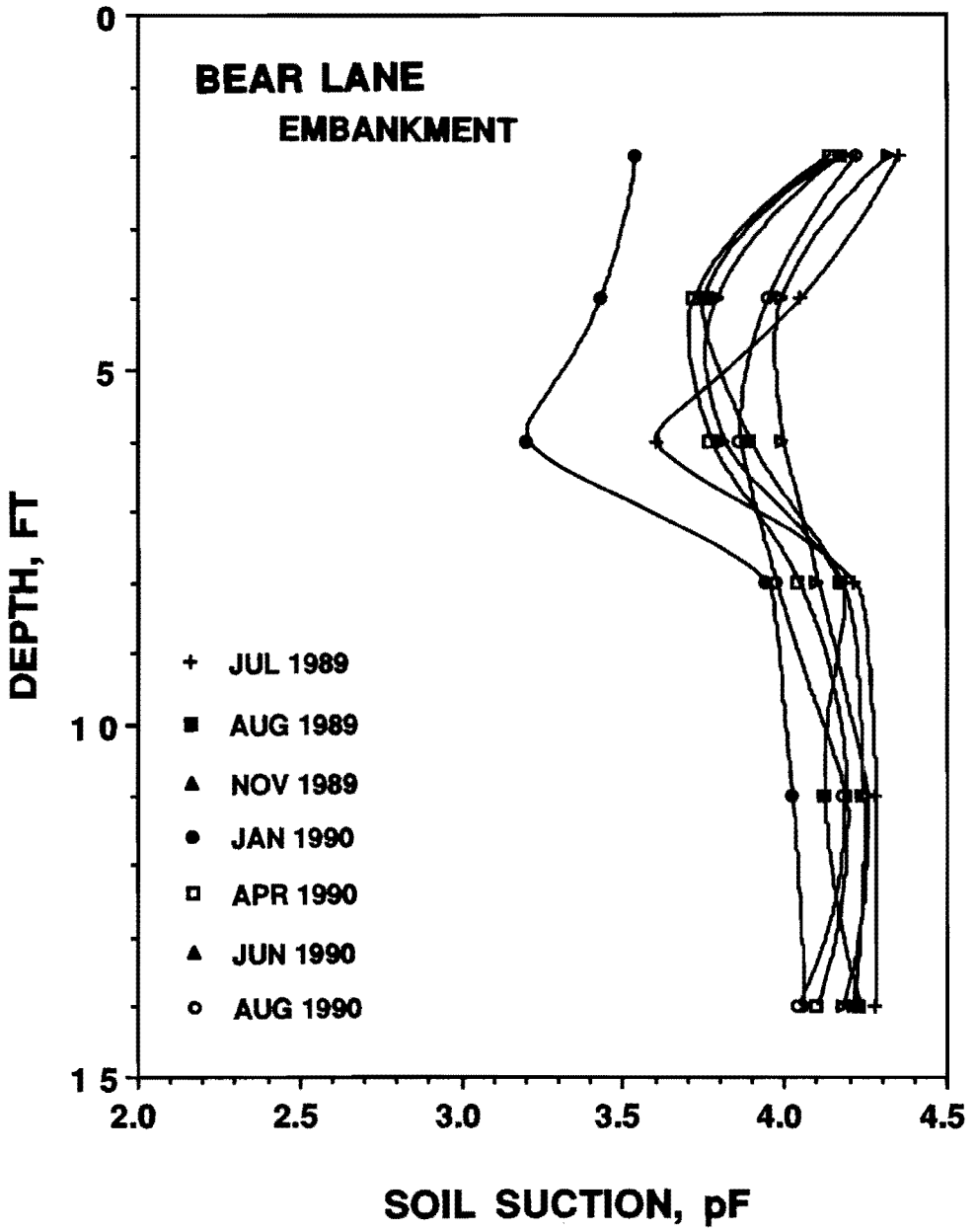

Fig. 4.27. Soil suction vs. time for field measurements obtained from sensors installed in the clay embankment at the Bear Lane test site.

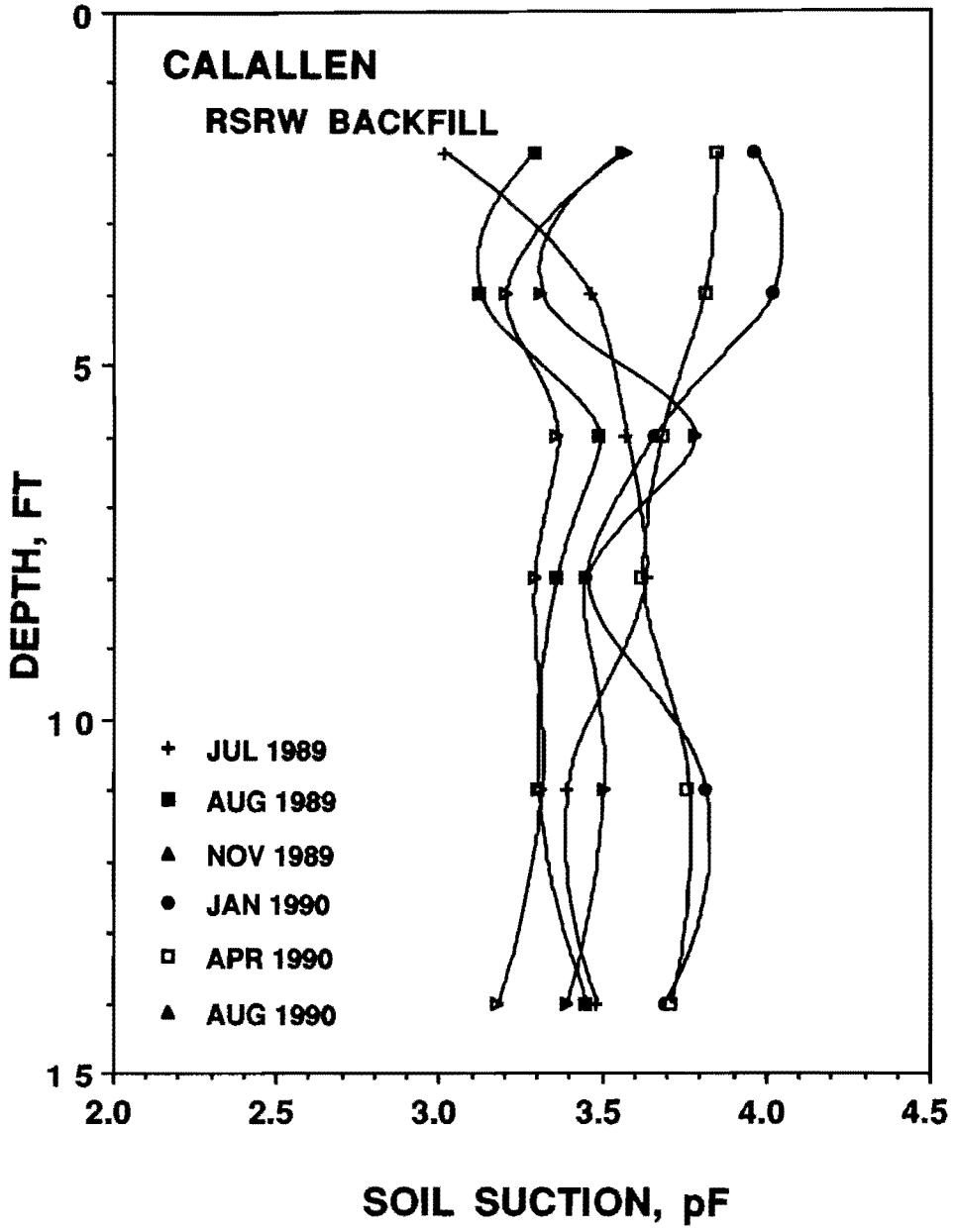

Fig. 4.28. Soil suction vs. time for field measurements obtained from sensors installed in the cohesionless backfill at the Calallen test site.

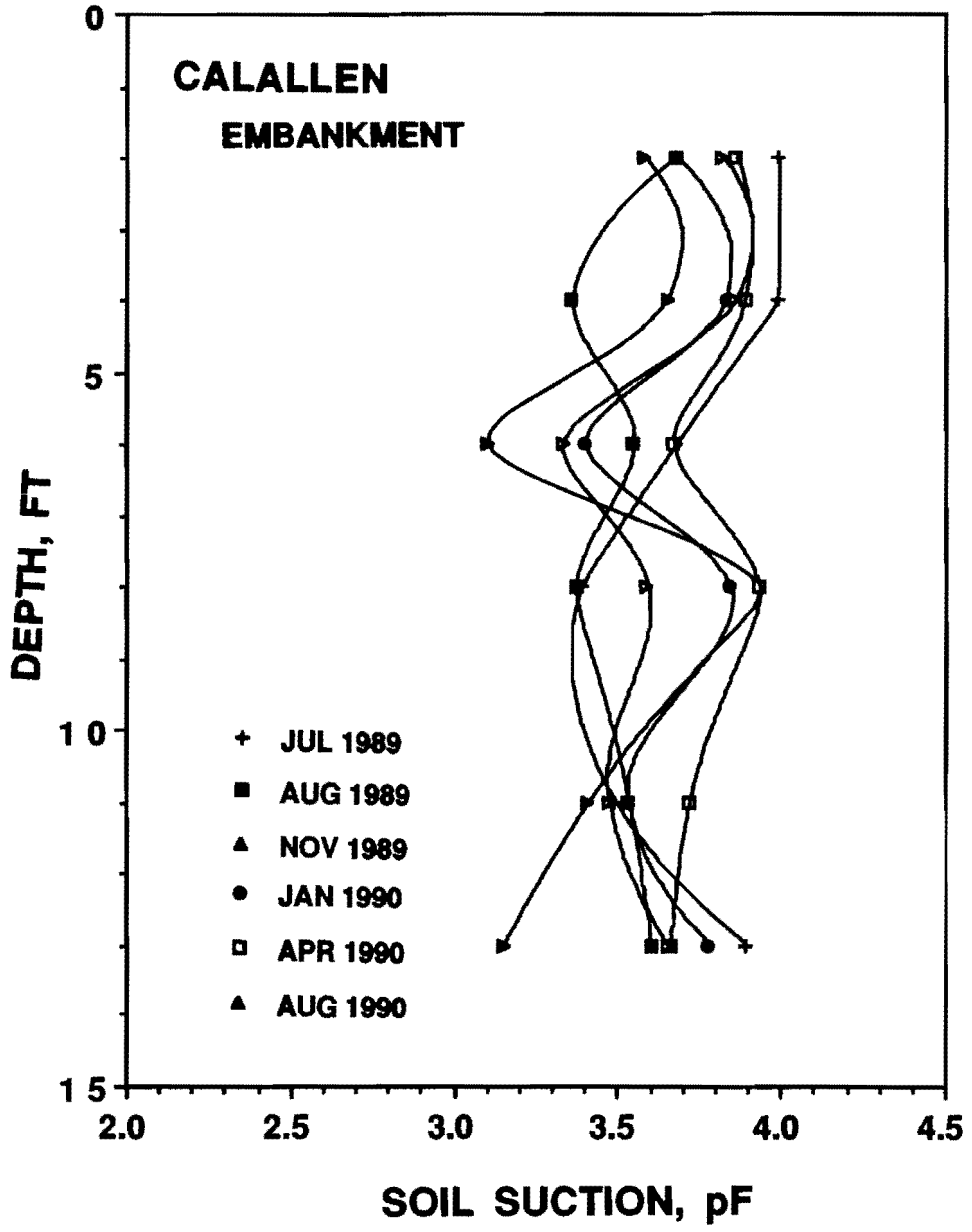

Fig. 4.29. Soil suction vs. time for field measurements obtained from sensors installed in the embankment soil at the Calallen test site.

The Thornthwaite Moisture Index for Corpus Christi for the 12-month period September, 1988 - August, 1989 was -32.9 in./yr and the index for the next 12-month period through the end of the study was -31.5 in./yr. Both periods were considerably drier than the mean. As pointed out in Section 3.B., these two periods were respectively, the 4th and 6th driest 12-month periods in the recorded climate history of Corpus Christi. Thus, it would be expected that some drying of the high-PI clay embankments would have already occurred by the time the pavement was placed at these two sites.

5. CONCLUSIONS AND RECOMMENDATIONS

A. CONCLUSIONS

Field observations made prior to the start of the study showed that the location of the cracking in the pavement was occurring parallel to the highway alignment and that the cracking was only being noted on embankments retained by reinforced soil retaining walls. It was further noted that the location of the cracking with respect to the retained embankment structure approximated the location of the interface between the clay embankment and the cohesionless soil backfill used behind the RSRW walls. During the study it was confirmed that the crack location closely approximated the interface location, with the crack "stair-stepping" inward as the embankment became higher; this was consistent with the longer reinforcement strips used with the higher walls.

Coring at the crack locations by SDHPT District 16 personnel showed that the crack was wider at the bottom than at the top, suggesting that the force causing the fracture was being applied at the bottom of the pavement structure. Thus, it was hypothesized that the source of the cracking was lateral drying of the high-PI clay embankment soil subsequent to placement of the pavement. To test the hypothesis, a series of laboratory studies were conducted using soil obtained from the same source as that used in constructing the actual embankments and RSRWs. The laboratory studies showed that substantial shrinkage of the high-PI soil away from the sand backfill of the RSRW could occur. The tests also showed that when lateral shrinkage of the clay occurred, a crack propagated through the overlying flexible base immediately above the interface gap. A final test to determine if the shrinkage forces generated by the shrinking clay could also induce a crack in HMAC pavement was inconclusive because the HMAC used in the experiment more strongly adhered to the walls of the test device than to the underlying flexible base and contact was subsequently lost between the HMAC and the caliche base. No transfer of shrinkage forces in the form of frictional forces from the caliche to the HMAC occurred.

Measurements made of the changes of soil moisture conditions in the clay soil during the laboratory test series indicate that soil suction pressures as high as 90 atmospheres could be developed in the soil as it underwent the shrinkage process. Conversion of the lateral suction pressures to laterally-induced stresses in the soil showed that the shrinkage stresses could sig-

nificantly exceed the tensile strength of HMAC. Thus, it was concluded that the hypothesis had been proved, i.e., the source of the longitudinal cracking being observed in SDHPT District 16 was lateral shrinking of the high-PI clay embankments subsequent to placement of the pavement.

Soil moisture monitoring instruments were placed in three field locations within SDHPT District 16: two in high-PI clay embankments and one in a sandy clay embankment. The purpose of the instrumentation was to measure changes in soil moisture conditions occurring subsequent to placement of the pavement. However, the sensor locations were not paved until the very end of the study period. As a result, sensor measurements were inconclusive with respect to reporting changes occurring beneath the paved structure. Measurements made over the one-year measurement period, however, showed that some 25 atmospheres of soil suction pressure variations due only to changes in the climate occurred while the completed embankment awaited paving.

Thus, the principal conclusion resulting from this study is that the longitudinal cracking that was observed in District 16 pavements is the result of lateral shrinking of the high-PI clay embankment soil away from its interface with the cohesionless RSRW backfill subsequent to placing pavement over the embankment-wall structure. It is further concluded that the cracking is more likely to occur when the pavement is placed over wetter embankment soil than when placed over soil that is drier, i.e., pavement placed during or immediately following drought periods is less likely to experience this type of cracking than pavement placed during or immediately following a wet period.

B. RECOMMENDATIONS

1. Possible Solutions. Based on the conclusions reported above, several possible recommendations were developed and discussed with SDHPT District 16 engineering personnel. These possible solutions were:

(a) *Geotextile Friction Breaker.* A strip of geofabric is placed between the subgrade and the flexible base, extending several feet on either side of the interface between the clay embankment and the select sand backfill to act as a bond breaker or friction eliminator between the clay embankment subgrade and the flexible base. The objective is to eliminate any tensile stress which might occur in the flexible base as a result of the clay embankment shrinking as it dries.

(b) *Sand Subbase.* A thin lift of sand--similar to the select material used behind the reinforced soil wall--is placed between the clay embankment subgrade and the flexible base to

act as a bond breaker or friction eliminator between the clay embankment soil and the flexible base. For construction simplicity, the sand lift would extend completely across the top surface of the embankment.

(c) *Construct Embankment of RSRW Select Backfill.* The objective of this proposal is to avoid any soil shrinkage at all by completely constructing the embankment of select cohesionless material.

(d) *Spray Cut-Back Asphalt as a Sealer.* Once the clay embankment is completed, a cut-back asphalt is sprayed over the embankment surface to effectively seal the soil moisture within the embankment and prevent soil drying and subsequent shrinkage. If a vertical interface between the clay embankment and the select cohesionless RSRW backfill is subsequently constructed, the vertical interface would also require sealing prior to placing the backfill.

(e) *Construct a Zone of Mixed Soil Across the Interface.* A volume of mixed soil (high-PI clay mixed with a predetermined quantity of cohesionless soil to produce a lesser-PI material) is placed at the interface between the clay embankment and the RE wall select backfill. By reducing the quantity of shrink-susceptible soil, lesser stress would be transmitted to the pavement system should the mixed soil experience drying.

(f) *Membrane Friction Reducer/Separator Along Interface.* This proposal, a variation of Proposal B.1(a), would construct the clay embankment and RSRW in the same manner in which it is currently constructed. However, before any flexible base is installed, either one or two layers of geotextile or plastic membrane is placed over a predetermined width along the alignment of the clay-sand interface. This material would prevent any bonding between the flexible base materials and the underlying clay or sand and avoid any transfer of tensile stress into the flexible base should drying of the clay and subsequent volumetric shrinkage occur.

(g) *Build Up to a Specified Depth With Clay and Complete the Embankment with Sand.* This is a variation on Proposal B.1(c).

(h) *Let Cracks Occur, Repair Crack, and Re-Top.* This method proposes to not change anything in the present construction procedure, allowing cracks to occur. After the cracks have formed, they are then milled out or veed-out, the prepared crack filled, and then the final riding surface of pavement is placed.

(i) *Sand Trench.* The embankment and RSRW are constructed in the same manner as they are currently being constructed. Prior to placement of the flexible base, the interface is deeply and widely veed-out. The vee-shaped trench is then backfilled with a less than 15-PI cohesive material. The flexible base is then placed which is then followed by the asphalt concrete

pavement. Should drying of the clay embankment and subsequent lateral shrinkage occur, the shrinkage stresses would not be transmitted through the low-PI soil material in the wide vee-trench and the pavement structure would not experience a lateral stressing.

2. Discussion of Possible Solutions. In concert with District 16 engineers, each of the proposed possible solutions were considered and discussed at length.

(a) *Geotextile Friction Breaker.* In considering current construction techniques, it is thought that it would be very difficult to maintain a sufficiently "smooth" surface over which the geotextile is to be placed to ensure that some degree of interlock does not occur through the fabric. Thus, although this method may have potential, it is not considered to be practical at the present time.

(b) *Sand Subbase.* This solution is considered to be the most practical of all the solutions; however, actual paving techniques may prove this method to be difficult to employ.

(c) *Construct Embankment of RSRW Select Backfill.* Although many structures have been constructed in this manner, it is not a practical solution for District 16. The availability of locally available acceptable cohesionless soil is limited. Thus, embankments must be constructed from cohesive soils and all locally available cohesive soils are all heavy clays (high-PI soils). Therefore, this solution, while being a very successful solution in other locations, is not considered to be an applicable solution for District 16 without importing large quantities of cohesionless soils.

(d) *Spray a Cut-Back Asphalt as a Sealer.* Although this is a simple solution and can provide a very effective seal to prevent changes in soil moisture conditions, it is thought that such a seal will be very difficult to maintain during the construction period between application of the sealer and placement of the pavement. Thus, unless construction project traffic can be kept off the sealed embankment, this solution is considered to be impractical.

(e) *Construct a Zone of Mixed Soil Across the Interface.* This solution is being employed on a project currently under construction in District 16. Its success will be evaluated in the future.

(f) *Membrane Friction Reducer/Separator Along Interface.* The same concerns associated with Proposal B.2(a) apply to this proposed solution.

(g) *Build Up to a Specified Depth with Clay and Complete the Embankment with Sand.* A variation between Proposal B.2(b) and B.2(c), this possible solution is considered to have the same potential as the two earlier solutions and to have the same application concerns.

(h) *Let Crack Occur, Repair Crack, and Re-Top.* District 16 engineers consider this solution to likely be the most cost effective and to be quite practical. A concern is the occurrence of reflective cracking if the longitudinal cracks are inadequately repaired.

(i) *Low-PI Soil Trench.* Although this method avoids providing a point source of crack propagation through the flexible base immediately above the clay-sand interface, there is concern that there might still be sufficient frictional force transmitted to the flexible base by the clay outside the sand wedge. Thus, this method may only transfer the location of the cracking from the shoulder of the pavement to the right driving lane.

Of these nine possible solutions, only four are considered to be applicable at the present time. Of the four possible solutions considered to have the most merit, the following recommendations are made in the order of expected success:

1. Construct a zone of mixed soil with a lower PI across the clay-sand interface.
2. Construct a sand subbase of at least 3 in. in thickness between the flexible base and the clay subgrade (combines two solutions).
3. Let the crack occur, repair the cracks, and apply a final topping lift of HMAC.
4. Spray cut-back asphalt to encapsulate the clay embankment.

APPENDIX A: REFERENCES

Al-Hussaini, M. and Perry, E.G. (1978), "Field Experiment of Reinforced Earth Wall," *Proc.*, Symposium on Earth Reinforcement, Pittsburgh, PA, April 27, ASCE, New York, NY, pp. 127-156.

Almi, I., Bacot, J., Lareal, P., Long, N.T., and Schlosser, F. (1973), "Etude d'adherence Sol-Armatures," *Proc.*, Ninth International Conference on Soil Mechanics and Foundation Engineering, Moscow.

American Association of State Highway and Transportation Officials (1986), AASHTO Designation T 180-86, "The Moisture-Density Relations of Soils Using a 10-lb [4.54 kg] Rammer and an 18-in. [457 mm] Drop," pp. 648-655.

American Association of State Highway and Transportation Officials (1986), AASHTO Designation T 99-86, "The Moisture-Density Relations of Soils Using a 5.5-lb [2.5 kg] Rammer and a 12-in. [305 mm] Drop," pp. 326-333.

American Association of State Highway and Transportation Officials (1986), Standard Specifications for Transportation Materials and Methods of Sampling and Testing, Part II, Methods of Sampling and Testing, August, 14th Ed.

Aslyng, H.C. (1963), *Soil Physics Terminology*, International Soil Science Society, Bulletin 23, 7 pp.

Austin, S. (1987), "Estimating Shrink/Swell in Expansive Soils Using Soil Suction," Master's Thesis, Department of Civil Engineering, Texas Tech University, Lubbock, TX.

Baker, R., Kassif, G., and Levy, A. (1973), "Experience with a Psychrometric Technique," *Proc.*, Third International Conference on Expansive Soils, Haifa, Israel, pp. 83-95.

Baquelin, F. (1978), "Construction & Instrumentation of Reinforced Earth Walls in French Highway Administration," *Proc.*, Symposium on Earth Reinforcement, Pittsburgh, PA, April 27, ASCE, New York, NY, pp. 186-201.

Bassett, R.H. and Last, N.C. (1978), "Reinforcing Earth Below Footings and Embankments," *Proc.*, Symposium on Earth Reinforcement, Pittsburgh, PA, April 27, ASCE, New York, NY, pp. 202-231.

Bloodworth, M.E. and Page, J.B. (1957), "Use of Thermistors for the Measurement of Soil Moisture and Temperature," Soil Science of America Proceedings, Vol. 21, pp. 11-15.

Bolton, M.D., Choudhurry, S.P., and Pang, P.I.R. (1978), "Reinforced Earth Walls: A Centrifugal Model Study," Symposium on Earth Reinforcement, Pittsburgh, PA, April 27, ASCE, New York, NY, pp. 252-281.

Bomba, S.J. (1968), "Hysteresis and Time-Scale Invariance in a Glass-Bead Medium," Ph.D. Dissertation, University of Wisconsin, Madison, WI.

Bowles, J.E. (1982), *Foundation Analysis and Design*, 3rd Edition, McGraw-Hill Book Co., New York, NY.

Brown, R.W. (1970), "Measurement of Water Potential with Thermocouple Psychrometers: Construction and Application," Intermountain Forest and Range Experiment Station, Ogden, UT (Research Paper INT-80) USDA Forest Service.

Brown, R.W. and Bartos, D.L. (1982), "A Calibration Model for Screen-Caged Peltier Thermocouple Psychrometers," Intermountain Forest and Range Experiment Station, Ogden, UT (Research Paper INT-293) USDA Forest Service, July.

Buckingham, E. (1907), *Studies on the Movement of Soil Moisture*, U.S. Dept. of Agriculture Bureau of Soils, Bulletin 38.

Castro, G. (1969), "Liquefaction of Sands," Ph.D. Dissertation, Harvard University; reprinted as Harvard Soil Mechanics Series No. 81, 112 pp.

Chang, J.C. and Forsyth, R.A. (1977), "Finite Element Analysis of Reinforced Earth Wall," *Journal of the Geotechnical Engineering Division*, ASCE, Vol. 103, No. GT7, pp. 711-724.

Chen, X.Q. and Lu, Z.W. (1984), "Calculation of Movement of Building Foundation of Expansive Soils," *Proc.*, 5th International Conference on Expansive Soils, Adelaide, South Australia, May 21-23, pp. 175-178.

Cheng, M and Shi, Z. (1988), "Laboratory Model Test and Research of the Reinforced Earth Wall," *Proc.*, International Geotechnical Symposium on Theory and Practice of Earth Reinforcement, October 5-7, Fuknoka, Japan, pp. 505-509.

Comuzzie, D.G. (1989), Supervising Resident Engineer, State Department of Highways and Public Transportation, District 16, Corpus Christi, TX, December.

D'Appolonia, D.J., Whitman, R.V., and D'Appolonia, E.D. (1968), "Settlement of Spread Footings in Sand," *Journal of the Soil Mechanics and Foundation Division*, ASCE, Vol. 94, No. SM3, pp. 1011-1043.

Dalton, F.N. and Rawlins, S.L. (1968), "Design Criteria for Peltier-Effect Thermocouple Psychrometers," *Soil Science*, Vol. 105, No. 1, pp. 12-17.

Darbin, M., Jailloux, J.M., and Montuelle, J. (1978), "Performance and Research on the Durability of Reinforced Earth Reinforcing Strips," *Proc.*, Symposium on Earth Reinforcement, Pittsburgh, PA, April 27, ASCE, New York, NY, pp. 305-333.

Design Analysis Associates, Inc. (1989), *HydroNET User's Manual and Reference Guide, Version 2.3*.

Dixon, J.B. and Weed, S.B., Eds. (1977), *Minerals in Soil Environments*, Soil Science Society of America, Madison, WI.

Evans, D.D. (1965), "Gas Movement," *Methods of Soil Analysis*, Part 1, Monographs, American Society of Agronomists, Madison, WI, pp. 319-330.

Fawcett, R.C. and Collis-George, N. (1967), "A Filter-Paper Method of Determining the Moisture Characteristics of Soil," *Australian Journal of Experimental Agriculture and Animal Husbandry*, Vol. 7, pp. 162-167.

Gardner, R. (1937), "A Method of Measuring the Capillary Tension of Soil Moisture Over a Wide Moisture Range," *Soil Science*, Vol. 43, pp. 277-283.

Gardner, W. (1920), "The Capillary Potential and Its Relation to Soil Moisture Constants," *Soil Science*, Vol. 10, pp. 357-359.

Gardner, W.R. (1958), "Laboratory Studies of Evaporation from Soil Columns in the Presence of Water Table," *Soil Science*, Vol. 86, pp. 2-24.

Gibson, R.E. (1967), "Some Results Concerning Displacements and Stresses in a Non-Homogeneous Elastic Half Space," *Geotechnique*, Vol. 17, pp. 58-67.

Goode, J.C. (1982), "Heave Prediction and Moisture Migration Beneath Slabs on Expansive Soils," Master's Thesis, Department of Civil Engineering, Colorado State University, Fort Collins, Colorado.

Goughnour, R.G. and DiMaggio, J.A. (1978), "Soil-Reinforcement Methods on Highway Projects," Symposium on Earth Reinforcement, Pittsburgh, PA, April 27, ASCE, New York, NY, pp. 371-399.

Gromko, G.J. (1974), "Review of Expansive Soils," *Journal of the Geotechnical Division*, ASCE, Vol. 100, No. GT6, Proc. Paper 10609, June, pp. 667-687.

Haines, W.B. (1930), "Studies in the Physical Properties of Soils. V: The Hysteresis Effect in Capillary Properties and the Modes of Moisture Distribution Associated Therewith," *Journal of Agricultural Science*, Vol. 20, pp. 97-116.

Hausmann, M. and Lee, I.K. (1976), "Strength Characteristics of a Reinforced Soil," *Proc.*, International Symposium on New Horizons in Construction Materials, Lehigh University, edited by H.Y. Fang, Vol. 1, pp. 165-176.

Hillel, D. (1982), *Introduction to Soil Physics*, Academic Press, Inc., 1250 Sixth Ave., San Diego, CA.

Holtz, W.G. and Gibbs, H.J. (1954), "Engineering Properties of Expansive Clays," *Proc.*, ASCE, Vol. 80.

Holtz, W.L. and Loibbs, H.J. (1956), "Engineering Properties of Expansive Clays," Transactions, ASCE Vol. 121, pp. 641-677.

Ingles, O.G. (1962), "Bonding Forces in Soils, Part 3: A Theory of Tensile Strength for Stabilized and Naturally Coherent Soils," *Proc.*, First Conference of the Australian Road Research Board, Vol. I, pp. 1025-1047.

Ingles, O.G. (1968), "Soil Chemistry Relevant to the Engineering Behavior of Soils," Chapter 1, *Soil Mechanics, Selected Topics,* edited by I.K. Lee, Elsevier, New York, NY.

Ingvalson, R.D., Oster, J.D., Rawlins, S.L., and Hoffman, G.J. (1970), "Measurement of Water Potential and Osmotic Potential in Soil with a Combined Thermocouple Psychrometer and Salinity Sensor," *Proc*, Soil Science Society of America, Vol. 34, pp. 570-574.

Jaky, J. (1944), "The Coefficient of Earth Pressure at Rest," *Journal of Society of Hungarian Architects & Engineers*, pp. 355-358.

Janbu, N. (1972), "Slope Stability Computation," Embankment Dam Engineering: Casagrande Volume, edited by R.C. Hirschfield and S.J. Poulos, John Wiley & Sons, New York, NY, pp. 47-86.

Johnson, L.D. (1973), "Influence of Suction on Heave in Expansive Soils," *Miscellaneous Paper S-73-17*, U.S. Army Engineer Waterways Experiment Station, Vicksburg, MS, April.

Jones, D.E and Holtz, W.G. (1973), "Expansive Soils - The Hidden Disaster," *Civil Engineering - ASCE*, Vol. 43, No. 8, New York, NY, August, pp. 49-51.

Juran, I., Schlosser, E., Long, N.T., and Legeay, G. (1978), "Full Scale Experiment on a Reinforced Earth Bridge Abutment in Lille," *Proc.*, Symposium on Earth Reinforcement, Pittsburgh, PA, April 27, ASCE, New York, NY, pp. 556-584.

Kassiff, G., Livneh, M., and Wiseman, G. (1969), *Pavement on Expansive Clays*, Israel Institute of Technology, Jerusalem, Academic Press, Israel, pp. 125-157.

Katti, R.K., Bhangale, E.S., and Moza, K.K. (1983), "Lateral Pressure in Expansive Soil With and Without Non-Swelling Soil Layer Application to Earth Pressure on Cross Drainage Structures in Canals and Key Walls in Dams," Part I (Studies on K_o condition), Technical Report No. 32, Central Board of Irrigation & Power, New Delhi, India, 102 pp.

Krohn, J.P. and Slosson, J.E. (1980), "Assessment of Expansive Soils in the United States," *Proc.*, 4th International Conference on Expansive Soils, Denver, CO, ASCE, New York, NY, Vol. 1, June, pp. 569-608.

Ladd, C.C. (1960), "Mechanisms of Swelling by Compacted Clay," *Highway Research Board Bulletin 245*, Washington, DC, pp. 10-26.

Lambe, T.W. (1964), "Methods of Estimating Settlement," *Proc.*, ASCE Settlement Conference, Northwestern University (June).

Lee, K.L., Adams, B.D., and Vagneron, J.J. (1972), "Reinforced Earth Walls," Report No. 7233, UCLA-ENG-7233, University of California, Los Angeles, CA, April.

Lee, K.L. (1978), "Mechanisms, Analysis and Design of Reinforced Earth State-of-the-Art Report," *Proc.*, Symposium on Earth Reinforcement, Pittsburgh, PA, April 27, ASCE, New York, NY, pp. 62-76.

Long, N.T., et al. (1983), "Soil-Reinforcement Friction in a Triaxial Test," *Proc.*, Eighth European Conference on Soil Mechanics and Foundation Engineering; Improvement of Ground, Helsinki, Vol. 1, pp. 381-384.

Low, P.F. (1968), "Mineralogical Data Requirements in Soil Physical Investigations," *Mineralogy in Soil Science and Engineering*, Soil Science Society of America, Special Publication No. 3, pp. 1-34.

Lytton, R.L. (1969), "Theory of Moisture Movement in Expansive Clays," *Research Report No. 118-1*, The Center for Highway Research, the University of Texas at Austin.

Lytton, R.L. and Nachlinger, R.R. (1969), "Continuum Theory of Moisture Movement and Swell in Expansive Clays," *Research Report No. 118-2*, The Center for Highway Research, University of Texas at Austin, September.

Lytton, R.L. and Kher, R.K. (1970), "Prediction of Moisture Movement in Expansive Clays," *Research Report No. 118-3*, The Center for Highway Research, University of Texas at Austin, May.

Lytton, R.L. (1977), "Foundation in Expansive Soil," *Numerical Methods in Geotechnical Engineering*, McGraw-Hill, Inc., New York, NY, pp. 427-457.

Lytton, R.L. (1987), Personal Communication, May.

McKeen, R.G. (1977), "Characterizing Expansive Soils for Design," presented at the Joint Meeting of the Texas, New Mexico, and Mexico Sections of the ASCE, Albuquerque, NM, October 6-8.

McKeen, R.G. (1980), "Field Studies of Airport Pavements on Expansive Clays," *Proc.*, 4th International Conference on Expansive Soils, Denver, CO, pp. 242-261.

McKeen, R.G. (1981), "Design of Airport Pavements for Expansive Soils," New Mexico Engineering Research Institute, Albuquerque, NM (DOT/FAA/RD-81/25), Systems Research & Service Development Service, Washington, DC, January.

McKeen, R.G. (1985), "Validation of Procedures for Pavement Design on Expansive Soils," New Mexico Engineering Research Institute, Albuquerque, NM (DOT/FAA/PM-85/15), Program Engineering and Maintenance Service, Washington, DC, July.

McKittrick, D.P. (1978), "Reinforced Earth: Application of Theory and Research to Practice," Symposium on Soil Reinforcing and Stabilizing Techniques, New South Wales Institute of Technology and the University of New South Wales, Sydney, Australia, October.

McQueen, I.S. and Miller, R.F. (1968), "Calibration and Evaluation of a Wide-Range Gravimetric Method for Measuring Moisture Stress," *Soil Science*, Vol. 106, pp. 225-231.

Miller, E.E. and Miller, R.D. (1955), "Theory of Capillary Flow: I. Practical Implications," *Soil Science Society of America Proceedings*, Vol. 19, pp. 271-275.

Mitchell, J.K. (1976), *Fundamentals of Soil Behavior*, John Wiley & Sons, Inc., New York, NY.

Mitchell, J.R. and Gardner, W.S. (1975), "In Situ Measurement of Volume Change Characteristics," State-of-the-Art Report, *Proc.*, ASCE Speciality Conference on In Situ Measurement of Soil Properties, Raleigh, NC, Vol. II, p. 333.

Mohan, D. (1966), "Engineering Problems In Expansive Soils of India," *Indian Builder*, Vol. 14/9, pp. 22-24.

Naresh, D.N., Rafnam, M.V., and Subrahmanyam, G. (1988), "An Experimental Study on the Performance of a Prototype Reinforced Earth Embankment," *Proc.*, International Geotechnical Symposium on Theory on Earth Reinforcement, October 5-7, Fukuoka, Japan, pp. 443-448.

Olson, R.E. and Langfelder, L.J. (1965), "Pore Water Pressures in Unsaturated Soils," *Journal of the Soil Mechanics and Foundations Division*, ASCE, Vol. 91, No. SM4, pp. 127-150.

Patten, H.E. (1909), *Heat Transference in Soils*, USDA Bureau of Soils - Bulletin 59.

Peck, A.J. (1968), "Theory of the Spanner Psychrometer, I. The Thermocouple," *Agricultural Meteorology*, Vol. 5, pp. 433-447.

Phene, D.J., Hoffman, G.J., and Rawlins, S.L. (1971), "Measuring Soil Matric Potential In Situ by Sensing Heat Dissipation Within a Porous Body: I. Theory and Sensor Construction," Soil Science Society of America Proceedings, Vol. 35, pp. 27-33.

Philip, J.R. (1964), "Similarity Hypothesis for Capillary Hysteresis in Porous Materials," *Journal of Geophysic Resources*, Vol. 69, pp. 1553-1562.

Picornell, M. (1985), "The Development of Design Criteria to Select the Depth of a Vertical Moisture Barrier," Vol. 1, Ph.D. Dissertation, Department of Civil Engineering, Texas A&M University, College Station, TX.

Ponce, V.M and Bell, J.M (1971), "Shear Strength of Sands at Extremely Low Pressures," *Journal of the Soil Mechanics and Foundation Division*, ASCE, Vol. 97, No. SM4, pp. 625-638.

Ravina, I. and Low, P.F. (1972), "Relation Between Swelling, Water Properties, and b-Dimension in Montmorillinite-Water Systems," *Clays and Clay Minerals*, Vol. 20, pp. 109-123.

Rawlins, S.L. (1966), "Theory for Thermocouple Psychrometers Used to Measure Water Potential In Soil and Plant Samples," *Agricultural Meteorology*, Vol. 3, pp. 293-310.

Rawlins, S.L. and Dalton, F.N. (1967), "Psychrometric Measurement of Soil Water Potential Without Precise Temperature Control," *Soil Society of America Proceedings*, Vol. 31, pp. 297-301.

Richards, B.G. (1967), "Moisture Flow and Equilibria in Unsaturated Soils for Shallow Foundations," *Permeability and Capillarity of Soils*, ASTM STP 417, American Society for Testing and Material, pp. 4-34.

Romanoff, M. (1975), "Underground Corrosion," National Bureau of Standards Circular, 579.

Sattler, P. and Fredlund, D.G. (1989), "Use of Thermal Conductivity Sensors to Measure Matric Suction in the Laboratory," Canadian Geotechnical Journal, Vol. 26, pp. 491-498.

Schick, T. (1988), Personal Communication, The Reinforced Earth Company, Grand Prairie, TX, April.

Schlosser, F. and Long, N.T. (1969), "Comportement de la Terre Armee a l'Appareil Triaxial," Activity Report, Laboratoire Central des Ponts et Chaussees.

Schlosser, F and Vidal, H. (1969), "Reinforced Earth," Bulletin de Liaison des Laboratoires Routiers-Ponts et Chaussees, No. 41, Paris, November.

Schlosser, F. and Long, N.T. (1974), "Recent Results in French Research on Reinforced Earth," *Journal of the Construction Division*, ASCE, Vol. 100, No. C03, September, pp. 223-237.

Schlosser, F. (1978), "La Terre Armee: Historique, Development Actuel et Futur," *Proc.*, Symposium on Soil Reinforcing and Stabilizing Techniques in Engineering Practice, Sydney, Australia.

Schlosser, F. and Elias, V. (1978), "Friction in Reinforced Earth," *Proc.*, Symposium on Earth Reinforcement, Pittsburgh, PA, April 27, ASCE, New York, NY, pp. 735-763.

Schmertmann, J.H. (1970), "Suggested Method for Screw-Plate Load Test," Special Procedures for Testing Soil and Rock for Engineering Purposes, Fifth Ed., ASTM Special Technical Publication No. 479, pp. 81-85.

Schofield, R.K. (1935), "The pF of the Water in Soil," *Transactions*, 3rd International Conference of Soil Science, Vol. 2, pp. 37-48.

Shaw, B. and Baver, L.D. (1939), "An Electrothermal Method for Following Moisture Changes of Soil *In Situ*," Soil Science Society of America Proceedings, Vol. 4, pp. 78-83.

Snethen, D.R., Johnson, L.D., and Patrick, D.M. (1977), "An Investigation of Natural Microscale Mechanisms That Cause Volume Change in Expansive Clays," U.S. Army Engineer Experiment Station, Soil and Pavement Laboratory, Vicksburg, MS, January.

Snethen, D.R. and Johnson L.D. (1980), "Evaluation of Soil Suction from Filter Paper," Geotechnical Laboratory, U.S. Army Engineer Waterways Experiment Station, Vicksburg, MS (Project No. 4A161101A91D, Task 02), June.

Spanner, D.C. (1951), "The Peltier Effect and Its Use in the Measurement of Suction Pressure," *Journal of Experimental Botany*, Vol. 2, No. 5, pp. 145-168.

Statement of the Review Panel (1960), "Engineering Concepts of Moisture Equilibria and Moisture Changes in Soils," *Proc.*, Moisture Equilibria and Moisture Changes in Soils Beneath Covered Areas: A Symposium in Print, Butterworths, Australia, pp. 7-21.

Tavenas, F.A., Blanchette, G., Leroueil, S., Roy, M., and LaRochelle, P. (1975), "Difficulties in the In Situ Determination of the K_o in Soft Sensitive Clays," *Proc.*, ASCE Speciality Conference on In Situ Measurement of Soil Properties, Raleigh, NC, Vol. I, pp. 450-476.

Texas State Department of Highways and Public Transportation (1982), "Standard Specifications for Construction of Highways, Streets, and Bridges," Texas State Dept. of Highways and Public Transportation, Austin, TX.

Texas State Department of Highways and Public Transportation (1989), "Manual of Testing Procedures," Vol. I, "Test Method No. Tex-114-E Compaction Ratio Method for Selection of Density of Soils and Base Materials in Place," December, 16 pp.

Timoshenko, S.P. and Goodier, J.N. (1970), *Theory of Elasticity*, 3rd Edition, McGraw-Hill Book Co., New York, NY.

Topp, G.C. and Miller, E.E. (1966), "Hysteresis Moisture Characteristics and Hydraulic Conductivities for Glass-Bead Media," Soil Science Society of America Proceedings, Vol. 30, pp. 156-162.

Topp, G.C. (1969), "Soil Water Hysteresis Measured in a Sandy Loam and Compared with the Hysteresis Domain Model," Soil Science Society of America Proceedings, Vol. 33, pp. 645-651.

Uzan, J., Livneh, M., and Shklarsky, E. (1973), "Two-Dimensional Restrained Shrinkage of Remoulded Heavy Clay," *Proc.*, Third International Conference on Expansive Soils, Haifa, Israel, pp. 137-141.

Vesic, A.S. (1970), "Tests on Instrumental Piles, Ogeechee River Site," JSMFD, ASCE, Vol. 96, No. SM2, March, pp. 561-584.

Vidal, H. (1966), "Reinforced Earth: A New Material for Public Works", Annales, de 1, Institut Technique due Batiment et des Travans Pubbis, 1.9, pp. 224-233.

Vidal, H. (1969), "The Principle of Reinforced Earth," *Soil Theories: Reinforced Earth, Displacements, Bearing, and Seepage*, Highway Research Board Record, No. 282, pp. 1-16, National Academy of Sciences, National Academy of Engineering, Washington, DC.

Vidal, H. (1969), "The Development and Future of Reinforced Earth," Symposium on Earth Reinforcement, Pittsburgh, PA, ASCE, New York, NY.

Vidal, M.H. (1978), "The Development and Future of Reinforced Earth," Keynote Address, *Proc.*, Symposium on Earth Reinforcement, Pittsburgh, PA, April 27, ASCE, New York, NY, pp. 1-61.

Walkinshaw, J.L. (1975), "Reinforced Earth Construction" Report No. FHWA-DP-18, Department of Transportation, Federal Highway Administration, Region 15, Arlington, VA.

Wiebe, H.H. et al. (1971), "Measurement of Plant and Soil Water Status," *Utah Agricultural Bulletin*, No. 484, 71 pp.

Wimsatt, J. and McCullough, B.F. (1989), "Subbase Friction Effects on Concrete Pavements," *Proc.*, 4th International Conference on Concrete Pavement Design and Rehabilitation, April 18-20, Purdue University, pp 3-22.

Wray, W.K. (1984), "The Principle of Soil Suction and Its Geotechnical Engineering Applications," *Proc.*, 5th International Conference on Expansive Soils, Adelaide, South Australia, May, pp. 114-118.

Wray, W.K. (1987), "Evaluation of Static Equilibrium Soil Suction Envelopes for Predicting Climate-Induced Soil Suction Changes Occurring Beneath Covered Surfaces," *Proc.*, 6th International Conference on Expansive Soils, New Delhi, December 1-3, pp. 235-240.

Wray, W.K. (1989), "Mitigation of Damage to Structures Supported on Expansive Soils," Vol. 1, Final Report, National Science Foundation, Washington, DC, March.

Yong, R.N and Warkentin, B.P. (1966), *Introduction to Soil Behavior*, McMillan Co., New York, NY.

APPENDIX B: SOIL SUCTION CONVERSION FACTORS

1 Bar = 0.987 Atmospheres (Atm)
= 14.503 Pounds/square inch (psi)
= 1,019.784 Centimeters of water (cm H_2O)
= 100.000 Kilopascals (kPa)
= 1.0×10^6 Dynes/square centimeter (dyne/cm^2)

1 ATM = 1.013 Bars
= 14.695 psi
= 1,033.296 cm H_2O
= 101.325 kPa
= 1.013×10^6 dyne/cm^2

1 cm H_2O = 9.806×10^{-4} Bars
= 9.678×10^{-4} Atm
= 1.422×10^{-2} psi
= 9.806×10^{-2} kPa
= 9.806×10^2 dyne/cm^2

1 psi = 6.895×10^{-2} Bar
= 6.805×10^{-2} Atm
= 70.314 cm H_2O
= 6.895 kPa
= 6.895×10^4 dyne/cm^2

1 kPa = 1.000×10^{-2} Bars
= 9.869×10^{-3} Atm
= 0.145 psi
= 10.198 cm H_2O
= 1.000×10^{-4} dyne/cm^2

APPENDIX C

PROPOSED TYPICAL SECTION

FOR MAIN LANES

WITH RETAINING WALLS

(Provided by SDHPT 16 from Construction
Drawings for SH 358 Project)

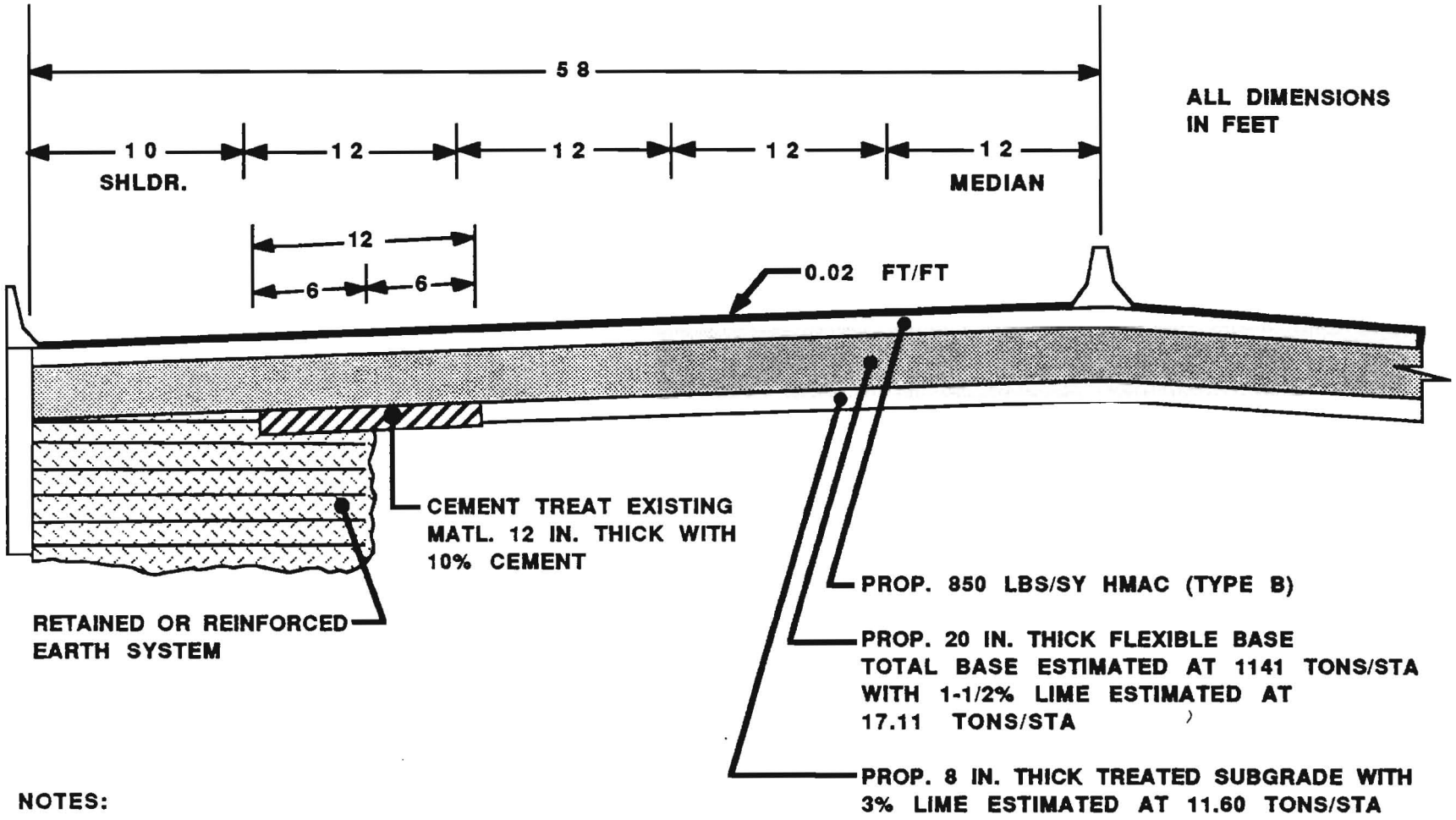

NOTES:

1. Type B HMAC 850 Lbs/Sy to be placed in 3 courses
2. Type B HMAC 550 Lbs/Sy to be placed in 2 courses
3. 20 in. flexible base to be placed in 2 courses
4. Salvaged base shall usually be placed in the 1st course base
5. Concrete traffic barrier shall be placed on the Type B HMAC